A Genetic, Anatomical, and Functional Analysis of Nucleus Ambiguus Neurons Controlling Digestive and Cardiorespiratory Functions

Tatiana Clarissa Coverdell
Eagle River, Alaska

M.S. Biological and Physical Sciences, University of Virginia, 2019
B.S. Biochemistry, Hillsdale College, 2017

A Dissertation presented to the Graduate Faculty of the
University of Virginia in Candidacy for the
Degree of Doctor of Philosophy

Department of Pharmacology

University of Virginia
January 2023

ABSTRACT

The nucleus ambiguus (nAmb), a region found within the medullary reticular formation of the brainstem, controls aspects of swallowing, vocalization, and cardiorespiratory function through its innervation of the pharynx, striated esophageal muscle, larynx, heart, and airways, covering a diverse range of physiological functions. Despite the importance of this region, little was known about what neuronal subtypes exist within the nucleus ambiguus, which organ(s) each subtype innervates, and how they control physiological functions. Thus, identification of these neuronal subtypes within the nucleus ambiguus and their control of respiration, heart function, vocalization, and swallowing were significant knowledge gaps in both the field of neuroscience as well as cardiovascular, respiratory, and digestive medicine. The following studies outlined in this thesis have identified three molecularly distinct neuronal subtypes localized in the nucleus ambiguus. Based on their gene expression and previous studies, we predicted that each molecularly distinct neuron subtype has a different physiological role. We used recombinase-driver mice to access each nucleus ambiguus neuron subtype. Our data shows that one of these nucleus ambiguus subtypes innervates the esophagus; another innervates the pharynx and larynx; and a third innervates the heart. Furthermore, when we optogenetically activated the subtype that innervated the esophagus, we saw esophageal contraction, but no change in heart rate. When we optogenetically activated the subtype that innervated the heart, we saw an immediate and drastic decrease in heart rate. We next focus on elucidating the functional role of the third subtype in pharyngeal and laryngeal control, as well as the necessity of these nucleus ambiguus neuronal subtypes for functional control. Taken together, this data supports the model that the nucleus ambiguus is composed of multiple genetically defined

labeled lines that project to individual organs and control those organ related functions. Overall, these studies provide three major advances to understanding the neuronal control of esophageal and cardiorespiratory function: (1) identifies the primary motor and parasympathetic neurons for the esophagus and heart molecularly, anatomically, and functionally, (2) reveals a genetic logic for the functional organization of the nucleus ambiguus; and (3) comprehensively characterizes the gene expression profile of esophageal motor neurons and cardiac vagal preganglionic neurons, which can be mined for potential drug targets to treat swallowing and cardiorespiratory disorders.

ACKNOWLEDGEMENTS

I would like to thank my mentors, Profs. John Campbell and Steve Abbott, for their continual support, mentorship, and guidance. I could not have asked for a better co-mentorship. Thank you, John and Steve, for giving me the freedom and support to explore science, to develop as a scientist, and to learn so many techniques, concepts, and management skills. I am so grateful for the wealth of opportunities that your mentorship has provided.

I would also like to thank all members of the Campbell Lab and Abbott Lab who have been supportive colleagues and collaborators. I am grateful for your insight and companionship. Thank you also to the undergraduates who worked on these projects with me. Your support on the projects did not go unnoticed and you made great contributions to many different experiments. Thanks for providing me with an opportunity to learn how to mentor.

I would like to thank my committee members: Profs. Doug Bayliss, Paula Barrett, Michael Scott, Thurl Harris, John Campbell, and Steve Abbott. Thank you for your continual feedback and constant support – not only on my research projects and funding, but also in my career as well. Thank you for your invaluable advice on my projects and graduate school. And lastly, thank you for encouraging me to pursue the career paths that seemed like an ideal fit for me and for your support in my next career phase.

Thank you, Pharmacology Department and BIMS program, for supporting me throughout graduate school, but especially in my transition from my first lab to my final ones.

I would also like to thank two fellow graduate students who have been much more than just colleagues to me. To Shayla and Maira: thank you for your friendship during my time here; for being such great listeners and companions throughout graduate school; for being so genuinely supportive; and for your consistency and reliability. I wish you both the best of luck in your future careers and I look forward to seeing all of your future successes.

Thank you to my family for your support and honesty. To my parents: thank you for providing me with the training and support that is essential to where I am now. Thank you for never having a low expectation of me and for teaching me the importance of diligence and independence. Thank you to my siblings for your brutal honesty and genuine support. You have certainly helped keep me grounded. I would also like to thank my mother and her mother for inspiring me in my career trajectory through their own lives.

And lastly, I want to thank my fiancé, Shin, for supporting me all the way from my first week of graduate school to my last. Words cannot express the positive impact that you have made on my time here. I am looking forward to moving on to the next phases of career and life with you by my side.

TABLE OF CONTENTS

SUMMARY OF FIGURES

SUMMARY OF ACRONYMS

12N	hypoglossal nucleus
5-HT	5-hydroxytryptamine
5-HT3R	5-hydroxytryptamine 3 receptor
AV	atrioventricular
CaTCh	calcium-permeable channelrhodopsin 2
CGRP	calcitonin gene related peptide
ChAT	choline acetyltransferase
CRF2	corticotrophin-releasing factor type 2
CVN	cardiac vagal preganglionic neuron
d.a.b.	dorsal accessory branch of SLN
DMV	dorsal motor nucleus of the vagus
DVC	dorsal vagal complex
ECG	electrocardiogram
Ext	external branch of SLN
FISH	fluorescence in situ hybridization
GERD	gastroesophageal reflux disease
GRP	gastrin releasing peptide
GVE	general visceral efferents
HP	hyopharyngeus muscle
Int	internal branch of SLN
IO	inferior olivary nucleus
IX	glossopharyngeal nerve

Kir2.4	inwardly rectifying potassium channel 2.4
LES	lower esophageal sphincter
LRN	lateral reticular nucleus
MDH	medullary dorsal horn
nAmb	nucleus ambiguus
nNOS	neuronal nitric oxide synthase
NOS	nitric oxide synthase
Npy2r	neuropeptide Y Y2 receptor
NTS	nucleus tractus solitarius
OLC	oligodendrocyte lineage cells
Olig3	oligodendrocyte transcription factor 3
PACAP	pituitary adenylate cyclase activating polypeptide
PAG	mesencephalic periaqueductal gray
PC	principal component
PLAP	placental alkaline phosphatase
py	pyramidal tract
r.a.	ramus anastomoticus
RLN	recurrent laryngeal nerve
RNA FISH	RNA fluorescence in situ hybridization
RSA	respiratory sinus arrythmia
sgRNA	single guide RNA
SIDS	suddent infant death syndrome
SLN	superior laryngeal nerve

scRNA-seq	single cell RNA-sequencing
sNuc-seq	single-nuclei RNA-sequencing
Sp5	spinal trigeminal nucleus
ssDNA	single-stranded DNA
SVE	special visceral efferents
Tlx3	t-cell leukemia homeobox 3
Tshz3	teashirt 3
UES	upper esophageal sphincter
UMAP	uniform manifold approximation and projection
Uts2b	urotensin 2b
VIP	vasoactive intestinal peptide
VNS	vagus nerve stimulation
X	vagus nerve

CHAPTER 1: GENERAL INTRODUCTION

Neuronal control over the body's organs is governed by the interplay between sensory and motor neurons. The vagus nerve, known as the longest cranial nerve, projects to major organ systems involved in vocalization, breathing, heart function, and digestion, among other physiological processes (Neuhuber and Berthoud, 2021). The efferent vagus originates from neurons in two major nuclei in the brainstem: the dorsal motor nucleus of the vagus (DMV) and the nucleus ambiguus (nAmb) (Gibbons, 2019). Both of these nuclei are identifiable by their location in the brainstem, but more specifically, by their universal expression of the marker choline acetyltransferase (ChAT) (Neuhuber and Berthoud, 2021).

The DMV is located in the dorsomedial medulla and contains neurons that innervate multiple organs including the heart, stomach, smooth muscle of the esophagus, liver, pancreas, small intestine, spleen, and colon, thus playing a major role in digestion and in some cardiorespiratory functions (Liddle, 2018; Mawe et al., 2018; Rogers and Hermann, 2012; Schubert and Peura, 2008). A recent study showed that the DMV is composed of seven molecularly defined neuronal subtypes, two of which specifically innervate the stomach and connect with distinct enteric neuron populations (Tao. et al., 2021). These results support the theory that vagal neurons are organized into "functional units" that project to distinct organs to control unique organ functions (Chang et al., 2003; Huang et al., 1993; Rogers et al., 1999). Many also wonder if the same organizing principle exists within the nucleus ambiguus.

For almost 200 years, the nucleus ambiguus has been studied to further understand its parasympathetic inputs to the heart and airways, as well as its motor inputs to the striated

esophagus, larynx, and pharyngeal muscles (Bieger and Hopkins, 1987; Holstege et al., 1983a; Lawn, 1966a; Powley et al., 2013a; Taylor et al., 1999; Taylor et al., 2014). Given the complexity of this region, much study has been devoted to understanding whether there are subtypes of neurons within the nucleus ambiguus that distinctly project to different organs. Previous studies have identified some distinguishing characteristics between nucleus ambiguus neuron groups. For example, nucleus ambiguus neurons innervating the esophagus, larynx, and pharynx, together known as special visceral efferent (SVE) neurons or branchiomotor neurons, are largely distinct in their anatomy and function (Bieger and Hopkins, 1987; Holstege et al., 1983a; McGovern and Mazzone, 2010; Nunez-Abades et al., 1992). In addition to its motor neurons, the nucleus ambiguus contains parasympathetic pre-ganglionic neurons, also known as general visceral efferent (GVE) neurons, which innervate the smooth muscles in the heart, lungs, and lower airways (Mazzone and Canning, 2013; McAllen and Spyer, 1978; Nosaka et al., 1979). These general visceral efferents synapse with postganglionic neurons in the smooth and cardiac muscles to influence these organ functions. Studies in the rat indicated that the nucleus ambiguus is subdivided into two longitudinal divisions — a dorsal division housing the special visceral efferent neurons, and a ventral division housing the general visceral efferents neurons (Bieger and Hopkins, 1987). Below is a brief introduction into what is already known regarding the functional role of the nucleus ambiguus in swallowing, vocalization, heart function, and respiration.

1.1. CONTROL OF SWALLOWING BY VAGAL MOTOR NEURONS

1.1.1 Basic Introduction and Clinical Relevance

Swallowing is a complex process that is subdivided into three primary phases — the oral phase, pharyngeal phase, and esophageal phase (Diamant, 1989; Goyal and Cobb, 1981; Ingelfinger, 1958; Kahrilas, 1992; Roman and Gonella, 1987). The entire process of transporting food from the mouth to the stomach involves around 50 different striated muscles and some smooth muscles in the esophagus (Panebianco et al., 2020) controlled by motor neurons that are subject to inputs from a central pattern generator for swallowing (Carpenter, 1989; Doty, 1968; Jean, 1990; Roman and Gonella, 1987). All the muscles involved in the oral and pharyngeal phases are striated; thus, both the oral and pharyngeal phases are controlled by motor neuron pools in the brainstem, including the nucleus ambiguus, that provide motor input to these oral and pharyngeal muscles during swallowing (Carpenter, 1989; Doty, 1968; Jean, 1990; Miller, 1982). In contrast to the complexity of the oral and pharyngeal phases of swallowing, the esophageal phase of swallowing is much simpler and consists of peristaltic contractions that push the bolus from the upper esophageal sphincter to the stomach. The striated muscles of the esophagus receive innervation from the nucleus ambiguus. Thus, the nucleus ambiguus is involved in two of the three phases of swallowing, providing motor input to the pharyngeal muscles, laryngeal muscles, and striated esophageal muscles.

Dysphagia, or difficulty swallowing, is a serious medical condition that affects thousands of people worldwide per year (Panebianco et al., 2020; Robbins, 1999). Not only does dysphagia significantly reduce quality of life, but it can also lead to serious consequences, such as malnutrition, aspiration pneumonia, and death. Often, dysphagia affects aging patients as a secondary manifestation of aging related diseases, such as stroke, Alzheimer's disease, and Parkinson's disease, but is also implicated in other diseases

including Huntington's disease, multiple sclerosis, and muscular dystrophy (Suh et al., 2009).

Many dysphagia cases are neurogenic, meaning that they originate from issues in the central and/or peripheral nervous system (Panebianco et al., 2020; Robbins, 1999). Oropharyngeal dysphagia is most common and affects the oral and pharyngeal phases of swallowing. Most of the oropharyngeal dysphagia cases are due to issues relating to the upper esophageal sphincter (UES), which either over-constricts or does not relax when the bolus is ready to enter the esophagus (Wolf, 1990). Esophageal dysphagia is less common, but often manifests as diffuse esophageal spasms, achalasia, or gastroesophageal reflux disease (GERD) (Tack and Pandolfino, 2018; Wolf, 1990). Esophageal spasms involve non-coordinated contractions of the esophagus, whereas achalasia refers to a failure of the lower esophageal sphincter to relax when the bolus of food is ready to enter the stomach. Gastroesophageal reflux disease is also a common swallowing disorder that is caused by excessive relaxation of the lower esophageal sphincter, which allows the stomach contents to backflow into the esophagus (Tack and Pandolfino, 2018).

Management of dysphagia is still limited and often focused on rehabilitation therapy, pharmacological approaches such as anticholinergic drugs, and surgical interventions. For example, one therapy for dysphagia involves injections of botulinum toxin into the muscle of the upper or lower esophageal sphincter (Restivo et al., 2006). While this is fairly easy to perform, it must be done constantly and the treatment gradually loses its efficacy (Costantini et al., 2022). Other therapies are primarily surgical and invasive. Thus, there is a greater need for more effective and less invasive treatments of dysphagia. More specifically, a better understanding of the neurons that innervate the

pharyngeal, upper esophageal sphincter, esophageal, and lower esophageal sphincter (LES) muscles could lead to better and more targeted therapies to address dysphagia.

1.1.2 Pharyngeal Phase of Swallowing

The pharynx is a multifunctional organ that is involved in swallowing, breathing, and vocalization (Jean, 2001a). During swallowing, it contracts to push ingested material towards the esophagus. The pharynx is subdivided into the oropharynx and the nasopharynx (Miller, 2002). The oropharynx is right above the larynx, whereas the nasopharynx is behind the soft palate.

While the oral phase of swallowing is entirely voluntary, the pharyngeal phase of swallowing is irreversible once started and one of the more complex phases of swallowing, involving the coordination of both excitatory and inhibitory events (Doty, 1968). This phase starts with the contraction of the mylohyoid muscle, followed by contraction of the anterior digastric and internal pterygoid muscles (Doty, 1968). In the initial start of the pharyngeal phase of swallowing, the soft palate raises to the lateral and posterior walls of the pharynx, which closes off the nasal cavity from any potential passage of the bolus into the nasal cavity (Matsuo and Palmer, 2008). At a similar time, the bolus of material is pushed downwards through the constriction of the pharyngeal muscles. Together with the geniohyoid, stylohyoid, styloglossus, posterior tongue, superior constrictor, palatoglossus, and palatopharyngeus muscles (Figure 1-1), the pharyngeal phase of swallowing proceeds until the bolus of ingested material arrives at the upper esophageal sphincter, which is constricted at rest (Doty, 1968; Doty and Bosma, 1956). Constriction of the pharyngeal

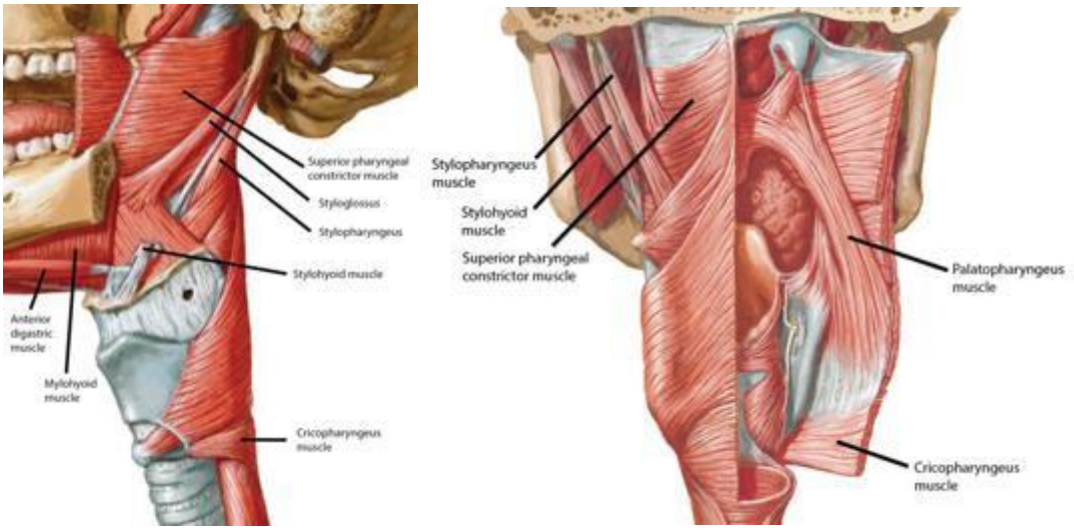

Figure 1-1. Anatomy of the pharyngeal muscles.

Published in Netter, F.H. Netter Atlas of Human Anatomy, 4th edn (Elsevier) .

Figure 1-1 Legend

Lateral view (left panel) and dorsal (right panel) view of the pharyngeal muscles, including the mylohyoid, anterior digastric, stylohyoid, styloglossus, posterior tongue, superior constrictor, and palatopharyngeus

muscles also causes the pharynx to become shorter, which helps the bolus move to the esophagus more efficiently (Matsuo and Palmer, 2008).

Two key reflexes are heavily centered around the pharyngeal phase of swallowing: the gag reflex and the apneic reflex (Miller, 2002). The gag reflex is a reflex that is stimulated by an object touching the back of the throat around the tonsils, which then triggers the pharyngeal muscles to contract in order to expel the object from the back of the throat. In this way, it protects from choking or potentially swallowing something harmful. The apneic reflex in responsible for stopping breathing during a swallow. This prevents potential aspiration of the bolus into the airway.

Pharyngeal muscles receive neuronal inputs via the superior laryngeal nerve and the pharyngeal nerve, which are both branches of the vagus nerve (Figure 1-2)(Kobler et al., 1994a; Mu and Sanders, 2007). The superior laryngeal nerve innervates the cricothyroid, thyropharyngeus, semicircular muscle (also called the cricopharyngeus muscle in humans), and upper esophagus muscle (Kobler et al., 1994a; Mu and Sanders, 2007). The semicircular muscle is a sphincter-like muscle that connects the pharyngeal muscles and the esophagus (Kobler et al., 1994a). The pharyngeal nerve innervates the hyopharyngeus, thyropharyngeus, semicircular muscle, and palatophargeus muscles (Kobler et al., 1994a; Mu and Sanders, 2007).

Motor neurons projecting through the superior laryngeal and pharyngeal nerves to innervate the pharyngeal muscle are primarily located in the nucleus ambiguus (Carpenter, 1989; Doty, 1968; Miller, 1982). Many studies have indicated that there is a rostral to caudal organization of nucleus ambiguus neurons innervating the esophagus, pharynx, and

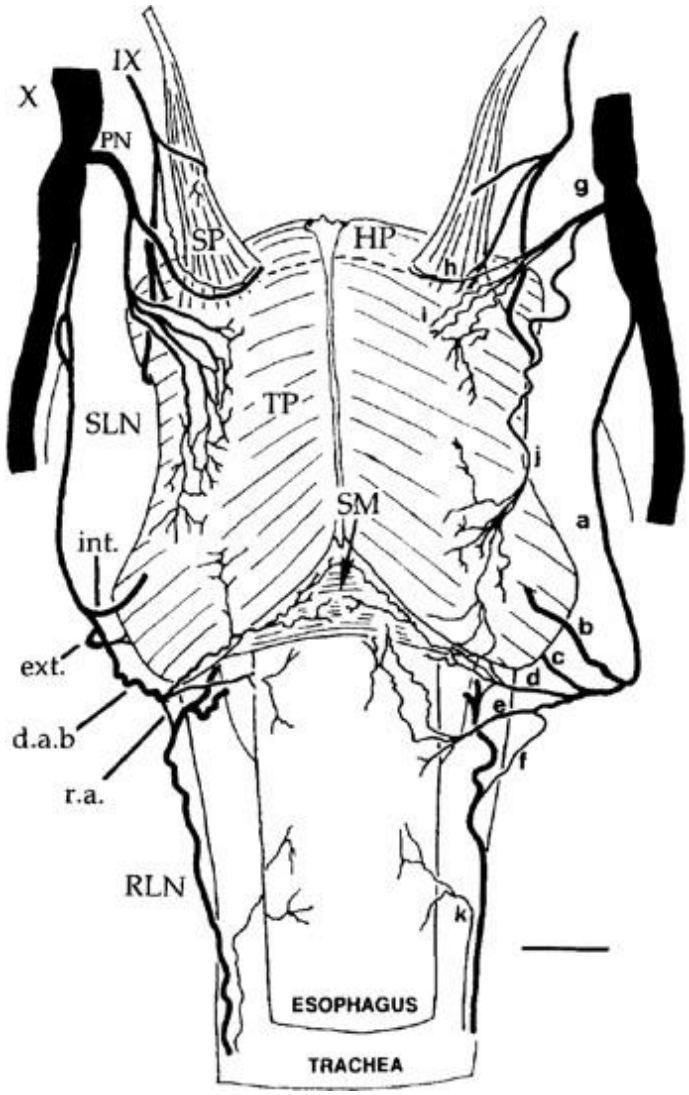

Figure 1-2. Representation of the innervation of the dorsal surface of the rat pharynx and upper esophagus

Published in Kobler, J., Datta, S., Goyal, R., and Benecchi, E. (1994). Innervation of the Larynx, Pharynx, and Upper Espohageal Sphincter of the Rat. THE JOURNAL OF COMPARATIVE NEUROLOGY *349*, 129-147.

Figure 1-2 Legend

Dorsal view of the pharynx, esophagus, and nerve innervation in the rat. IX, glossopharyngeal nerve; X, vagus nerve; SLN, superior laryngeal nerve; RLN, recurrent laryngeal nerve; HP, hyopharyngeus muscle; int, internal branch of SLN; ext, external branch of SLN; d.a.b. dorsal accessory branch of SLN; r.a. ramus anastomoticus. Scale bar = 1 mm

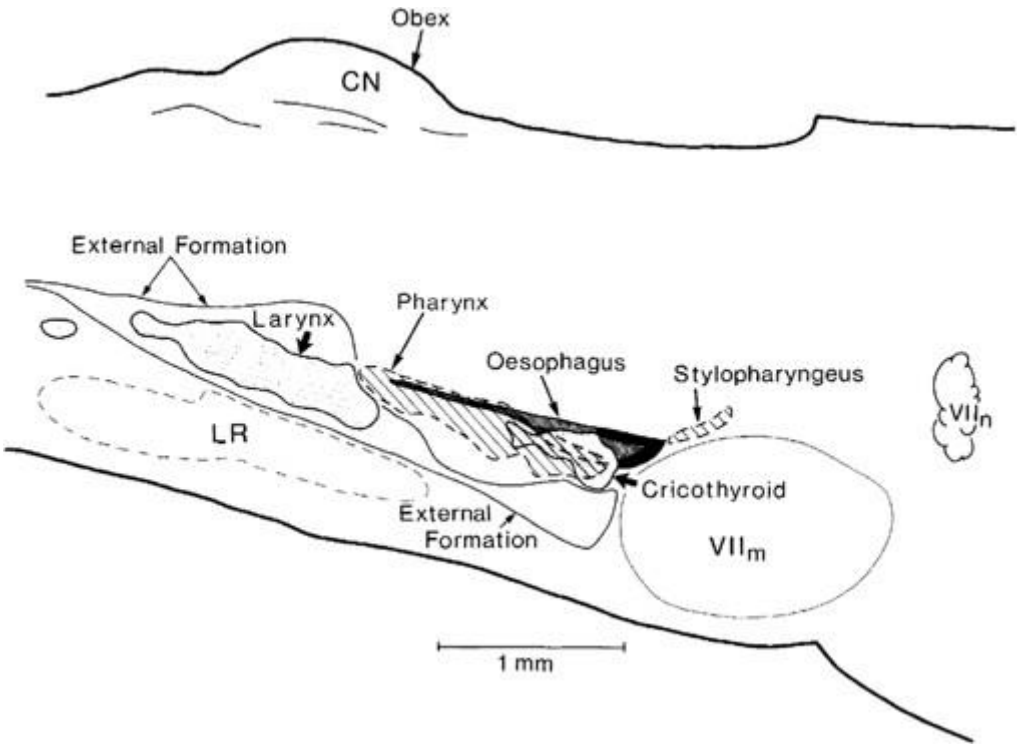

Figure 1-3. Viscerotopic organization of nucleus ambiguus projections.

Published in Bieger, D., and Hopkins, D. (1987). Viscerotopic representation of the upper alimentary tract in the medulla oblongata in the rat: the nucleus ambiguus. The Journal of comparative neurology *262* 546-562.

Figure 1-3 Legend

Viscerotopic organization of nucleus ambiguus projections to the larynx, pharynx, and esophageal muscles. The rostral nucleus ambiguus sends projections primarily to the esophagus. The semi-compact nucleus ambiguus sends projections to the pharynx. The loose nucleus ambiguus sends projections to the larynx.

larynx (Figure 1-3)(Bieger and Hopkins, 1987 ; Lawn, 1964, 1966a, b). Neurons projecting to the pharynx are localized to the semi-compact nucleus ambiguus and well as a rostral extension of the compact formation (Bieger and Hopkins, 1987). Retrograde tracing studies have additionally shown that neurons projecting to the cricothyroid are in the semi-compact nucleus ambiguus and those projecting to the cricoarytenoid are in the loose nucleus ambiguus (Hayakawa et al., 1999).

In addition to a viscerotopic organization of nucleus ambiguus projections, there are some known molecular identifiers for pharyngeal nucleus ambiguus neurons, which can give some clues as to whether there are nucleus ambiguus neuronal subtypes that specifically project to the pharynx to control aspects of swallowing. More broadly, one marker of relevance to pharyngeal projecting neurons is the inwardly rectifying potassium channel, Kir2.4 (gene name: *Kcjn14*) (Topert et al., 1998). This marks motor neurons that innervate striated muscle. More specifically, another study in anesthetized rats found that intravenously injecting 5-hydroxtryptamine (5-HT) increased activity of the pharyngeal branch of the vagus nerve, which was abolished with a 5-HT3 receptor (5-HT3R)(gene name: *5Htr3a*) antagonist (Yoshioka et al., 1994). Injection of 5-HT also increased pharyngeal pressure, which was abolished with a 5-HT3R antagonist. Thus, 5-HT3R could serve as an identifying molecular marker for nucleus ambiguus pharyngeal projecting neurons.

1.1.3 Esophageal Phase of Swallowing

The esophageal phase of swallowing is relatively simple compared to the oral and pharyngeal phases. Following the opening of the upper esophageal sphincter (UES), the

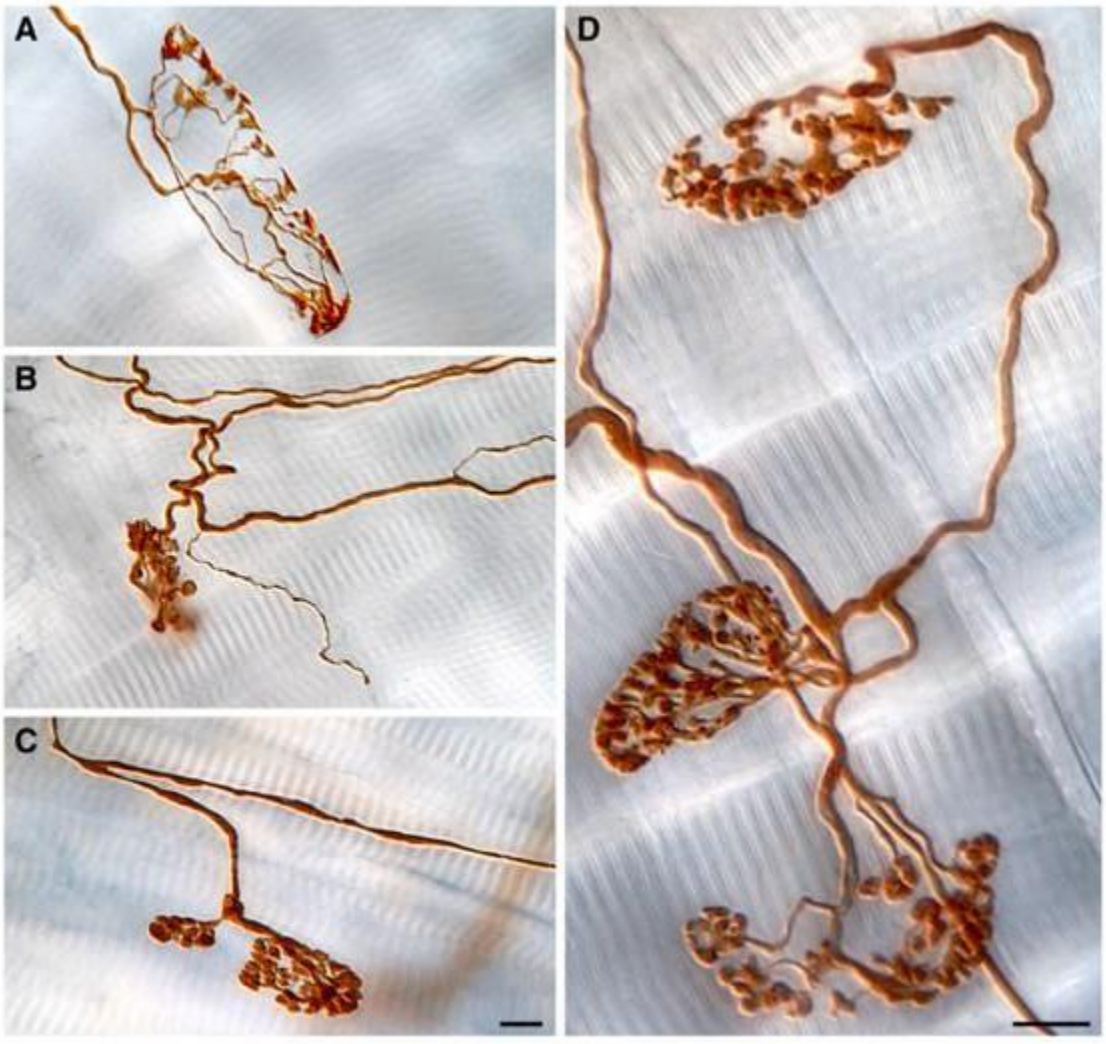

Figure 1-4. Vagal motor endplates innervating esophageal striated muscle.

Published in Powley, T.L., Mittal, R.K., Baronowsky, E.A., Hudson, C.N., Martin, F.N., McAdams, J.L., Mason, J.K., and Phillips, R.J. (2013). Architecture of vagal motor units controlling striated muscle of esophagus: peripheral elements patterning peristalsis? Auton Neurosci *179*, 90-98.

Figure 1-4 Legend

Vagal innervation of esophageal striated muscles. A) Axonal innervation of longitudinal esophageal muscle. B) Innervation of circular esophageal muscle. C) View of longitudinal muscle innervation. Smaller accessory endplate with larger unit. D) Another motor neurite producing three endplates on longitudinal muscle fibers. Scale bar in D = 10 μm for Panel D.

esophageal phase of swallowing involves a series of peristaltic relaxations and contractions of the esophagus to move ingested material from the mouth to the stomach (Jean, 2001a). The upper esophageal sphincter consists of both pharyngeal and esophageal muscles: the inferior pharyngeal constrictor muscle, the cricopharyngeus muscle, and the upper esophagus. In the absence of a swallow, the upper esophageal sphincter remains closed by tonic muscle contraction. However, when a swallow is initiated, the cricopharyngeus muscles relaxes and the suprahyoid and thyrohyoid muscles contract to open the upper esophageal sphincter. When the bolus arrives at the upper esophageal sphincter, it exerts further pressure which helps it to open completely, allowing passage of the bolus from the pharynx to the esophagus.

The esophagus in humans consists of both striated and smooth muscles. Whereas humans have an upper (cervical) esophagus of striated muscle and a lower esophagus of smooth muscle, rodents have a fully striated esophagus (Shiina et al., 2005). Peristalsis, which is a series of wave-like contractions that work together to push the bolus from the pharynx to the stomach, is thought to be generated by the sequential activation of esophageal motor fibers from proximal to distal esophagus (Gidda and Goyal, 1984; Goyal and Chaudhury, 2008a). The striated esophagus has two muscular layers: an external layer that contracts longitudinally, and an inner layer that contracts circularly. The longitudinal fibers shorten the esophagus while the circular fibers contract peristaltically to push ingested material toward the stomach (Edmundowicz and Clouse, 1991). The release of acetylcholine at the endplates on the striated muscle of the esophagus acts on nicotinic receptors to stimulate contraction.

Following passage of the bolus from the pharynx to the esophagus, the lower esophageal sphincter (LES) then opens to allow the bolus to move from the esophagus to the stomach. The lower esophageal sphincter is composed of smooth muscle and receives both excitatory and inhibitory input, both of which work together to keep the lower esophageal sphincter closed in a resting state (excitatory input) until it needs to open to allow for swallowing or vomiting (Goyal and Chaudhury, 2008b). There are two primary lower esophageal reflexes: swallow-associated lower esophageal relaxation and transient lower esophageal relaxation (Goyal and Chaudhury, 2008b). Swallow-associated lower esophageal relaxation occurs during swallowing to allow for the bolus to enter the stomach. Within seconds of the initiation of swallowing, the lower esophageal sphincter relaxes and continues to stay relaxed for a few minutes. On the other hand, transient lower esophageal relaxation occurs in response to gastric distension and inputs from abdominal vagal afferents. This allows for eructation (belching) or emesis (vomiting).

Interestingly, esophageal striated muscle fibers appear to have a one-to-one ratio of muscle endplates per muscle fiber (Figure 1-4)(Powley et al., 2013a), which is commonly the case with muscles that require precisely controlled movement (as opposed to larger muscles like the biceps, which require less motor control and have many fibers innervated by a neuron) (Desmedt, 1981; Duchateau and Enoka, 2011). Thus, it appears the esophageal striated muscle is under fine motor control.

The external and internal layers of striated esophageal muscles in rodents are innervated by the same motor neurons (Powley et al., 2013a) and work in synchrony (Mittal et al., 2006). The striated esophageal muscle is innervated by neurons in the rostral compact formation of the nucleus ambiguus (Figure 1-3)(Bieger and Hopkins, 1987). In addition to

esophageal projecting nucleus ambiguus neurons being identifiable by their location, there are also some molecular markers that appear to be present in nucleus ambiguus esophageal neurons. One study showed that over 70% of nucleus ambiguus neurons projecting to the esophagus expressed the protein calcitonin gene related peptide (CGRP), whereas less than 22% of neurons projecting to the trachea or larynx were CGRP positive. Thus, CGRP could serve as a marker of nucleus ambiguus esophageal neurons (P.N. McWILLIAM, 1989). Furthermore, substance P, neuronal nitric oxide synthase (nNOS), vasoactive intestinal peptide (VIP), neurofilament, calretinin, and calbindin are absent from neurons projecting to the esophagus (Mazzone and Canning, 2013; McGovern and Mazzone, 2010). Lastly, a study in rats showed that the esophagus mucosa, longitudinal muscle, and lower esophageal sphincter had abundant expression of corticotrophin-releasing factor type 2 (CRF2) – another potential marker of nucleus ambiguus esophageal motor neurons (Wu et al., 2007a).

Studies have shown that the lower esophageal sphincter is innervated by the DMV. Anatomically distinct populations of the DMV neurons control relaxation and contraction of the lower esophageal sphincter. Previous studies have shown there is also a viscerotopic organization within the DMV – neurons in the caudal DMV are the inhibitory lower esophageal sphincter population, whereas those in the rostral DMV are the excitatory lower esophageal sphincter population (Rossiter et al., 1990).

1.1.4 Laryngeal Involvement in Swallowing

The larynx is a multifunctional organ that is involved in swallowing, breathing, and vocalization (Shiba et al., 1999). Although primarily thought of in the context of

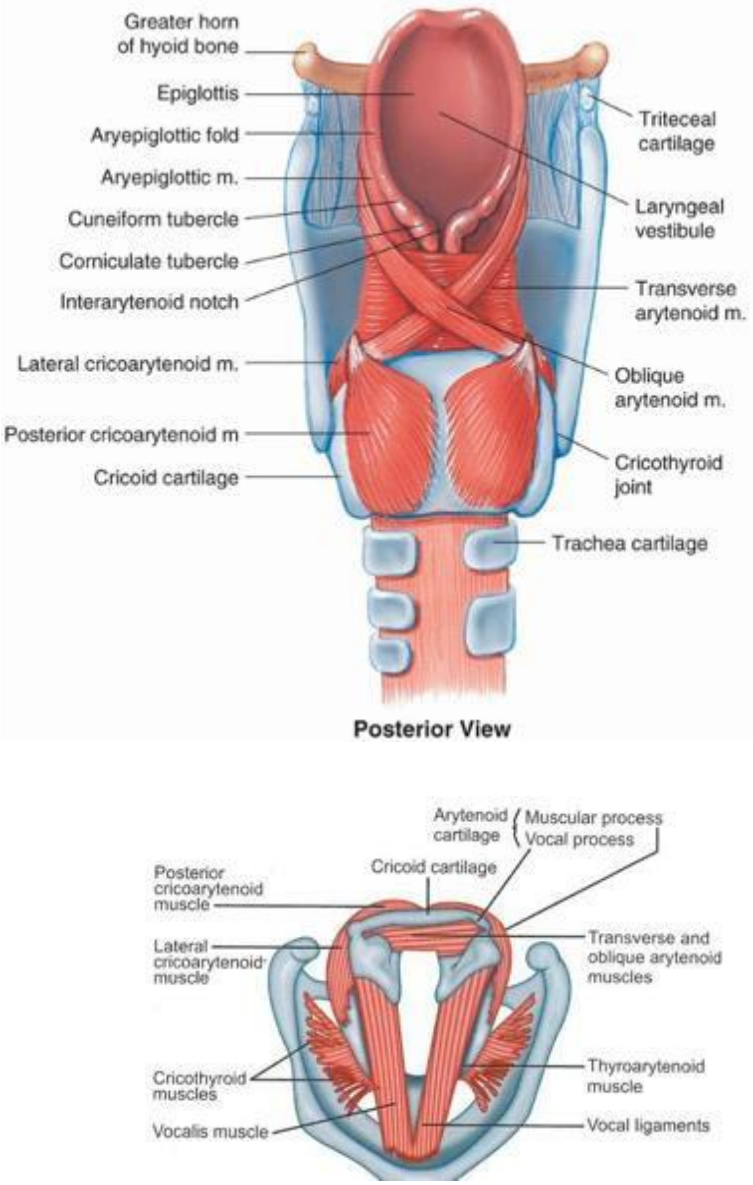

Figure 1-5. Anatomy of the Larynx.

Illustration taken from Lippincott Williams & Wilkins, 2000 and from Sataloff, R.T., Chowdhury, F., Portnoy, J., Hawkshaw, M.J., Joglekar S. Surgical Techniques in Otolaryngology – Head and Neck Surgery: Laryngeal Surgery. New Delhi, India: Jaypee Brothers Medical Publishers, 2013. (Sataloff et al., 2013)

Figure 1-5 Legend.

Ventral view (top panel) and top view (bottom panel) of the larynx, including the vocal cords, trachea, epiglottis, cricoarytenoid, thyroarytenoid, and arytenoid muscles

vocalization, it is also important for swallowing and protection of the airways since the glottis — the vocal cords and space between them — closes to prevent aspiration of food or liquid. Any entry of substances into the upper airway other than air activates chemoreceptors in the epiglottis, which further prompts closure of the glottis.

This process involves several muscles of the larynx including the cricothyroid, thyroarytenoid, and cricoarytenoid (Figure 1-5)(Kobler et al., 1994a), and is primarily a protective mechanism to prevent aspiration of ingested material. The suprahyoid and thyrohyoid muscles bring the hyoid bone and the larynx upward, which helps to seal the airways from food or liquid aspiration. Rotation of the arytenoids by the intrinsic laryngeal muscles adjusts the vocal cords. Ventromedial rotation causes the vocal cords to come together, which closes the glottis. This involves the coordination of the thyroarytenoid, interarytenoid, and lateral cricoarytenoid muscles. These laryngeal muscles work together as a valve able to withstand pressures as high as 250-300 mmHg in humans (Compton et al., 1973; Sharpey-Schafer, 1953).

The recurrent laryngeal nerve innervates the intrinsic laryngeal muscles, cricoarytenoid muscles, and the esophagus (Kobler et al., 1994a; Mu and Sanders, 2007). The recurrent laryngeal nerve provides innervation to all intrinsic laryngeal muscles except for the cricothyroid, which instead receives input via the superior laryngeal nerve. Retrograde tracing studies have shown that neurons projecting to the larynx are located in the caudal, loose region of the nucleus ambiguus (Bieger and Hopkins, 1987). A more detailed understanding of the motor input to the larynx will be discussed in the following section.

1.2 CONTROL OF VOCALIZATION BY NUCLEUS AMBIGUUS NEURONS

In addition to swallowing, the larynx plays a very important role in vocalization and breathing. Two motor systems are responsible for vocalization: the emotional motor system and the volitional motor system (Holstege and Subramanian, 2016). Vocalizations involving emotions, such as crying or laughing, are produced via the emotional motor system. This system is heavily reliant on the mesencephalic periaqueductal gray (PAG) and limbic regions such as the anterior cingulate, insula, and orbitofrontal cortical areas. In humans, the volitional motor system is responsible for more intelligent vocalizations, such as speech. This system involves the motor cortex. Both systems eventually rely on motor neurons innervating the face, mouth, tongue, larynx, pharynx, diaphragm, and intercostals to produce sound.

The process of vocalization is not fully understood; however, it appears that it is heavily controlled by neuronal inputs to the larynx, specifically to the cricothyroid muscle. The process of vocalization begins when the vocal cords come together to narrow the glottis (Zhang, 2016). At a similar time, the lungs expel air which, passing through the glottis, produces vibration of the vocal cords. The previous model for vocalization was that sound was produced when nerve impulses caused vocal cord vibrations; however, this theory was disproven by studies in cadavers in which the larynx produced sound when subglottic pressure was increased.

The larynx receives motor inputs via the superior and recurrent laryngeal nerves, which contain the axons of cell bodies located primarily in the caudal, loose nucleus ambiguus (Figure 1-3). Many studies have looked for genes that are involved in vocalization. These genes may give clues as to which nucleus ambiguus neurons are

involved in vocalization. One study found that CGRP is present in the larynx and is involved in the activity of sensory and motor pathways of the superior laryngeal nerve (Bauman et al., 1999). A study in newborn mutant mouse pups showed that mice with oligodendrocyte transcription factor 3 (*Olig3*) or T-cell leukemia homeobox 3 (*Tlx3*) knocked out significantly impacted vocalization, with pups either not able to vocalize at all, or weak and sparse calls (Hernandez-Miranda et al., 2017). However, these deletions primarily affected the nucleus tractus solitarius (NTS), which directly synapses onto the nucleus ambiguus. In songbirds, the gene urotensin 2b (*Uts2b*) is expressed in the pre-motor nucleus and is necessary for male songbirds to communicate aspects of learned vocalization (Bell et al., 2019). Multiple studies have explored the role of the gene *Foxp2* in vocalization. Mice and humans with disruption or knockout of *Foxp2* had significant challenges in producing vocalizations (French et al., 2007; Fujita et al., 2008; Shu et al., 2005). However, it's unclear where in the neural circuitry of vocalization the *Foxp2* gene plays the greatest role, as it has been found in the thalamus, striatum, cortex, hippocampus, and cerebellum (Urbanus et al., 2020). Deletion of the gene Teashirt 3 (*Tshz3*) causes significant breathing impairment and death of nucleus ambiguus neurons, including those located in the subregion of the nucleus ambiguus containing laryngeal projecting neurons (Caubit et al., 2010). Finally, a study looking at MET receptor tyrosine kinase+ neurons in the nucleus ambiguus showed that they projected to the esophagus and muscles around the larynx (Kamitakahara et al., 2017). Furthermore, deletion of MET in the hindbrain significantly impairs vocalization and causes a significant reduction of nucleus ambiguus neurons (Kamitakahara et al., 2021). Thus, it's possible that some of these genes may be acting in laryngeal motor neurons to control vocalization.

Dysfunction of laryngeal reflexes can have serious consequences. For example, the laryngeal adductor reflex is a reflex in which the glottis closes in response to stimuli other than air, followed by coughing and swallowing (Altschuler, 2001; Bartlett, 1989; Wang et al., 2016). This serves to prevent aspiration of food or liquid into the airways. Improper control of this reflex can result in aspiration of food or liquid as well as glottal closure that does not cease, thus preventing an airflow and resulting in apnea. It is thought that this could be a reason for sudden infant death syndrome (SIDS); however, this is not fully known (Leiter and Bohm, 2007; Thach, 2008). Thus, much could be gained from a more thorough understanding of laryngeal inputs and function.

1.3 CONTROL OF CARDIAC FUNCTION BY NUCLEUS AMBIGUUS NEURONS

Heart rate and other cardiac functions are controlled by the interplay between sympathetic (via sympatho-excitatory neurons) and parasympathetic (via cardiac vagal preganglionic neurons [CVNs]) branches of the autonomic nervous system (Gourine et al., 2016). Cardiac vagal preganglionic neurons project their axons via the vagus nerve to postganglionic neurons. Here, they release acetylcholine to activate postganglionic cardiac neurons via ganglionic nicotinic receptors, which then activate muscarinic receptors (Olshansky et al., 2008). At the same time, CVN activity suppresses sympathetic inputs to the heart. Heart rate is then reduced by the inhibition of sympathetic input to the heart and also by hyperpolarization of sinus node cells. This whole process culminates in a decrease in heart rate, atrioventricular (AV) conduction, and ventricular contractility.

Neurons in both the DMV and the nucleus ambiguus innervate the heart. Studies have shown that stimulation of the nucleus ambiguus and vagus nerve powerfully reduces

heart rate (Coote, 2013). Thus, it is thought that cardiac vagal preganglionic neurons in the nucleus ambiguus tonically suppress heart rate at rest.

The nucleus ambiguus also mediates key cardiac reflexes, including respiratory sinus arrhythmia (RSA) and the arterial baroreflex (Hayano et al., 1996; Yasuma and Hayano, 2004). Respiratory sinus arrhythmia describes the phenomenon in which heart rate increases with inspiration and decreases with expiration. This improves the efficiency of pulmonary gas exchange and circulation. Cardiac vagal preganglionic neurons suppress heart rate during respiratory sinus arrhythmia, as the nucleus ambiguus receives synaptic inputs from respiratory neurons. In other words, cardiac vagal preganglionic neurons are inhibited during inspiration and activated during expiration.

The cardiovagal arterial baroreflex describes a positive feedback loop where changes in blood pressure reflexively drives compensatory changes in cardiac function (Wehrwein and Joyner, 2013). This reflex involves activation of stretch receptors on sensory neurons innervating the carotid bifurcation and aortic arch that signal to neurons in the nucleus tractus solitarius (NTS) and stimulate cardiac vagal preganglionic neurons. The nucleus ambiguus is crucial for this reflex – lesioning the nucleus ambiguus, but not DMV, blocks the cardiovagal arterial baroreflex (Cheng et al., 2004).

Cardiac vagal preganglionic neurons in the nucleus ambiguus have some molecular identifiers. For example, pituitary adenylate cyclase activating polypeptide (PACAP; gene name: *Adcyap1*) marks cholinergic axons innervating guinea pig cardiac ganglia to modulate cardiac neuron excitability and is a potential marker of cardiovagal neurons within the nucleus ambiguus (Calupca et al., 2000). Additionally, neuropeptide Y Y2

receptor (gene name: *Npy2r*) has been demonstrated to play a role in modulating parasympathetic activity to the heart (Smith-White et al., 2002).

Cardiovagal activity is not only a measure of general health, but it also predicts risks and recovery from adverse cardiac events. For example, respiratory sinus arrhythmia (RSA) is mediated by cardiac vagal preganglionic neurons and is an indicator of cardiac health. In addition, low levels of parasympathetic cardiac activity have been associated with hypertension, sudden cardiac death, and heart failure (Mendelowitz, 1996b). Clinical studies looking at vagal nerve stimulation (VNS) in heart failure patients have shown significant improvements in quality-of-life and cardiac performance metrics when parasympathetic cardiac activity is increased; however, these studies have been limited due to off target effects and risk of infection during implant surgery (Franciosi et al., 2017; Garamendi-Ruiz and Gomez-Esteban, 2019). Other attempts to increase vagal tone have involved enhancing cholinergic signaling or activating cholinergic receptors (Liu et al., 2019), but these approaches also have unwanted side effects. More specific targeting of cardiac vagal preganglionic neurons to increase cardiovagal tone would likely reduce side effects and off-target effects. Opening the door to assessment of molecular changes in cardiac vagal preganglionic neurons in the context of cardiovascular disease, as well as developing tools for manipulating and targeting these subtypes, will reveal novel therapeutic targets for the treatment of cardiovascular disease.

1.4 CONTROL OF RESPIRATION BY NUCLEUS AMBIGUUS NEURONS

The airways pass air to and from the lungs, where exchange of carbon dioxide for oxygen occurs to allow cells and organs to function (Mazzone and Canning, 2013). In order

to optimize this process, the airways adapt to accommodate changes in physiological demands, illness, or irritants. The wall of the trachea dilates or constricts based on these changes in physiological demands. Illness or irritants can also cause coughing, airway constriction, or glottal closure. Additionally, airway glands secrete mucous that aids in removing irritants and pathogens.

Autonomic inputs from the parasympathetic and sympathetic nervous systems are responsible for regulating smooth muscle airway tone in response to the body's ever-changing physiological demands. Signaling from vagal preganglionic neurons to the airways causes constriction, increased blood flow, and submucosal gland secretion (Haxhiu et al., 2000). On the other hand, signaling by sympathetic neurons innervating the airways relaxes them; however, in humans, this is very sparse.

Parasympathetic preganglionic neurons that innervate the airways are found within the nucleus ambiguus and the DMV (Haselton et al., 1992). Specifically, these neurons are primarily housed within the rostral nucleus ambiguus and external formation of the nucleus ambiguus as found in a study in ferrets. Cholera toxin B-subunit was injected into the wall of the trachea to retrogradely label neurons projecting from the rostral and external nucleus ambiguus (Kc et al., 2004). Studies have indicated that vagal preganglionic neurons innervating the airways are ChAT positive (Kc et al., 2004). Additionally, the marker VIP marks airway neurons (Kc et al., 2004). Lastly, studies have shown that although some nucleus ambiguus neurons express NOS, neurons innervating the airways do not. Thus, there are some current molecular identifiers of nucleus ambiguus airway projecting neurons. Taken together, these markers can be used to identify and access nucleus ambiguus neuron subtypes in order to study their projections and functional roles.

Dysfunction of vagal preganglionic inputs to the airways can have profound consequences such as respiratory disorders, asthma, chronic obstructive pulmonary disease, and pulmonary hypertension. For example, patients with asthma have increased vagal tone, which leads to excessive bronchoconstriction and mucus secretion (Molfino et al., 1993). Thus, a greater understanding of the neural circuitry involving airway regulation could aid in treatment of airway related dysregulation.

CHAPTER 2. GENETIC ENCODING OF AN ESOPHAGEAL MOTOR CIRCUIT

2.1 SUMMARY

Motor control of the striated esophagus originates in the nucleus ambiguus (nAmb), a vagal motor nucleus that also contains upper airway motor neurons and parasympathetic preganglionic neurons for the heart and lungs. We disambiguate nucleus ambiguus neurons based on their genome-wide expression profiles, efferent circuitry, and ability to control esophageal muscles. Our single-cell RNA sequencing analysis predicts three molecularly distinct nucleus ambiguus neuron subtypes and annotates them by subtype-specific marker genes: Crhr2, Vipr2, and Adcyap1. Mapping the axon projections of the nucleus ambiguus neuron subtypes reveals that Crhr2^{nAmb} neurons innervate the esophagus, raising the possibility that they control esophageal muscle function. Accordingly, focal optogenetic stimulation of cholinergic Crhr2+ fibers in the esophagus results in contractions. Activating Crhr2^{nAmb} neurons has no effect on heart rate, a key parasympathetic function of the nucleus ambiguus, whereas activating all of the nucleus ambiguus neurons robustly suppresses heart rate. Together, these results reveal a genetically defined circuit for motor control of the esophagus.

2.2 INTRODUCTION

Primary motor neurons for the striated esophagus reside in the nucleus ambiguus (nAmb), an evolutionarily conserved vagal nucleus that also provides motor input to laryngeal and pharyngeal muscles (Bieger and Hopkins, 1987; Holstege et al., 1983a; Lawn, 1966a; Powley et al., 2013a; Taylor et al., 1999; Taylor et al., 2014). Nucleus

ambiguus neurons innervating the esophagus, larynx, and pharynx, together known as special visceral efferent (SVE) neurons, are largely distinct in their anatomy and function (Bieger and Hopkins, 1987; Holstege et al., 1983a; McGovern and Mazzone, 2010; Nunez-Abades et al., 1992). In addition to its motor neurons, the nucleus ambiguus contains parasympathetic pre-ganglionic neurons, also known as general visceral efferent (GVE) neurons. These GVE neurons control smooth and cardiac muscles of the cardiorespiratory system (Mazzone and Canning, 2013; McAllen and Spyer, 1978; Nosaka et al., 1979). The cellular heterogeneity of the nucleus ambiguus has made it difficult to isolate the esophageal motor neurons experimentally, limiting what is known about their molecular identity and organization.

Neuron subtypes can be classified based on differentially expressed genes, which can then be leveraged to access and genetically manipulate each subtype. We used this approach to identify nucleus ambiguus neuron subtypes and generate hypotheses about their roles in esophageal control. Targeting each nucleus ambiguus neuron subtype with intersectional genetic strategies, we then tested our hypotheses by (1) mapping the axon projections of the subtypes to the upper airways and esophagus and (2) optogenetically activating the subtypes in vivo to assess their control of esophageal muscle and heart rate. Our studies uncovered one molecular subtype of nucleus ambiguus neurons that selectively innervates the esophagus. Activating these neurons caused esophageal contractions but did not affect heart rate. Together, our results suggest a genetic logic to the organization of the nucleus ambiguus and identify its esophageal motor neurons by their gene expression, anatomy, and function.

2.3 RESULTS

2.3.1 Molecular Identification of Nucleus Ambiguus Neuron Subtypes

Neuron subtypes can be classified based on differentially expressed genes, which can then be leveraged to access and genetically manipulate each subtype. We used this approach to identify nucleus ambiguus neuron subtypes and generate hypotheses about their roles in digestive, vocalization, and cardiorespiratory control. Targeting each nucleus ambiguus neuron subtype with novel genetic strategies, we then tested our hypotheses by (1) mapping the axon projections of the subtypes to the upper airways, esophagus, and heart, and (2) optogenetically activating the subtypes in vivo to assess their control of esophageal muscle, pharyngeal muscle, vocalization, breathing, and heart rate.

To identify nucleus ambiguus neuron subtypes in mice, we profiled their genome-wide mRNA expression by single-nuclei RNA-sequencing, sNuc-Seq (Habib et al., 2016; Todd et al., 2020). To enrich for nucleus ambiguus neurons in our analysis, we used a mouse line which expresses Cre recombinase downstream of the endogenous Chat gene locus (Chat-Cre; (Rossi et al., 2011). We first validated Cre activity in that mouse line by crossing it to a Cre reporter strain, H2b-TRAP (Roh et al., 2017), which fluorescently labels cells with Cre activity. We then labeled all peripherally-projecting nAmb neurons using a systemically injected retrograde tracer, Fluorogold (Cheng and Powley, 2000; Leong and Ling, 1990). Cre recombinase activity was present in 100% of Fluorogold-labeled nucleus ambiguus neurons (396 of 396 neurons; n = 3 mice, Figure 2-1), indicating that all peripherally-projecting nucleus ambiguus neurons have Chat-Cre activity. Furthermore, we used RNA fluorescence in situ hybridization (RNA FISH) to co-localize Cre mRNA with Chat mRNA in nAmb neurons of Chat-Cre mice and observed that all Cre+ cells were

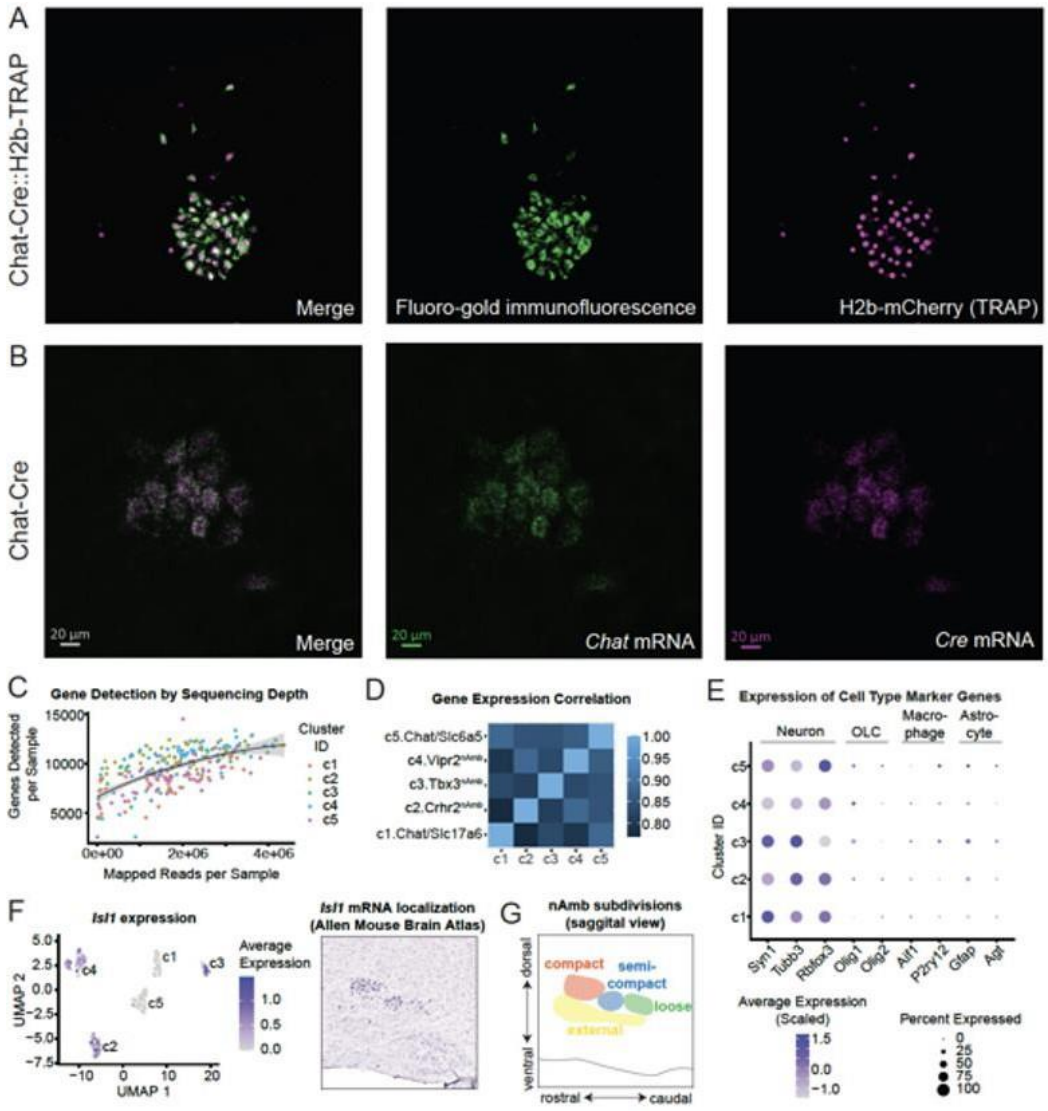

Figure 2-1. Validation of Chat-Cre Activity and Anatomical and Cellular Identity.

Figure 2-1 Legend

A. Co-localization of Fluoro-gold and H2b-mCherry in the nAmb of Chat-Cre::H2b-TRAP mice (n=3 mice).
B. Co-localization of Cre mRNA and Chat mRNA in the nAmb of Chat-Cre mouse by RNA fluorescence in situ hybridization (RNA FISH; image representative of 3 mice; 103 of 103 Chat+ neurons were also Cre+; no Cre mRNA detected in hindbrain cells that did not express Chat).
C. Relationship of sequencing depth to gene detection in individual sNuc-seq samples (dots, colored by cluster identity)
D. Pairwise correlation of gene expression profiles between each pair of cell clusters
E. Cluster-level expression of neuron, oligodendrocyte lineage cells (OLC), macrophage, and astrocyte marker genes
F. Left, log-normalized expression of the nAmb marker gene, Isl1, superimposed on UMAP. Right, in situ hybridization (ISH) of Isl1 mRNA in a sagittal section of the nAmb (Allen Mouse Brain Atlas, experiment 597) (Lein et al., 2007).
G. Map of nAmb subregions based on Isl1 ISH data.

also Chat+ (103 of 103 of Chat+ neurons were also Cre+; Cre mRNA was only detected in hindbrain cells that expressed Chat; n = 3; Figure 2-1). Thus, our results indicate that the Chat-Cre mouse expresses Cre in all Chat+ and peripherally-projecting nucleus ambiguus neurons.

To fluorescently label nucleus ambiguus neurons for sNuc-Seq, we injected a Cre-dependent AAV vector, AAV-DIO-H2b-mCherry, into the ventrolateral medulla of Chat-Cre mice, then isolated single, mCherry+ cell nuclei from the nucleus ambiguus area and sequenced their mRNA with Smart-seq2 to near-saturating depth for gene detection (Picelli et al., 2014) Removing low-complexity transcriptomes (<2,000 genes per nucleus) left 238 single-nuclei transcriptomes for further analysis. Clustering these based on their expression of highly variable genes yielded five cell clusters, which we annotated based on cluster-enriched marker genes (Figure 2-2). These cell clusters differed substantially in their expression of transcription factors, receptors, and other genes (Figure 2-1 & 2-2).

We then compared cluster-level gene expression to identify the cell type represented by each cluster. Confirming their identity as cholinergic neurons, all clusters expressed the neuron marker genes Tubb3 and Syn1, the cholinergic marker gene Chat, but little to no glial marker genes (Figure 2-1). However, only three of the five clusters expressed the nucleus ambiguus marker genes Isl1 and Phox2b (Figure 2-1 & 2-2), supporting their identity as nucleus ambiguus neurons. Our analysis identified candidate molecular markers for these three nucleus ambiguus neuron subtypes: *Crhr2*, *Vipr2*, and *Adcyap1*. The two other clusters appear to have originated from a nearby Chat+ region, as they express genes found around but not in the nucleus ambiguus (Slc17a6, Slc6a5; Figure

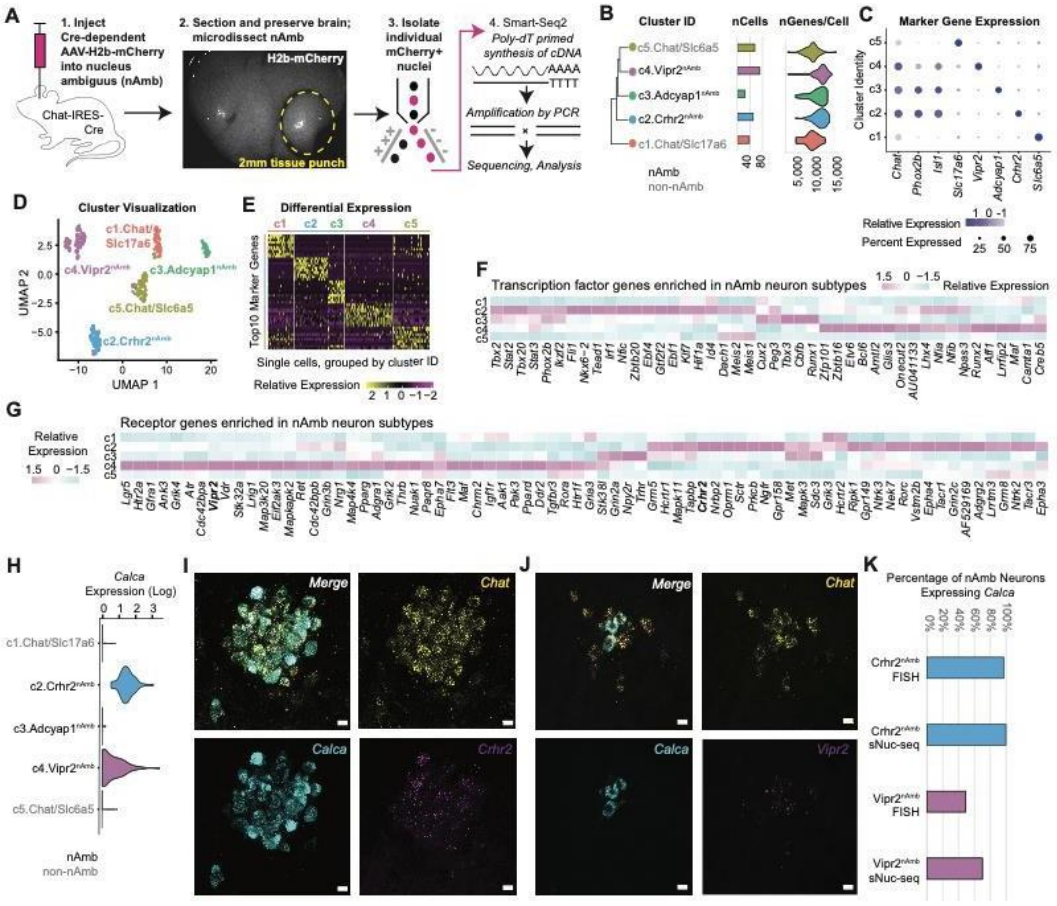

Figure 2-2. Molecular Identification of Nucleus Ambiguus Neuron Subtypes

Figure 2-2 Legend

A. Schematic of single-nuclei RNA-seq (sNuc-seq) workflow.
B. Relatedness of neuron clusters, number of cells per cluster, and number of genes detected per cell.
C. Dot plot of nAmb regional genes (*Chat*, *Phox2b*, *Isl1*) and cluster marker genes.
D. UMAP (Uniform Manifold Approximation and Projection) visualization of clustered data.
E. Single-cell expression heatmap of top marker genes for each cluster.
F. Cluster-level average expression of transcription factor genes.
G. Cluster-level average expression of receptor genes.
H. Violin plots of *Calca* expression.
I. Fluorescence *in situ* hybridization of *Calca*, *Chat*, and *Crhr2* mRNA in the "compact" (rostral) nAmb.
J. Fluorescence *in situ* hybridization of *Calca*, *Chat*, and *Vipr2* mRNA in the "semi-compact" (caudal) nAmb.
K. Percentage of *Calca* expressing $Crhr2^{nAmb}$ neurons and $Vipr2^{nAmb}$ neurons in FISH and sNuc-seq studies. nAmb neurons identified in FISH by systemic Fluorogold labeling and in sNuc-seq by *Isl1* expression. The numbers of *Calca*+ cells as a fraction of the total cells in that group are shown in parentheses.

2-2) (Anderson et al., 2016b; Sherman et al., 2015; Tanaka et al., 2003). Based on their molecular differences, we hypothesized that the three nucleus ambiguus neuron subtypes play distinct physiological roles.

Interestingly, two nucleus ambiguus subtypes, Crhr2^{nAmb} neurons and Vipr2nAmb neurons, expressed the gene *Calca*, which encodes calcitonin gene-related peptide (CGRP; 7). CGRP is enriched in esophageal and airway motor neurons in mammals (Lee et al., 1992; McWilliam et al., 1989). To confirm Calca expression in vivo, we performed fluorescence in situ hybridization (FISH) and detected Calca transcript in approximately 97% of Crhr2^{nAmb} neurons and 49% of Vipr2^{nAmb} (102 of 105 Chat+Crhr2+ neurons were also Calca+; 115 of 232 Chat+Vipr2+ neurons were also Calca+; Figure 2-1). By comparison, our sNuc-seq analysis detected Calca expression in 100% and 70% of the same populations (Figure 2-1). Overall, our sNuc-seq analysis predicts three subtypes of nucleus ambiguus neurons and suggests that the Calca-expressing subtypes, Crhr2^{nAmb} and Vipr2^{nAmb}, may be motor neurons for the esophagus and upper airways.

2.3.2 Vipr2 and Crhr2 Transcripts Mark Anatomically Distinct Nucleus Ambiguus Neurons

In rodents, nucleus ambiguus neurons innervating the esophagus, larynx, and pharynx reside in different subregions (Bieger and Hopkins, 1987; Holstege et al., 1983b; McGovern and Mazzone, 2010), named based on their relative cell densities as the compact, semi-compact, and loose nucleus ambiguus (Figure 2-3). To map the location of Crhr2^{nAmb} neurons and Vipr2^{nAmb} neurons, we performed FISH for Vipr2, Crhr2, and Chat mRNA transcripts in the medulla oblongata of wild type mice after labeling all nucleus

ambiguus neurons with systemically administered Fluorogold (n=3 mice). Essentially all Fluorogold-labeled nucleus ambiguus neurons contained Chat mRNA (e.g., 115 of 116, or >99% of Fluorogold+ cells were also Chat+; Figure 2-1; n= 3 mice), indicating that all peripherally-projecting nucleus ambiguus neurons are cholinergic and validating our choice of Chat to target nucleus ambiguus neurons for sNuc-seq. Importantly, we observed little to no colocalization of Vipr2 and Crhr2 in Chat+ nucleus ambiguus neurons, which agrees with the near lack of Vipr2 and Crhr2 co-expression in our sNuc-seq dataset (Fig. 2-3) and suggests that these genes mark distinct populations of nucleus ambiguus neurons. Our sNuc-Seq analysis detected slightly more overlap in expression of the other markers, between Adcyap1 and Crhr2 and between Adcyap1 and Vipr2 (Figure 2-3). Overall, our sNuc-seq analysis of nucleus ambiguus neurons suggests that Adcyap1, Vipr2, and Crhr2 are expressed by mostly non-overlapping populations of nucleus ambiguus neurons (Figure 3-1).

To validate our sNuc-Seq results, we used RNA FISH to co-localize Adcyap1, Vipr2, and Crhr2 mRNA in nucleus ambiguus neurons, as again labeled by systemic Fluorogold. Our RNA FISH analysis estimates that $Crhr2^{nAmb}$ neurons and $Vipr2^{nAmb}$ neurons constitute 46% and 35% of all nucleus ambiguus neurons, respectively (n=3 mice; 84 of 182 nucleus ambiguus neurons were Crhr2+ only, 64 of 182 nucleus ambiguus neurons were Vipr2+ only; Figure 2-3). The remaining nucleus ambiguus neurons were either $Adcyap1^{nAmb}$ neurons (7%; 13 neurons), Adcyap1+/Vipr2+ neurons (3%; 6 neurons) or did not express any of the three marker genes (8%; 15 neurons). Together, our results indicate that the vast majority of nucleus ambiguus neurons (89%) express either Adcyap1, Vipr2, or Crhr2 and so likely represent distinct subtypes of nucleus ambiguus neurons.

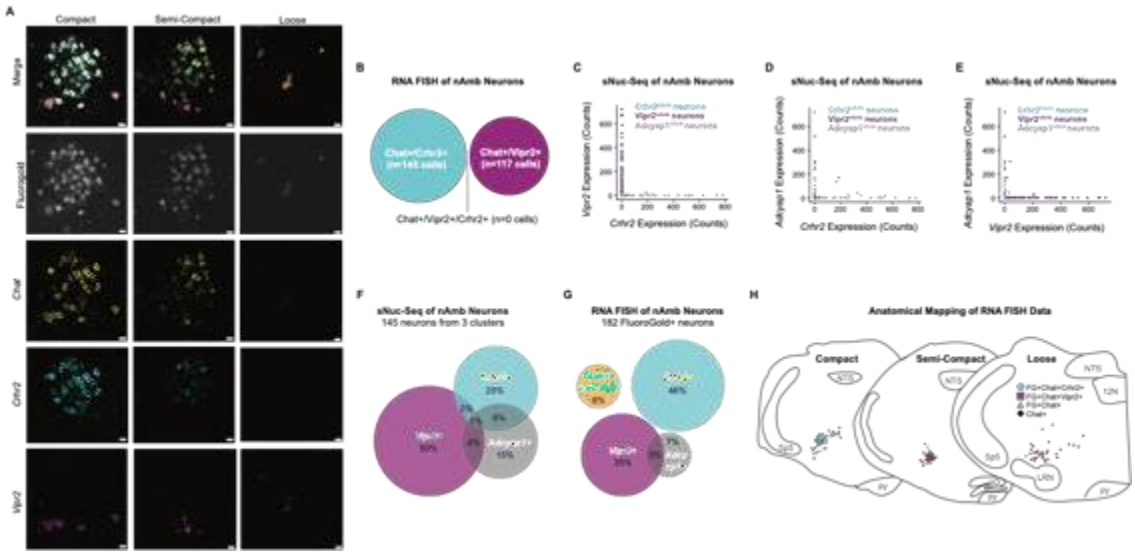

Figure 2-3. Vipr2 and Crhr2 Transcripts Mark Anatomically Distinct Subtypes of Nucleus Ambiguus Neurons

Figure 2-3 Legend

A. Fluorescence in situ hybridization (FISH) of *Chat*, *Crhr2*, and *Vipr2* transcripts in the compact, semi-compact, and loose nAmb, co-localized with systemically administered Fluorogold (n=3 mice).
B. Venn diagram from FISH data showing lack of cellular colocalization between *Vipr2* transcripts and *Crhr2* transcripts.
C. Co-expression of *Vipr2* and *Crhr2* genes in neurons of the three nAmb neuron clusters in the sNuc-seq data.
D. Co-expression of *Adcyap1* and *Crhr2* genes in neurons of the three nAmb neuron clusters in the sNuc-seq data.
E. Co-expression of *Adcyap1* and *Vipr2* genes in neurons of the three nAmb neuron clusters in the sNuc-seq data.
F. Venn diagram of *Crhr2, Vipr2*, and *Adcyap1* expression among neurons in the three nAmb neuron clusters, as detected by sNuc-Seq. Expression counts of >1 were considered positive expression.
G. Venn diagram of *Crhr2, Vipr2*, and *Adcyap1* mRNA as detected by RNA FISH (n=3 mice). nAmb neurons were labeled by systemic injection of the retrograde tracer, Fluorogold.
H. Rostral to caudal distribution of *Chat*+/*Vipr2*+ and *Chat*+/*Crhr2*+ neurons throughout the extent of the nAmb (n=3 mice). DVC, dorsal vagal complex; Sp5, spinal trigeminal nucleus; 12N, hypoglossal nucleus; LRN, lateral reticular nucleus; IO, inferior olivary nucleus; py, pyramidal tract. Compact nAmb: –6.47mm through –6.75mm from bregma, Intermediate nAmb: –6.83mm through –7.10mm from bregma, loose nAmb: -7.19mm through –7.46 mm from bregma.

Mapping the anatomical distribution of Crhr2^{nAmb} neurons and Vipr2^{nAmb} neurons revealed that these subtypes mostly occupy opposite ends of the nucleus ambiguus (n=3 mice; Figure 2-3). The Crhr2^{nAmb} neurons were enriched in the compact and semi-compact nucleus ambiguus (Figure 2-3), where most esophageal and pharyngeal motor neurons reside (Bieger and Hopkins, 1987; McGovern and Mazzone, 2010). On the other hand, Vipr2^{nAmb} neurons were found predominantly in the semi-compact and loose nucleus ambiguus (Figure 2-3), suggesting they may be pharyngeal and laryngeal motor neurons, respectively (Bieger and Hopkins, 1987; McGovern and Mazzone, 2010).

2.3.3 Crhr2^{nAmb} Neurons and Vipr2^{nAmb} Neurons Separately Innervate the Esophagus and Upper Airways.

Given the distinct molecular and anatomical profile of Crhr2^{nAmb} and Vipr2^{nAmb} neurons, we investigated whether these nucleus ambiguus subtypes also differ in which tissues they innervate. To map the axon projections of the nucleus ambiguus, we injected an AAV that Cre-dependently expresses a placental alkaline phosphatase (AAV-FLEX-PLAP) into the ventrolateral medulla of Cre driver mouse lines (n=6 mice; Figure 3-2; (Prescott et al., 2020). We first established that this approach labels nucleus ambiguus neurons by injecting AAV-FLEX-PLAP in Chat-Cre mice. Following recovery, PLAP immunofluorescence was detected in 63% of ChAT immunoreactive neurons in the nucleus ambiguus area (98 ChAT+/PLAP+ out of 155 ChAT+ neurons, n=2 mice; Figure 2-4) distributed along the rostro-caudal extent of the nucleus. PLAP+ cholinergic neurons were also observed in the caudal aspect of the facial motor nucleus and cuneiform nucleus, but

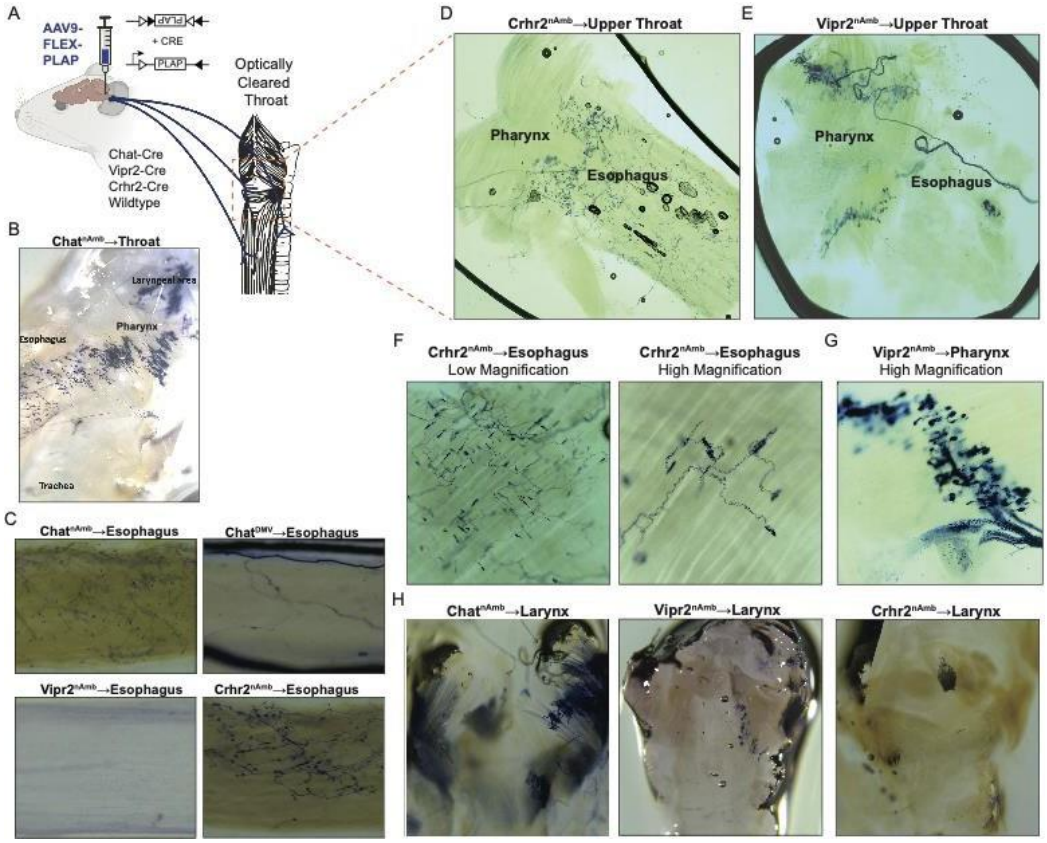

Figure 2-4. Crhr2^{nAmb} Neurons and Vipr2^{nAmb} Neurons Separately Innervate Esophagus and Pharynx

Figure 2-4 Legend

A. Schematic showing injection of AAV9-FLEX-PLAP into the nAmb of Chat-Cre (n=6 mice), Vipr2-Cre (n=5 mice), Crhr2-Cre (n=5 mice), and wildtype mice (n=3 mice). Portions of Fig. 3A were created with BioRender.com
B. PLAP-stained axons in the upper throat after injection in the nAmb of Chat-Cre mice.
C. PLAP-stained axons in the cervical esophagus after injections in the nAmb of Chat-Cre, Vipr2-Cre, Crhr2-Cre, and the DMV of Chat-Cre mice.
D. PLAP-stained axons in the lower pharynx and upper esophagus after injection into the nAmb of Crhr2-Cre mice (D) and Vipr2-Cre (E) mice.
F. Low and high magnification images of PLAP-stained axon terminals in the mid-esophagus after injection into the nAmb of Crhr2-Cre mice.
G. High magnification image of PLAP-stained axons in the pharyngeal muscles after injection into the nAmb of Vipr2-Cre mice.
H. PLAP-stained axon terminals in the larynx after injection into the nAmb of Chat-Cre, Vipr2-Cre, and Crhr2-Cre mice.

not in the DMV, another major source of vagal motor neurons, or the hypoglossal nucleus, which innervates the tongue. Injecting AAV-FLEX-PLAP in Cre-negative mice resulted in no detectable PLAP expression in the brainstem (Figure 2-4). Together, this evidence indicates that our injection of AAV-FLEX-PLAP into the ventrolateral medulla efficiently labels most nucleus ambiguus neurons while avoiding labeling of the DMV and hypoglossal nucleus, and that PLAP expression is limited to Cre expressing cells.

To visualize the axons of PLAP+ neurons, we performed a chromogenic reaction to stain the PLAP+ axons dark blue and then optically cleared the esophagus, airways, heart, lungs, and tongue (Prescott et al., 2020). Targeting PLAP to all peripherally-projecting nucleus ambiguus neurons ($Chat^{nAmb}$) labeled axons throughout the larynx, pharynx, and esophagus (n=6 mice), as well as sparse fibers on the trachea (Figure 2-4 & 2-5). We observed no PLAP stained axons from $Chat^{nAmb}$ neurons to the tongue, consistent with previous retrograde tracing studies showing that the nucleus ambiguus does not innervate the tongue in mouse (Stanek et al., 2014). Unexpectedly, however, we observed little to no PLAP labeled axons from $Chat^{nAmb}$ neurons to the lungs or heart (Figure 2-5), major targets of nucleus ambiguus parasympathetic neurons, indicating that our methods were not suitable for visualizing nucleus ambiguus innervation of these organs. Together, our anterograde tracing studies confirm that nucleus ambiguus neurons innervate the larynx, pharynx, esophagus, and trachea.

The DMV is another major source of vagal motor neurons, though is thought primarily to innervate subdiaphragmatic digestive organs. To characterize DMV projections to the cervical esophagus in mice, we repeated our PLAP studies but instead targeted Chat-Cre+ DMV neurons ($Chat^{DMV}$; n=3 mice). Our results showed PLAP-stained

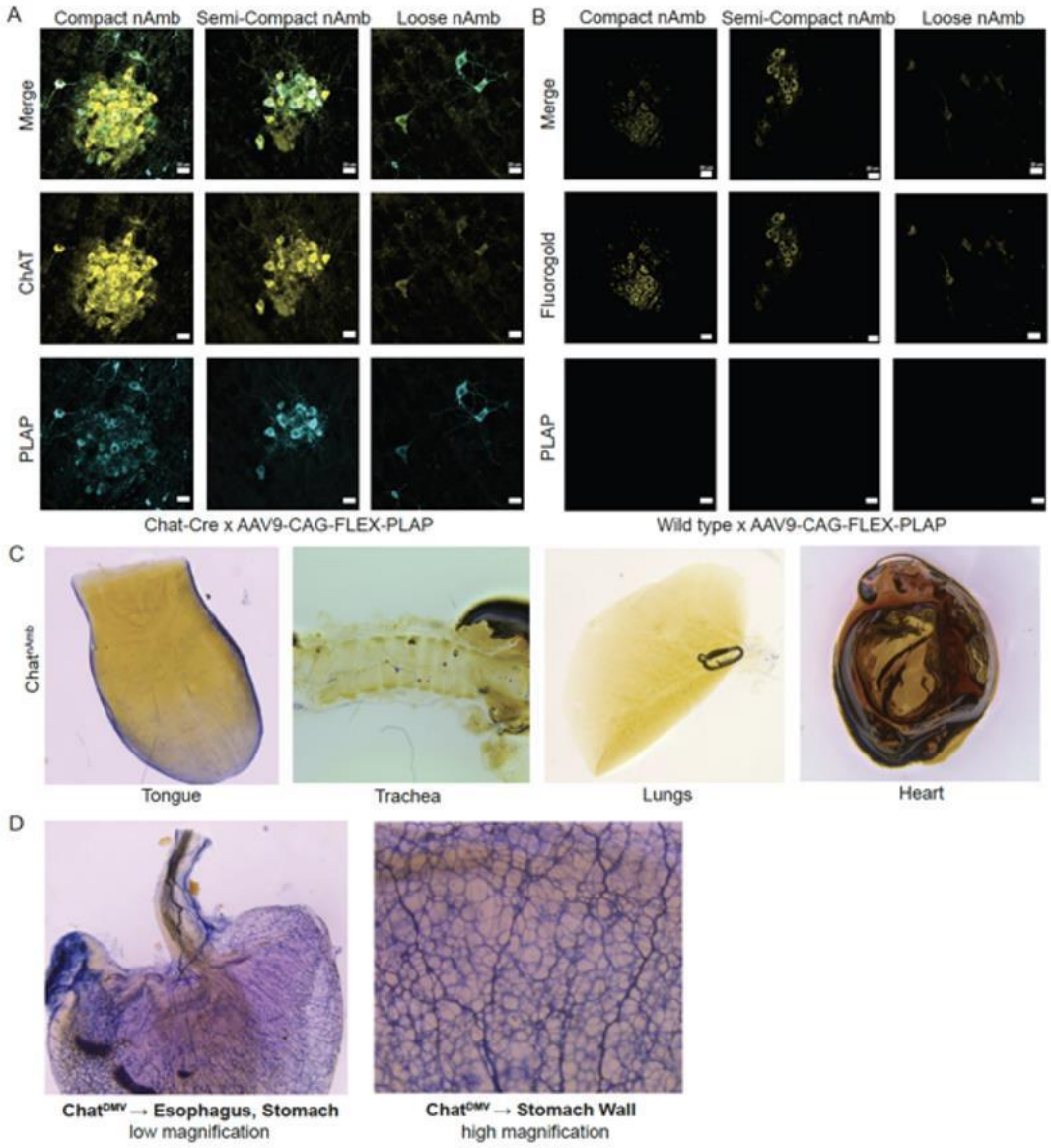

Figure 2-5. Immunofluorescence Images of AAV9-CAG-FLEX-PLAP Expression in Chat-Cre and Wild type Mouse Lines Confirm Successful Infection and Expression; ChatnAmb Innervation of the Tongue, Trachea, Lungs, and Heart; ChatDMV Innervation of the Esophagus and Stomach

Figure 2-5 Legend

A. Colocalization of ChAT and PLAP immunofluorescence in nAmb neurons after injection of AAV9-CAG-FLEX-PLAP into the nAmb of a Chat-Cre mouse (n=6 mice).
B. Colocalization of ChAT and PLAP immunofluorescence in nAmb neurons after injection of AAV9-CAG-FLEX-PLAP into the nAmb of a wildtype mouse (n=3 mice).
C. PLAP stained axons in the tongue, trachea, lungs, and heart of Chat-Cre mice following injection of AAV9-CAG-FLEX-PLAP into the nAmb. (n=6 mice)
D. PLAP stained axons in the esophagus and stomach of Chat-Cre mice following injection of AAV9-CAG-FLEX-PLAP into the DMV (n=3 mice). Higher magnification image of PLAP stained axons in the stomach wall of Chat-Cre mice following injection of AAV9-CAG-FLEX-PLAP into the DMV (n=3 mice).

Chat^{DMV} fibers branch extensively in the stomach wall (Figure 2-5) but not in the cervical esophagus, in contrast to what we observed of Chat^{nAmb} fibers (Figure 2-4). Stained nerves and fiber bundles from Chat^{DMV} neurons were evident along the esophagus but lacked the branching pattern and motor end plate-like morphology of the Chat^{nAmb} fibers. These results confirm that the nucleus ambiguus is the predominant source of motor innervation of the cervical esophagus in mice (Sang and Young, 1998).

To map the projections of Crhr2^{nAmb} neurons and Vipr2^{nAmb} neurons, we obtained Crhr2-Cre and Vipr2-Cre mice. We validated Cre expression in these mouse lines by co-localizing mRNA of the driver gene (i.e., Crhr2 or Vipr2) and Cre using RNA FISH. In Crhr2-Cre mice (n=3 mice), 79 of 82 Crhr2+ neurons were also Cre+. In Vipr2-Cre mice (n=4 mice), 57 of 57 Vipr2+ neurons were Cre+ (Figure 2-6). Importantly, in the hindbrain of both Cre mouse lines, Cre mRNA was limited to cells in which the driver gene mRNA was also detected, confirming the specificity of these Cre lines.

To map the projections of the Crhr2^{nAmb} neurons and Vipr2^{nAmb} neurons, we injected AAV-FLEX-PLAP into the ventrolateral medulla of Crhr2-Cre mice and Vipr2-Cre mice. This resulted in patterns of PLAP immunofluorescence which were consistent with the anatomical distribution of Crhr2^{nAmb} neurons and Vipr2^{nAmb} neurons (Figure 2-6). We observed no PLAP immunofluorescence in the DMV or the hypoglossal, suggesting that our injections did not reach these regions. While we did observe PLAP labeling in some neurons around the nucleus ambiguus, none of these neurons were FluoroGold positive, indicating that they do not project peripherally and so should not confound our anterograde tracing studies. These results suggest that the only peripherally-projecting neurons expressing PLAP were nucleus ambiguus neurons.

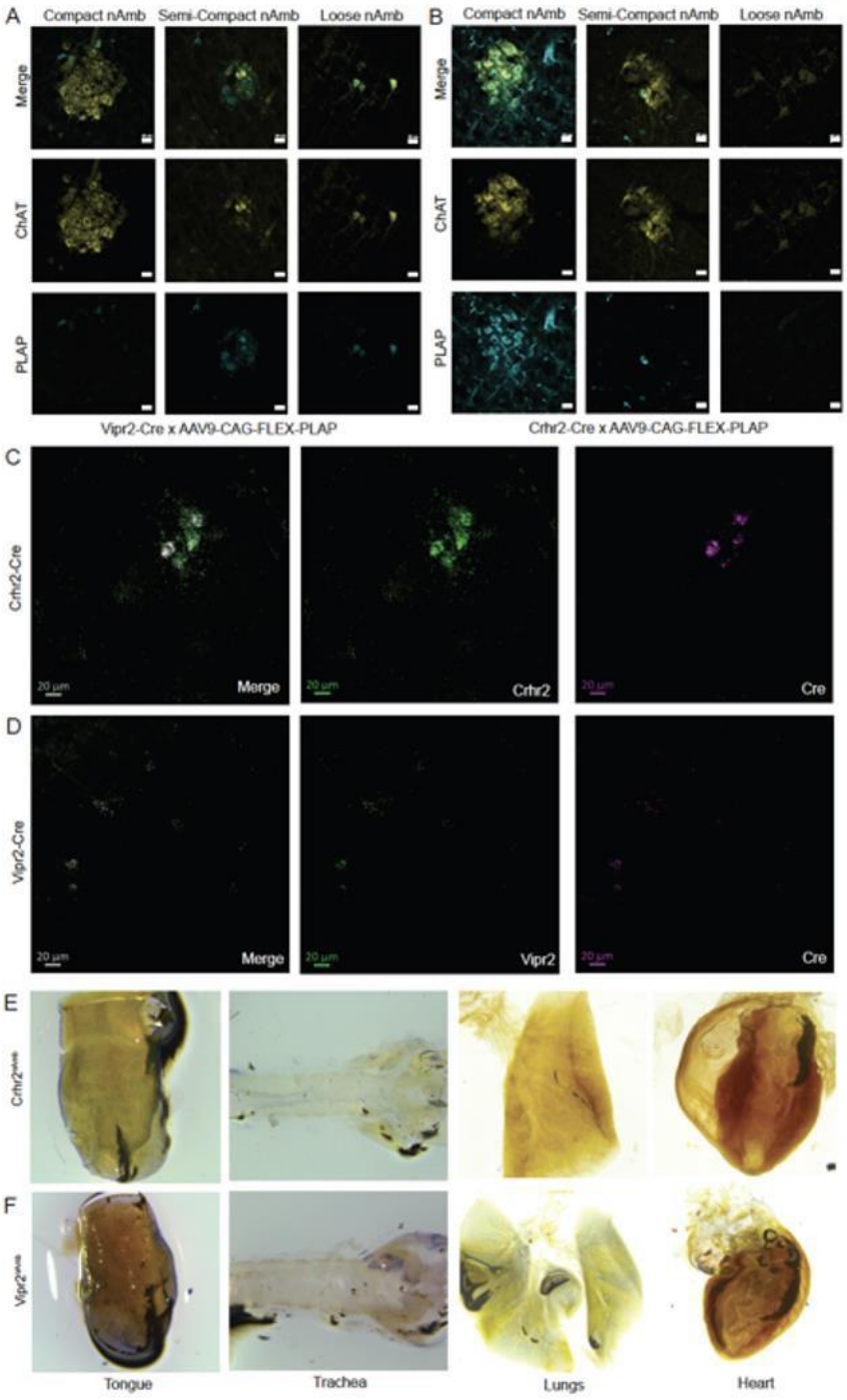

Figure 2-6. Immunofluorescence Images of AAV9-CAG-FLEX-PLAP Expression in Vipr2-Cre and Crhr2-Cre Mouse Lines Validate Infection and Expression; Validation of Crhr2-Cre and Vipr2-Cre Activity; Vipr2^{nAmb} and Crhr2^{nAmb} Innervation of the Tongue, Trachea, Lungs, and Heart

Figure 2-6 Legend

A. Colocalization of ChAT and PLAP immunofluorescence in nAmb neurons after injection of AAV9-CAGFLEX-PLAP into the nAmb of a Vipr2-Cre mouse (n=5 mice).
B. Colocalization of ChAT and PLAP immunofluorescence in nAmb neurons after injection of AAV9-CAGFLEX-PLAP into the nAmb of a Crhr2-Cre mouse (n=5 mice).
C. Co-localization of Cre mRNA and Crhr2 mRNA in the nAmb of Crhr2-Cre mouse by RNA fluorescence in situ hybridization (RNA FISH; image representative of 4 mice; 79 of 82, or 96%, Crhr2+ neurons were also Cre+; no Cre mRNA detected in hindbrain cells that did not express Crhr2).
D. Co-localization of Cre mRNA and Vipr2 mRNA in the nAmb of Vipr2-Cre mouse by RNA fluorescence in situ hybridization (RNA FISH; image representative of 3 mice; 57 of 57 Vipr2+ neurons were also Cre+; no Cre mRNA detected in hindbrain cells that did not express Vipr2).
E. Little to no PLAP stained axons in the tongue, trachea, lungs, and heart of Crhr2-Cre mice following injection of AAV9-CAG-FLEX-PLAP into the nAmb (n=5 mice).
F. Little to no PLAP stained axons in the tongue, trachea, lungs, and heart of Vipr2-Cre mice following injection of AAV9-CAG-FLEX-PLAP into the nAmb (n=5 mice).

We then chromogenically stained and optically cleared cervical tissues to visualize their innervation by Crhr2^{nAmb} and Vipr2^{nAmb} neurons (Figure 2-4). Stained fibers from Crhr2^{nAmb} neurons formed a dense plexus of blue-stained axons and terminations in the cervical and upper esophagus, but few to none were visible in the pharynx, larynx, or trachea. The esophageal Crhr2^{nAmb} fibers formed sparse motor endplates along perpendicular axes, suggesting they innervate both circular and longitudinal muscles (Powley et al., 2013b). In striking contrast, Vipr2^{nAmb} fibers did not visibly innervate the esophagus but did branch extensively in the pharynx, where they formed grape-like clusters of terminals in bands along an axis perpendicular to the muscle fibers, consistent with the structure of pharyngeal nerve fibers in rats (Kobler et al., 1994b).. When we imaged the larynx, we observed stained fibers from Chat^{nAmb} neurons and Vipr2^{nAmb} neurons but not from Crhr2^{nAmb} neurons. Collectively, these results indicate that the Crhr2^{nAmb} neurons selectively innervate the esophagus, whereas Vipr2^{nAmb} neurons selectively innervate the larynx and pharynx.

2.3.4. Activating Crhr2^{nAmb} Neurons Affects Esophageal Motor Activity but not Heart Rate.

Since they selectively innervate the esophagus, we hypothesized that Crhr2^{nAmb} neurons control esophageal motor activity. To investigate this, we used intersectional optogenetics to activate nucleus ambiguus subtypes while imaging motor responses in the esophagus. First, we intersectionally defined Crhr2^{nAmb} neurons and Vipr2^{nAmb} neurons by crossing Crhr2-Cre mice and Vipr2-Cre mice to a novel, knock-in Chat-Flp mouse line, which we first validated by co-localizing Chat mRNA with Flp RNA by RNA FISH (n=3;

121 Chat mRNA+ cells in the nAmb area were also Flp mRNA+, and vice versa; Figure 2-7). Then we bred the Cre::Flp mice to a transgenic intersectional mouse line that expresses Cre- and Flp- dependent CatCh, a calcium-permeable channelrhodopsin2 (Daigle et al., 2018). We used the offspring to optogenetically activate different nucleus ambiguus neuron populations as follows: all nucleus ambiguus neurons using Chat-Cre::Phox2b-Flp::CaTCh mice (Chat::Phox2b::CaTCh), Vipr2^{nAmb} neurons using Vipr2-Cre::Chat-Flp::CaTCh mice (Vipr2::Chat::CaTCh), and Crhr2^{nAmb} neurons using Crhr2-Cre::Chat-Flp::CaTCh mice (Crhr2::Chat::CaTCh). As a negative control, we also included a group of mice that Cre-dependently expressed ChR2 (Ai32 mice) but which were not crossed to a Cre expressing mouse line.

We performed focal photostimulation of the ventral surface of the esophagus in anesthetized, mechanically ventilated mice (Figure 2-7). This approach minimizes the chances of activating non-nAmb neurons because cholinergic nucleus ambiguus neurons are the principal source of motor innervation of the esophagus. Focal stimulation of the esophagus in Crhr2::Chat::CaTCh mice (n=4) produced time-locked movements localized to the site of stimulation that could be reliably identified in video recordings by blinded scorers (Figure 2-7). A similar result was obtained in experiments where all nucleus ambiguus neurons were targeted (Chat::Phox2b::CaTCh; n=3). Conversely, focal stimulation of the esophagus had no visible effect in Vipr2::Chat::CaTCh mice (n=4) or in negative controls (n=2)(Figure 2-7). To assess whether the movements evoked by photostimulation of the esophagus in Crhr2::Chat::CaTCh mice reflected constriction, we measured esophageal pressure during photostimulation with a balloon catheter. We photostimulated both focally in the esophagus and centrally through a fiber optic implanted

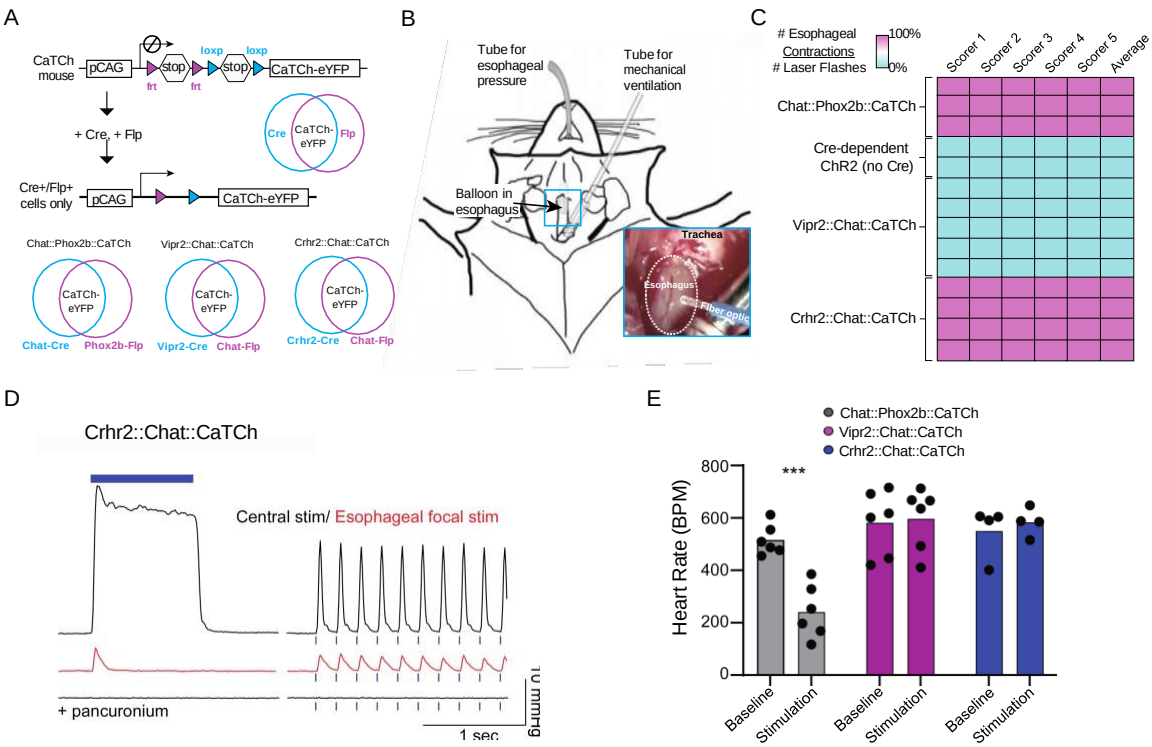

Figure 2-7. Crhr2^{nAmb} Neurons Selectively Control Esophageal Muscles

Figure 2-7 Legend

A. Intersectional optogenetics approach for activating all nAmb neurons, Vipr2^{nAmb} neurons, and Crhr2^{nAmb} neurons. CaTCh-eYFP expression is dependent on the presence of both Cre and Flp recombinases.
B. Schematic of experimental set-up for measuring esophageal function. Mouse is anesthetized and mechanically ventilated to expose the esophagus. A balloon is inserted in the esophagus to measure esophageal pressure and a fiber optic is placed above the esophagus for focal stimulation.
C. Blinded scoring of video data from optogenetic stimulation of esophagus in different genotype groups. Values represent the number of visible muscle contractions divided by the number of laser flashes observed during the video. (n=3-4 mice per genotype, 2 mice for negative control)
D. Representative pressure recordings from balloon pressure transducer in esophagus during photo-stimulation of Crhr2-Cre::Chat-Flp::CaTCh mouse via optical fiber either implanted in nAmb ("central") or placed over esophagus. Esophageal response before and after administration of pancuronium, a competitive inhibitor of nicotinic acetylcholine receptors at the neuromuscular junction.
E. Heart rate before and after photo-stimulation of Chat-Cre::Phox2b-Flp::CaTCh (n=6 mice), Vipr2-Cre::Chat-Flp::CaTCh (n=6 mice), and Crhr2-Cre::Chat-Flp::CaTCh (n=4 mice) mice via nAmb-implanted optical fiber (*** $P<0.001$ for baseline vs stimulation by Sidak's multiple comparison test; $F=[2,26]=8.538$; $P= 0.0014$).

over the nucleus ambiguus in the same mice. With both approaches, photostimulation resulted in abrupt increases in esophageal pressure that were frequency-dependent and time-locked to the pattern of photostimulation, with the effects of central stimulation being more robust (n=6). When the balloon catheter was retracted into the mouth, focal stimulation of the esophagus no longer produced detectable changes in pressure supporting the conclusion that focal stimulation results in contractions that are generated locally within the esophagus. Pressure changes were recorded in the mouth during central stimulation in Crhr2::Chat::CaTCh mice, which may be related to movements in the mouth secondary to strong contractions of the esophagus and/or the central activation of the axons of facial and hypoglossal motor neurons that express CaTCh+ in this mouse line. Pancuronium, a competitive inhibitor of nicotinic acetylcholine receptors, blocked the increases in esophageal pressure that occurred with both central and focal esophageal stimulation of Crhr2::Chat::CaTCh neurons (n=2)(Figure 2-7). These results indicate that Crhr2+, and not Vipr2+, labels cholinergic esophageal motor neurons that control the cervical esophagus through nicotinic receptor signaling.

Since we were unable to visualize nucleus ambiguus projections to the heart with the PLAP method, we assessed the effects of stimulating nucleus ambiguus neurons on heart rate in freely behaving mice instrumented to record EKG. We targeted $Chat^{nAmb}$ neurons (all nAmb neurons, n=6 mice), $Vipr2^{nAmb}$ neurons (n=6 mice), or $Crhr2^{nAmb}$ neurons (n=4 mice) for activation by implanting an optic fiber above the right nucleus ambiguus in the corresponding Cre::Flp::CaTCh lines (Figure 2-8). Stimulating the nucleus ambiguus in Crhr2::Chat::CaTCh or Vipr2::Chat::CaTCh mice resulted in small and variable changes in heart rate that were not different from negative controls, whereas

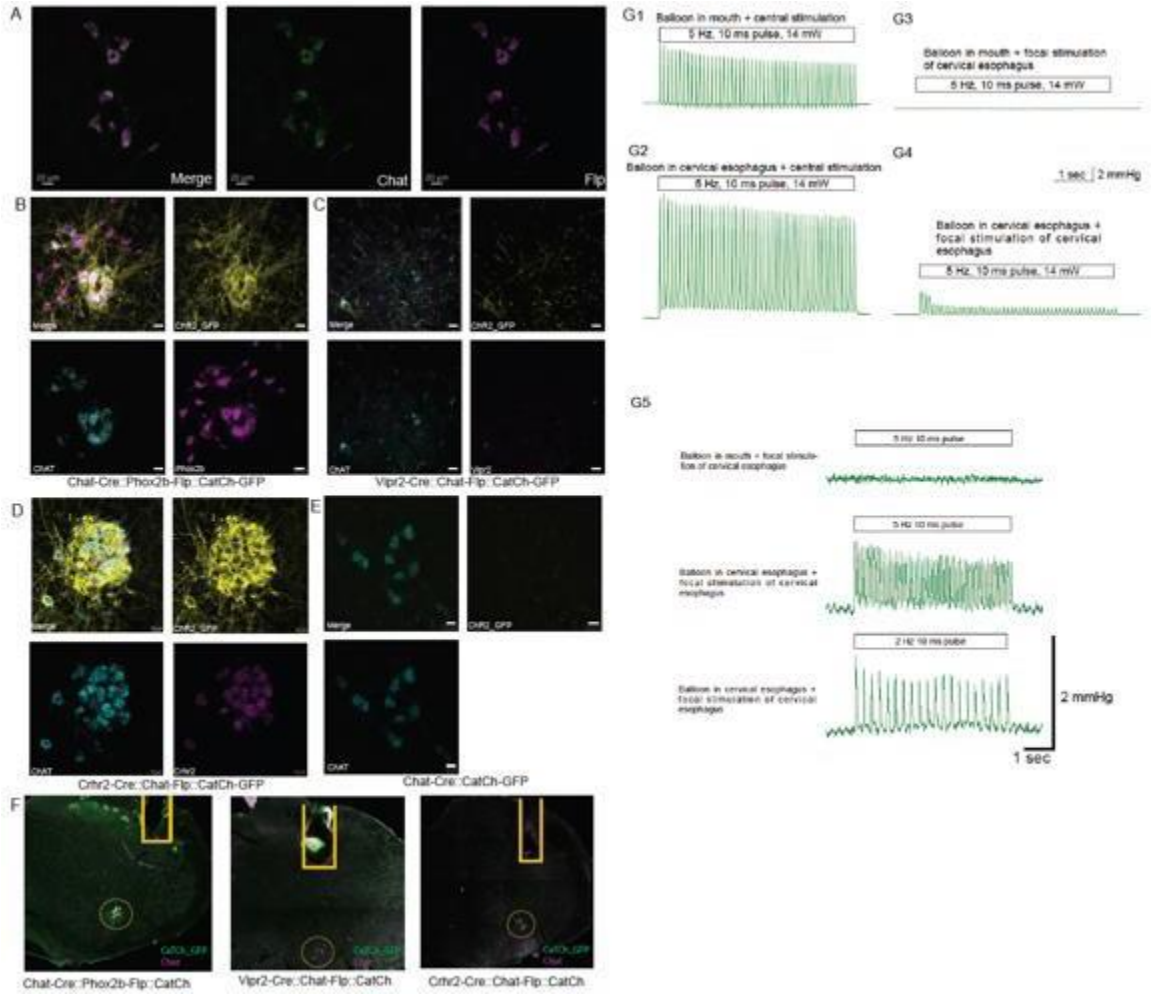

Figure 2-8. Validation of Chat-Flp Expression; Validation of Subtype Specific Cre::Flp::CatCh Mouse Lines and Fiber Implant Locations; Stimulation of Cholinergic Crhr2+ Neurons in the Brain and Esophagus Contracts the Cervical Esophagus.

Figure 2-8 Legend

A. Co-localization of Flp mRNA and Chat mRNA in the nAmb of Chat-Flp mouse by RNA fluorescence in situ hybridization (RNA FISH; image representative of 3 mice; 121 of 121 Chat+ neurons were also Flp+; no Flp mRNA detected in hindbrain cells that did not express Chat.
B. Co-localization of Chat RNA FISH, Phox2b RNA FISH, and eYFP immunofluorescence in Chat-Cre::Phox2b-Flp::CaTCh-eYFP mouse (n=3 mice).
C. Colocalization of Vipr2 RNA FISH, Chat RNA FISH, and eYFP immunofluorescence in Vipr2-Cre::Chat-Flp::CaTCh-eYFP mouse (n=3 mice).
D. Colocalization of Crhr2 RNA FISH, Chat RNA FISH, and eYFP immunofluorescence in Crhr2-Cre::Chat-Flp::CaTCh-eYFP mouse (n=3 mice).
E. Colocalization of Chat RNA FISH and eYFP immunofluorescence in Cre::CaTCh-eYFP mouse. (n=3 mice)
F. Representative images of optic fiber tracts, eYFP and ChAT immunofluorescence from Chat-Cre::Phox2b-Flp::CaTCh-eYFP, Vipr2-Cre::Chat-Flp::CaTCh-eYFP, and Crhr2-Cre::Chat-Flp::CaTCh-eYFP mice used for optogenetic experiments
G. Changes in pressure measured in the mouth and cervical esophagus generated by central and focal stimulation in Crhr2-Cre::Chat-Flp::CaTCh mice. Central stimulation (G1, G2) produced pressure deflections whether the balloon was positioned in the mouth (G1) or cervical esophagus (G2), however the peak amplitude of pressure deviations was the greatest when measured in the esophagus. Focal application of light on the cervical esophagus (G3, G4) produced pressure deviations when the balloon was positioned in the esophagus (G4), but not in the mouth (G3). Focal application of light on the cervical esophagus produces frequency-dependent increases in pressure deviations (G5).

stimulating all Chat^{nAmb} neurons using Chat::Phox2b::CaTCh mice immediately and significantly decreased heart rate by nearly half compared to baseline. The decrease in heart rate observed when activating all nucleus ambiguus neurons (Chat^{nAmb}) is likely due to a nucleus ambiguus neuron subtype which expresses Chat but not Vipr2 or Crhr2 (e.g., Adycap1^{nAmb} neurons). These results suggest Crhr2^{nAmb} and Vipr2^{nAmb} neurons are not cardiovagal preganglionic neurons. Of note, central stimulation produced time-locked whisking and movements localized to the head and neck in all Cre::Flp::CaTCh lines, but not in negative controls (Figure 2-8). The presence of oro-facial motor responses in these experiments suggests that central stimulation activates cranial motor neurons outside of the nucleus ambiguus, specifically in the hypoglossal and facial motor pools. Collectively, our data suggests that the nucleus ambiguus comprises genetically defined neuron subtypes which play distinct physiological roles. Of these neuron subtypes, our results indicate that Crhr2^{nAmb} neurons selectively innervate the esophagus and are capable of contracting esophageal muscles.

2.4 DISCUSSION

The nucleus ambiguus is the primary source of motor input to the larynx, pharynx, and cervical esophagus and of parasympathetic input to the heart, lungs, and airways. Combining single-cell transcriptomics, anterograde tracing, and intersectional optogenetics, our results identify three subtypes of nucleus ambiguus neurons and suggest that one subtype, Crhr2^{nAmb} neurons, are esophageal motor neurons. Crhr2^{nAmb} neurons innervate the esophagus and when activated, reliably contract the esophagus but do not affect heart rate. While previous studies showed that esophageal motor neurons occupy a

distinct subregion of the nucleus ambiguus, this study defines the molecular organization of these motor neurons and links it with their anatomy and function.

The molecular profiles of esophageal motor neurons may reveal insight into their physiology and function. For instance, morphine increases the rate of esophageal peristalsis in humans (Penagini et al., 1996), and our results show the gene encoding the morphine receptor, Oprm1, is highly enriched in the nucleus ambiguus esophageal motor neurons, $Crhr2^{nAmb}$ neurons. The gene expression profile for $Crhr2^{nAmb}$ neurons provided by our study, including many receptors, neuropeptides, and other signaling proteins, can be mined for pharmacological targets to treat diseases such as esophageal motility disorder.

Together with a recent study by Tao and colleagues (Tao et al., 2021), our results support a "labeled line" organization of vagal motor neurons. Tao et al. identifies seven molecular subtypes of vagal motor neurons in the DMV, the major source of parasympathetic input to the gut. Two DMV subtypes specifically innervate the glandular stomach but target neurochemically distinct enteric neurons. These findings raise the possibility that the functional units of the DMV (Huang et al., 1993) are genetically defined. Our study suggests a similar organization of the nucleus ambiguus, another vagal motor nucleus. Interestingly, genetic coding of cellular function is also true of vagal sensory neurons, which show a clear correspondence between molecular subtype and physiological role (Bai et al., 2019; Borgmann et al., 2021; Chang et al., 2015; Kupari et al., 2019; Prescott et al., 2020; Williams et al., 2016). Further, sympathetic preganglionic neurons in the spinal cord comprise transcriptionally diverse subtypes as well (Blum et al., 2021), raising the possibility that functionality may be genetically encoded throughout the autonomic nervous system.

We did not comprehensively assess the projections and function of the nucleus ambiguus populations marked by Vipr2 and Adcyap1 expression. Vipr2 appears to mark special visceral efferent neurons that innervate the pharynx and the larynx based on the distribution of Vipr2 in the nucleus ambiguus, their expression of Calca, and projections to pharyngeal and laryngeal muscles. The function of the third nucleus ambiguus population marked by Adcyap1 expression is less clear. As these neurons are molecularly distinct from the Crhr2^{nAmb} neurons and Vipr2^{nAmb} neurons, we speculate that these Adcyap1^{nAmb} neurons are parasympathetic, potentially cardiovagal preganglionic neurons. In guinea pig, cholinergic preganglionic axons in the cardiac ganglia contain PACAP (Calupca et al., 2000), the product of the Adcyap1 gene. Furthermore, PACAP activates parasympathetic cardiac neurons via the PAC1 receptor and causes bradycardia (Seebeck et al., 1996). More work is needed to establish the functional roles of the Vipr2^{nAmb} neurons and Adcyap1^{nAmb} neurons.

Our study also does not address the role of the DMV in esophageal function. Comprehensive tracing studies in rat indicate the innervation of the cervical esophagus originates almost entirely from the nucleus ambiguus (Bieger and Hopkins, 1987; Lee et al., 1992), whereas the DMV innervates the lower esophageal sphincter (Lang, 2009). Our data indicate that this is also true in mouse, as we observed projections from cholinergic DMV neurons to the stomach but not the cervical esophagus (Figures 3.2 & 3.3). Crhr2 was also not identified as a differentially expressed gene in Tao et al. and is not prominently expressed in the DMV based on Allen Mouse Brain Atlas RNA in situ hybridization data (Lein et al., 2007). Hence, the possibility that Crhr2 marks DMV esophageal motor neurons is limited. Outside of the nucleus ambiguus, Vipr2 and Crhr2 are expressed by other motor

neurons, including those controlling facial and tongue muscles. Therefore, it is likely that only within the nucleus ambiguus are these markers specific to neurons innervating the upper airways and cervical esophagus.

Our study raises several questions for further investigation. For instance, what is the physiological role of Crhr2^{nAmb} neurons? Our results indicate that they are capable of contracting esophageal muscle through nicotinic receptor signaling - does this represent physiological control, and is it necessary for esophageal function? Also, are all Crhr2^{nAmb} neurons capable of contracting the esophagus, or just a subset? Our sNuc-seq analysis relied on 145 nucleus ambiguus neurons, or only ~15% of the neurons present in one hemisphere of the adult mouse nucleus ambiguus (Sturrock, 1990). While our RNA FISH analysis shows that 92% of peripherally-projecting nucleus ambiguus neurons express Crhr2, Vipr2, and/or Adcyap1, our sNuc-seq analysis may underestimate the true diversity of neuron subtypes in the nucleus ambiguus. For instance, though our anterograde tracing data show that Crhr2^{nAmb} neurons innervate the esophagus, Crhr2^{nAmb} neurons may comprise subtypes, one or more of which could be esophageal motor neurons.

Three limitations to our study are noteworthy. First, our sNuc-seq analysis includes only male mice. Both males and females were used in our other studies, including the FISH validation of Crhr2^{nAmb} and Vipr2^{nAmb} subtypes, suggesting that the same subtypes present in male nucleus ambiguus are also present in female nucleus ambiguus. However, our results cannot exclude the possibility that additional neuron subtypes exist in the female nucleus ambiguus.

A second limitation is that our functional data relies on targeting neurons in the nucleus ambiguus using the intersection of genes which are not restricted to the nucleus

ambiguus. Vipr2 and to a lesser extent Crhr2, is expressed in cholinergic neurons supplying the facial and hypoglossal nerves. Consistent with this, movements of the tongue and whiskers were clearly visible during central optogenetic stimulation targeting the cell bodies in the nucleus ambiguus regardless of the particular combination of neurons targeted (e.g., Crhr2::Chat::CaTCh or Vipr2::Chat::CaTCh). During central stimulation of $Crhr2^{nAmb}$ neurons, the stimulation of neurons that contract the tongue in particular confounds interpretation of esophageal pressure changes with this approach. However, the effects of focal stimulation reflect changes that are generated only by axons in the cervical esophagus. Based on previous studies, these cholinergic axons principally arise from esophageal motor neurons in the nucleus ambiguus (Sang and Young, 1998). Hence, focal stimulation of the cervical esophagus provides a reasonably selective approach for identifying neurons with a motor function in this region.

A third limitation is that our results do not rule out the possibility that photo-activating the esophagus in Crhr2::Chat::CaTCh and Chat::Phox2b::CaTCh mice contracted the esophagus through indirect effects on other tissues. However, it is unlikely the esophageal contractions were secondary to effects on tongue muscles since the tongue is not known to be innervated by the nucleus ambiguus (Jean, 2001b; Stanek et al., 2014) and since our anterograde tracing with PLAP failed to detect tongue innervation by Chat nucleus ambiguus neurons (Figure 3-4). Also, it is unlikely that the esophageal contractions we observed were due to effects on the lower esophageal sphincter, since studies in ferrets have demonstrated that changes in lower esophageal sphincter pressure do not trigger esophageal contractions (Abrahams et al., 2002). Direct activation of esophageal neuromuscular circuits is therefore the most parsimonious explanation for the esophageal

contractions we observed when photo-stimulating esophagus in Crhr2::Chat::CaTCh and Chat::Phox2b::CaTCh mice.

Overall, our study provides three major advances to understanding the neural control of esophageal function: (1) identifies the primary motor neurons for the esophagus molecularly, anatomically, and functionally; (2) reveals a genetic logic for the functional organization of the nucleus ambiguus; and (3) comprehensively characterizes the gene expression profile of esophageal motor neurons, which can be mined for potential drug targets to treat swallowing disorders.

2.5 METHODS

2.5.1 Chat-p2a-Flp Mouse

Chat-p2a-Flp mice were generated using Easi-CRISPR method (Miura et al., 2018). Briefly, a single-stranded DNA (ssDNA) donor containing the p2a-Flp cassette, flanked by 100-base homology arms both up- and down-stream of the *Chat* stop codon was designed. A single guide RNA (sgRNA)(sequence: 5'-CCCACTAGCCAATGTCCTAC-3') was designed to induce the cut in the genome. For pronuclear injection, ssDNA donor, sgRNA and *Cas9* protein were co-injected into mouse fertilized eggs of FVB strain. Live-born pups were screened by PCR reactions, and the positives were then sequenced to confirm the correct insertion.

2.5.2 Single-Nuclei RNA-Sequencing

The ventrolateral medulla of five male Chat-Cre mice were injected with a Cre-dependent reporter virus, AAV-DIO-H2b-mCherry. Four weeks later, mice were rapidly

decapitated for brain extraction to avoid stress related changes in nuclear mRNA. Following immediate brain extraction, 1 mm thick coronal sections of hindbrain through the nAmb's full rostral-caudal extent (Bregma -6.5 mm to -8.0 mm) were cut and immersed in ice-cold RNA-later (Qiagen catalog # 76106). After at least 30 minutes in ice-cold RNA-later, the nucleus ambiguus was visualized under a fluorescence stereomicroscope (Zeiss Discovery V8) and dissected, then stored in RNA-later overnight at 4°C. On the next day, nucleus ambiguus tissue was homogenized and purified by density-gradient centrifugation into a single-nuclei suspension as previously described (Habib et al., 2016; Todd et al., 2020). The single-nuclei suspension was sorted by FACS to isolate one H2b-mCherry+ nucleus per well of three 96-well plates, which were then centrifuged at 2,500rcf, frozen on dry ice, and stored at -80°C until use. After purifying the RNA by RNA-clean SPRI reagents (1.5x ratio of SPRI to sample), cDNA libraries were generated from polyadenylated mRNA of each sample using Smart-Seq2 (Picelli et al., 2014) and then sequenced by Illumina Next-Seq 500. Reads were demultiplexed by bcl2fastq2 v2.20.0 (Illumina) and aligned to the mouse genome by STAR v2.6.1 (Dobin et al., 2013). Duplicates were removed with Picard Tools v2.18.21. Aligned reads were processed into a digital gene expression (DGE) file with Drop-Seq Tools v2.3.0 and tagged using ''GENCODE_M16_PRI'' annotation. Since the sNuc-seq protocol does not produce true UMIs, we considered any unique read (i.e., non-duplicated) as a unique "UMI-tagged" read for the Drop-Seq pipeline. An R software package for single-cell genomics analysis, Seurat v4.0 (Hao et al., 2021), was used to filter, scale, and normalize the data, then perform dimensionality reduction with principal component (PC) analysis on the top 2,000 most variable genes, cell clustering on the top 6 PCs, and differential expression analysis using

Wilcoxon Rank Sum test and default settings, as previously described (Tao et al., 2021; Todd et al., 2020). Low quality samples (<2000 genes detected per nucleus) were excluded from this analysis. Transcription factor and receptor gene lists were derived from the Panther v16.0 protein and gene classification site, http://www.pantherdb.org/ (Mi et al., 2021).

2.5.3 Fluorescence In Situ Hybridization (FISH)

FISH experiments were performed on brain tissue from mice that received one intraperitoneal injection of 2% Fluorogold (Fluorochrome) a minimum of 5 days prior to euthanasia. Mice were terminally anesthetized with ketamine (20 mg/kg) and xylazine (2 mg/kg) diluted in PBS, followed by transcardial perfusion with 0.9% saline plus heparin and 4% paraformaldehyde (Thomas Scientific). Brains were extracted and post-fixed for 24 hours at 4°C. Following fixation, brains were sectioned coronally at 30 - 35 um thickness on a vibratome (Leica). The day before FISH, the sections were rinsed in PBS and then mounted on slides (Fisher) and left to dry overnight. An ImmEdge Hydrophobic Barrier Pen was used to draw a barrier around the sections. The sections were then incubated in Protease IV in a HybEZ II Oven for 30 minutes at 40°C, followed by incubation with target probes (*Chat*, *Vipr2*, *Crhr2*, *Calca*, *Adcyap1*, and *Phox2b*) for 2 hours at 40°C. Slides were then treated with AMP 1-3, HRP-C1, HRP-C2, HRP-C3, and HRP Blocker for 15-30 minutes at 40°C, as previously described (Wang et al., 2012). FITC, Cy3, and Cy5 (Perkin Elmer) were used for probe visualization. Fluorogold was either imaged in its native state or visualized using immunofluorescence with a rabbit anti-Fluorogold primary antibody (Fluorochrome, 1:5000) overnight and a donkey anti-rabbit

647 secondary antibody (Thermo Scientific Cat# A31573, Lot# 2083195, 1:1000) for 2 - 4 hours. Images were taken using a confocal microscope (Zeiss). Cell distributions were mapped in Neurolucida software (version 11, MBF Bioscience) using an AxioImager M2 (Carl Zeiss). Composite maps of nAmb neurons reflect cells in 3 hemi-sections of the brainstem spanning 270 um in the rostro-caudal axis overlaid on a single wireframe representing the three levels of the nAmb. The three levels of the NAmb correspond to the following bregma levels according to Paxinos and Franklin (2013) (Compact nAmb: -6.47 mm through -6.75 mm from bregma, Intermediate NAmb: -6.83 mm through -7.10mm from bregma, loose nAmb: -7.19 mm through -7.46 mm from bregma).

2.5.4 Anterograde Tracing Viral Injections

Mice were anesthetized with ketamine (20 mg/kg) and xylazine (2 mg/kg) diluted in PBS and positioned into a stereotaxic apparatus (Kopf). A pulled glass micropipette was used for stereotaxic injections of an adeno-associated virus vector, AAV9-CAG-FLEX-PLAP (Prescott et al., 2020), a gift of Dr. Stephen Liberles (Harvard Medical School, Howard Hughes Medical Institute), using the following stereotaxic coordinates for the nucleus ambiguus: anterior/posterior -2.1, -2.4, -2.7 mm, lateral/medial +/- 1.3 mm, and dorsal/ventral -5.8 mm, from lambda; and anterior/posterior -0.1 mm, lateral/medial +/- 1.3 mm, and dorsal/ventral -0.1, -1.3 mm, from the calamus scriptorius. Following local anesthetization with bupivacaine, virus was injected (200 nl/injection, 2-3 injections/side) using a Nanoject III system. This injection strategy was designed to fully cover the nucleus ambiguus, not to restrict viral infection to only nucleus ambiguus neurons. The pipette was removed 3-5 minutes after injections, followed by wound closure using sutures or surgical

wound glue (Vetbond). Meloxicam SR (5 mg/kg; sustained release, SR) was injected subcutaneously for post-operative analgesia.

2.5.5 Placental Alkaline Phosphatase Staining

Following 3-4 weeks after AAV9-CAG-FLEX-PLAP injection, mice were terminally anesthetized with ketamine (20 mg/kg) and xylazine (2 mg/kg) diluted in PBS, followed by transcardial perfusion with 0.9% saline plus heparin then 4% paraformaldehyde (Thomas Scientific). The brains, esophagus, trachea, larynx, and lungs were collected and post-fixed for 24 hrs at 4°C. Following fixation, brains were sectioned coronally at 30 or 35 um thickness on a vibratome (Leica). A single series of sections per animal was used in histological studies to confirm injection site and PLAP expression. All subjects determined to be surgical "misses" based on little or absent reporter expression were excluded from analyses. The esophagus, lungs, upper airways, heart, and tongue were washed three times for 1 hour at room temperature in PBS, followed by incubation in alkaline phosphatase (AP) buffer (0.1 M Tris HCl pH 9.5, 0.1 M NaCl, 50 mM MgCl2, 0.1% Tween 20, 5 mM tetramisole-HCl) for two hours at 70 °C. Afterward, the samples were equilibrated to room temperature and then washed twice in AP buffer. AP activity was visualized with NCT/BCIP solution (ThermoFisher Scientific 34042) and stained samples were rinsed in AP buffer for 15 min, post-fixed in 4% PFA for 1 hr, and washed in PBS. Samples were then dehydrated through a series of ethanol washes (15% - 100%) and cleared using a 1:2 mixture of benzyl alcohol (Sigma-Aldrich 402834-500ML) and benzyl benzoate (Sigma-Aldrich B6630-1L). Whole mount images were taken using a

brightfield stereomicroscope (Leica M205 FCA Stereomicroscope with color camera) and fluorescence microscope (Echo Revolve).

2.5.6 Optogenetic Physiology

Cre-expressing mouse lines were crossed to Chat-Flp or Phox2b-Flp mouse lines to generate Cre::Flp lines, which were then crossed to transgenic mice that express eYFP tagged calcium-permeable channelrhodopsin 2 (CaTCh) only after recombination by both Cre and Flp recombinases. Mice from these Cre::Flp::CaTCh lines were implanted with an optical fiber over the nucleus ambiguus.

Optical fibers for central stimulation and headsets to record electrocardiogram (ECG) were implanted under anesthetized with ketamine (150 mg/kg) and dexmedetomidine (1 mg/kg). Depth of anesthesia was assessed by absence of the corneal and hind-paw withdrawal reflex. Body temperature was maintained at 37.2 ± 0.5 °C with a servo-controlled temperature pad (TC-1000; CWE). Following confirmation of anesthesia, mice were prepped for surgery, positioned in a stereotaxic headframe, and the local anesthetic, Bupivacaine (50 ul of 5 mg/ml), was injected at surgical sites. The tissue overlying the dorsal surface of the skull was retracted and the surface of the skull prepped for headset and optical fiber implants.

EKG headsets were constructed from 4-pin miniature connectors soldered to 2 lengths of Teflon-coated multi-strand stainless steel wire (AM-systems) for positive and negative leads and a stainless steel screw implanted in the skull for the ground. The screw was implanted above the frontal cortex and the leads were tunneled subcutaneously to opposing locations near the base of the ribcage. An optical fiber cannula constructed

(200um 0.39NA fiber, Thorlabs) was implanted to stimulated cell bodies in the nAmb neurons using the following coordinates from Lambda: Anterior/posterior: -2.1 mm, medial/lateral: +1.3 mm, dorsal/ventral: -5.0 mm for Crhr2-Cre::Chat-Flp::CaTCh mice. Fibers were only implanted on the right side of the brain. The same coordinates were used for Vipr2-Cre::Chat-Flp::CaTCh mice, but at a 10 degree angle to access these neurons, which are found in the caudal nAmb. The fiber and ECG headset was secured to the skull with dental cement and wounds were closed with sutures and surgical glue. Mice were given ketoprofen (5 mg/kg) for 3 days after surgery and allowed to recover for a minimum of 5 days before optogenetic physiology experiments.

To assess the cardiac effects of stimulating nucleus ambiguus neurons without anesthesia, mice were scuffed to connect the ECG head set and implanted fiber optic cannula to an amplifier and laser respectively. After a period of habituation to the recording set-up, stimulation was performed with a diode laser (473 nm; LaserGlow) controlled by Spike 2 software (CED). ECG (gain: 2K, band pass filter: 10-1000 Hz) signal was acquired (sampling rate: 1K) and heart rate calculated using Spike 2 software. Stimulation consisted of a 10 s period of stimulation at 10 Hz (5 ms pulse) with a power output at the tip of the connecting fiber of 12 mW.

To assess the esophageal effects of nucleus ambiguus stimulation, mice were anaesthetized with ketamine (150 mg/kg) and dexmedetomidine (1 mg/kg). Depth of anesthesia was assessed by absence of the corneal and hind-paw withdrawal reflex. Additional anesthetic was administered as necessary (10% of the original dose, intraperitoneal). Body temperature was maintained at 37.2 ± 0.5 °C with a servo-controlled temperature pad (TC-1000; CWE). Following induction of anesthesia, the fiber optic was

connected to the laser, and mice were then placed in a stereotaxic frame in the supine position. A midline incision followed by blunt dissection and retraction of overlying tissue was performed to expose the trachea. A tracheostomy was performed, and mice were mechanically ventilated with pure oxygen (MiniVent type 845; Hugo-Sachs Electronik). Mice were ventilated at volume of 150-250 uL and rate between 150-250 breaths/min. Mice were hyperventilated to eliminate spontaneous breathing efforts. The trachea was bisected and reflected exposing the anterior surface of the esophagus. Focal stimulation of the exposed surface of the esophagus was conducted using a multimode 200um fiber (0.39NA, Thorlabs) positioned using a micromanipulator. Stimulation was performed with a diode laser (473 nm; LaserGlow) controlled by Spike 2 software (CED). For video imaging of contractions with focal stimulation of the esophagus, 10 ms pulses of laser light (12 mW measured at the tip) was delivered at 2 or 5 Hz for between 5 - 10 s. Video was acquired with a high-speed color CMOS Camera mounted to the operating microscope. Videos were acquired at a framerate of 50-60 Hz. Video scoring was performed by scorers blinded to the genotype of the mice. Scorers were first trained to identify light-evoked contractions and then instructed to count contractions in each video. As the number of light pulses and thus contractions varied across individual videos, scorer accuracy is represented as the number of observed contractions as a percentage of laser flashes for each video.

Contractile force in the esophagus during optogenetic stimulation was assessed during cell-body stimulation of Crhr2^{nAmb} neurons. Mice were anesthetized as described above. Following induction of anesthesia, a fiber optic was connected to an implanted fiber optic cannula, and mice were then placed in a stereotaxic frame in the supine position. Mice were ventilated as described above. To measure contractile force in the esophagus, a

miniature latex balloon (Harvard Apparatus) and catheter filled with saline was advanced through the mouth into the upper esophagus. Placement was visually confirmed under an operating microscope. The balloon was connected to a pressure transducer and amplifier and filter (gain: 5K, band pass filter: 0.1-50 Hz, CWE inc.) The balloon was inflated with saline to a pressure between 20-50 mmHg during periods of stimulation. Stimulation was performed with a diode laser (473 nm; LaserGlow) controlled by Spike 2 software (CED). Stimulation consisted of a single 1 s pulse or a 10 s of stimulation at 2-10 Hz (5 ms pulse).

2.6 ATTRIBUTIONS

The majority of this chapter (text and figures) were taken from Coverdell TC, Abraham-Fan RJ, Abbott SBG, Campbell JN. Genetic encoding of an esophageal motor circuit. Cell Rep 2022 June 14.

2.7 ACKNOWLEDGMENTS

We gratefully acknowledge Patrice G. Guyenet and Ruth Stornetta for thoughtful discussion and feedback on the experimental design and manuscript; Bradford Lowell for the Chat-p2a-Flp mouse; Sara Prescott and Stephen Liberles for the AAV-FLEX-PLAP and histology method; Nathanial Heintz and Todd Anthony for the Crfr2a-EGFPCre transgenic mice; Patrice G. Guyenet and Hui Zong for co-acquisition of pilot funding; Ruth Stornetta for training in microscopy and Neurolucida; Daniel Stornetta for training in the RNAscope method; and Natalie Schiavone, Virginia Owen Trinkle, Veronica Gutierrez, Maisie Crook, and Zongfang Yang for technical support. We also acknowledge these core facilities: ICCB-Longwood Screening Facility at Harvard Medical School; the Bauer Core

Facility at Harvard University; and the Boston Nutrition Obesity Research Center Functional Genomics and Bioinformatics Core and Transgenic Mouse Core. Funding for this study was provided by a University of Virginia 3 Cavaliers award to J.N.C., Patrice G. Guyenet, and Hui Zong; NIH R01 HL148004to S.B.G.A.; NIH T32 GM007055 and NIH F31 HL158187 to T.C.C.; and a Pathway to Stop Diabetes Initiator Award 1-18-INI-14, NIH R01 HL153916, pilot grant funding, and transgenic core service from the Boston Nutrition Obesity Research Center (NIH grant no. P30 DK046200) and the Boston Area Diabetes Endocrinology Research Center (BADERC; NIH, grant no. P30 DK057521) to J.N.C.

2.8 AUTHOR CONTRIBUTIONS

T.C.C., S.B.G.A., and J.N.C. designed the experiments. J.N.C. generated the sNuc-seq data and T.C.C. analyzed it. T.C.C. performed the FISH and anterograde tracing studies. T.C.C. and S.B.G.A. performed the optogenetic studies. C.W. designed the Chat-p2a-Flp mouse. T.C.C. and R.-J.A.-F. imaged the anterograde tracing of organs. T.C.C., S.B.G.A., and J.N.C. prepared the figures. T.C.C., S.B.G.A., and J.N.C. wrote the manuscript, with input from all of the authors.

CHAPTER 3. GENETIC ENCODING OF CARDIOVAGAL NUCLEUS AMBIGUUS NEURONS

3.1 SUMMARY

Heart rate is controlled by the interplay of the parasympathetic and sympathetic nervous systems. Parasympathetic signaling to the heart reduces heart rate at rest and during cardiac reflexes such as the baroreflex, respiratory sinus arrythmia, and the diving reflex. The nucleus ambiguus (nAmb) is a primary source of parasympathetic control of heart rate. In addition to housing parasympathetic pre-ganglionic neurons that project to the heart and lungs, this nucleus also contains upper airway and esophagus motor neurons that project to the pharynx, larynx, and esophagus. We examine nucleus ambiguus neurons based on their genome-wide expression profiles, efferent circuitry, and ability to control heart rate. Our single-cell RNA sequencing analysis previously predicted three molecularly distinct nucleus ambiguus neuron subtypes and annotated them by subtype-specific marker genes: *Crhr2*, *Vipr2*, and *Npy2r*. Mapping the axon projections of nucleus ambiguus neuron subtypes reveals that the subtype marked by *Npy2r* innervates the heart, raising the possibility that they control heart rate. Accordingly, we find that optogenetic stimulation of cholinergic Npy2r+ neurons in the nucleus ambiguus reduces heart rate. Our previous studies have shown that the Crhr2^{nAmb} neurons project to and control esophageal function, whereas the Vipr2^{nAmb} neurons innervate the larynx and pharynx. Furthermore, optogenetic activation of both Vipr2^{nAmb} and Crhr2^{nAmb} subtypes results in no change in heart rate, thus ruling out the possibility that they control heart rate. Together, these results reveal a genetically defined circuit for parasympathetic control of heart rate.

3.2 INTRODUCTION

Heart rate is reduced by signaling from cardiovagal preganglionic neurons (CVNs), which reside primarily in the nucleus ambiguus, a hindbrain region that also provides motor input to the esophagus, pharynx, and larynx (Gourine et al., 2016). Cardiovagal preganglionic neurons in the nucleus ambiguus project their axons through the vagus nerve to cardiac ganglia, where they synapse on intrinsic cardiac neurons to activate cardiac neurons and suppress sympathetic input to the same cardiac neurons (Fisher et al., 2004; Gourine et al., 2016; Rajendran et al., 2018).

Dysfunction of the parasympathetic nervous system contributes to heart arrhythmias and heart failure (Mendelowitz, 1996b). Vagal nerve stimulation, an approach that activates the parasympathetic circuits between the brain and the heart, is currently undergoing clinical evaluation for the treatment of heart conditions (Garamendi-Ruiz and Gomez-Esteban, 2019). Clinical studies of vagal nerve stimulation in heart failure have reported significant improvements in quality-of-life measures and cardiac performance metrics (Garamendi-Ruiz and Gomez-Esteban, 2019). However, these studies have been limited due to off target effects and risk of infection during surgery. Other attempts to increase vagal tone have involved enhancing cholinergic signaling or activating cholinergic receptors (Liu et al., 2019), but these approaches also have unwanted side effects. More specific approaches to increasing cardiovagal tone would have fewer side effects. However, few therapeutic targets have been identified since the molecular profile of CVNs is largely uncharacterized.

Neuron subtypes can be identified by their differentially expressed genes, which can then be utilized to genetically access each subtype. To identify nucleus ambiguus

neuron subtypes in mice, we previously profiled their genome-wide mRNA expression by single-nuclei RNA sequencing (Coverdell et al., 2022; Habib et al., 2016). Our analysis uncovered three nucleus ambiguus subtypes (Crhr2^{nAmb}, Vipr2^{nAmb}, and Npy2r^{nAmb}), two of which we previously identified as projecting to the esophagus, pharynx, and larynx to control respective functions related to these organs (Coverdell et al., 2022).

Interestingly, the third nucleus ambiguus subtype, Npy2r^{nAmb} neurons, expressed markers that have been previously associated with cardiovagal neurons. One of these genes, pituitary adenylate cyclase activating polypeptide (gene name: *Adcyap1*), which encodes the protein PACAP, has been previously shown to mark cholinergic axons innervating guinea pig cardiac ganglia to modulate cardiac neuron excitability and is a potential marker of cardiovagal neurons within the nucleus ambiguus (Calupca et al., 2000). Additionally, two other receptors that have been previously demonstrated to play a role in modulating parasympathetic activity to the heart were also highly expressed in the third nucleus ambiguus cluster: neuropeptide Y Y2 receptor (gene name: *Npy2r*) and TRH receptors (gene name: *Trhr*) (Smith-White et al., 2002). Thus, we selected the markers *Adcyap1* and *Npy2r* to genetically access this third nucleus ambiguus subtype. Of note, we did not observe expression of the gene *Calca*, which encodes calcitonin gene-related peptide (CGRP), in the Npy2r^{nAmb} neurons. CGRP is enriched in esophageal and airway motor neurons in mammals (Lee et al., 1992; McWilliam et al., 1989). Overall, our single nuclei RNA-sequencing analysis uncovered three nucleus ambiguus neuron subtypes and suggests that the third subtype, marked by *Npy2r* and *Adcyap1*, may be cardiovagal preganglionic neurons projecting to the heart to reduce heart rate.

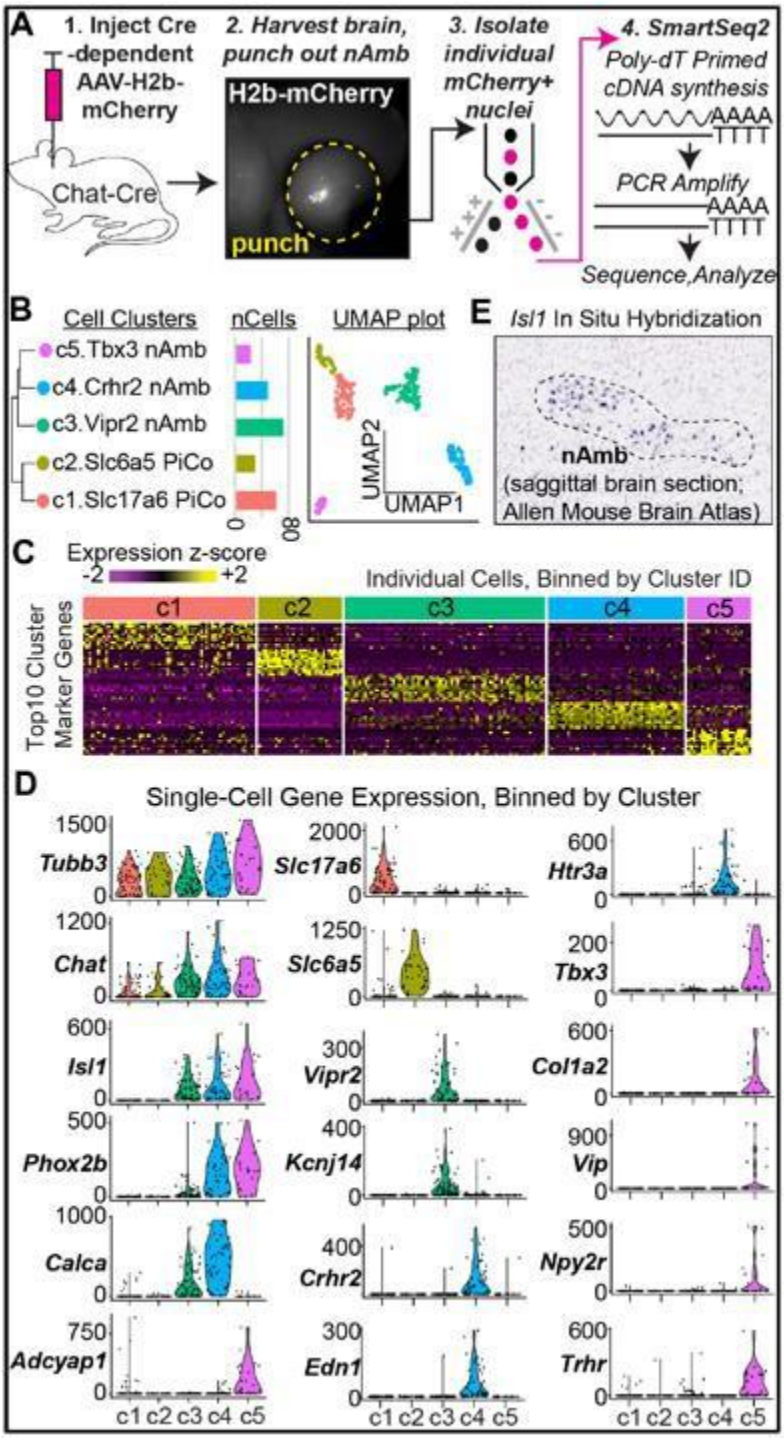

Figure 3-1. Molecular Identification of CVN Markers

Figure 3-1 Legend

A. Schematic of single-nuclei RNA sequencing (sNuc-seq) workflow
B. Relatedness of neuron clusters, number of cells per cluster, and UMAP (uniform manifold approximation and projection) visualization of clustered data
C. Single-cell expression heatmap of top marker genes for each cluster.
D. Violin plots of nAmb regional genes (Chat, Phox2b, Isl1) and cluster marker genes.
E. Isl1 in situ hybridization data from the Allen Brain Atlas showing the different subregions of the nAmb

We now explore the identity of the third subtype in control over heart rate. Targeting this nucleus ambiguus subtype with intersectional genetic approaches, we then test our hypothesis by (1) mapping the axon projections of the subtype to the heart and (2) optogenetically activating the subtype in vivo to assess its control over heart rate. Our results uncovered a molecularly distinct subtype of nucleus ambiguus neurons that innervates the heart. Activating this subtype immediately and profoundly decreased heart rate. Together, our results identify cardiovagal preganglionic neurons by their gene expression, anatomy, and function.

3.3 RESULTS

3.3.1 Npy2r and Adcyap1 Transcripts Mark Nucleus Ambiguus Neurons

To determine the locations of Npy2r+ neurons and Adcyap1+ neurons in the nucleus ambiguus, we performed RNA fluorescence in situ hybridization (FISH) for Npy2r, Adcyap1, and ChAT mRNA transcripts in the medulla oblongata of wild type mice. We previously labeled all nucleus ambiguus neurons with systemically administered Fluorogold and found that all Fluorogold-labeled nucleus ambiguus neurons contained ChAT mRNA (Coverdell et al., 2022), thus showing that all peripherally-projecting nucleus ambiguus neurons are cholinergic and validating our choice of ChAT to target nucleus ambiguus neurons for sequencing.

To validate our sequencing results and map the anatomical distribution of Adcyap1^{nAmb} and Npy2r^{nAmb} neurons, we used FISH to visualize Adcyap1, Npy2r, and Chat mRNA in nucleus ambiguus neurons, as labeled by Fluorogold. Our previous studies

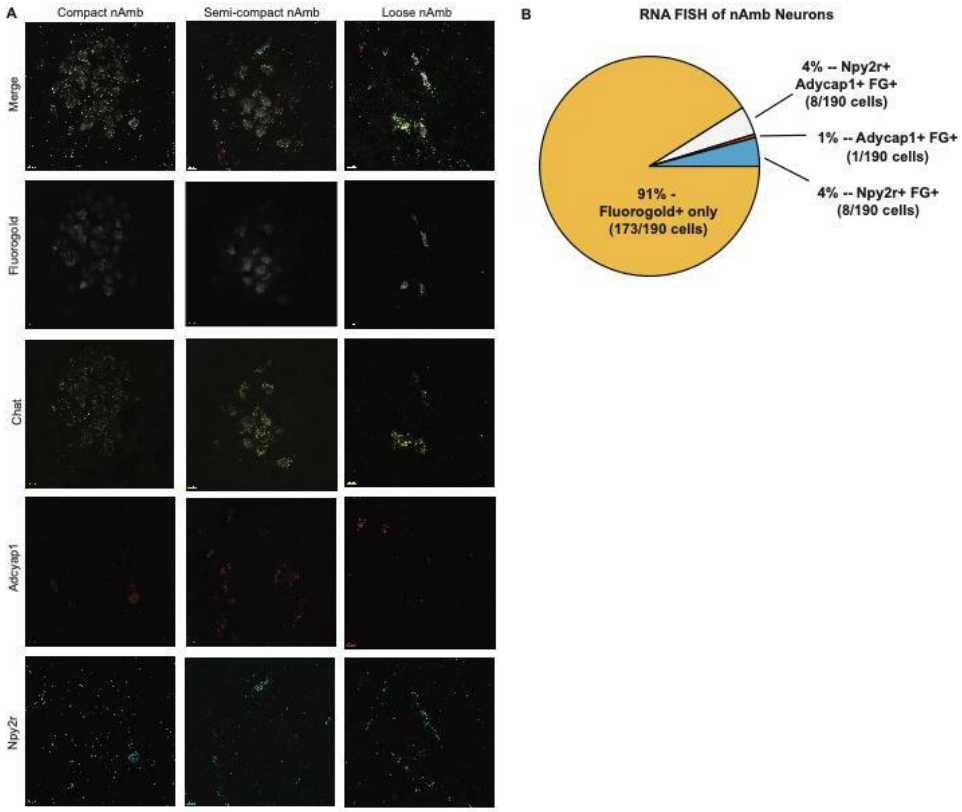

Figure 3-2. Adcyap1 and Npy2r Transcripts Mark Nucleus Ambiguus Neurons

Figure 3-2. Legend

A. Fluorescence in situ hybridization (FISH) of Chat, Adcyap1, and Npy2r transcripts in the compact, semi-compact, and loose nAmb, co-localized with systemically administered FluoroGold (n = 2 mice). Scale bar, 20 mm.
B. Breakdown of Npy2r and Adcyap1 neurons as a part of the entire nucleus ambiguus.

showed that the other two nucleus ambiguus subtypes marked by *Crhr2* and *Vipr2* were mostly distinct from the Adcyap1^{nAmb} neurons (Coverdell et al., 2022). As expected, we observed that the majority of nucleus ambiguus neurons had little to no expression of *Adcyap1* or *Npy2r* (173 of 190 (91%) of nucleus ambiguus neurons are *Adcyap1* and *Npy2r* negative, n=2), consistent with our previous study showing that approximately 84% of nucleus ambiguus neurons express the other two markers, *Crhr2* and *Vipr2*. We observed that 8% of nucleus ambiguus neurons expressed *Npy2r* (16/190 (8%) nucleus ambiguus neurons were Npy2r positive). Of these Npy2r^{nAmb} neurons, half of them also expressed *Adcyap1*. Thus, the Npy2r^{nAmb} and Adcyap1^{nAmb} neurons appear to be partially overlapping populations.

Our results also show that Npy2r^{nAmb} neurons are scattered throughout the compact, semi-compact, and loose nucleus ambiguus, consistent with previous research demonstrating that CVNs are not located in any specific subregion of the nucleus ambiguus (Takanaga et al., 2003). Of note, we did not detect Adcyap1^{nAmb} in the loose nucleus ambiguus, although we saw *Adcyap1* expression throughout the semi-compact and compact nucleus ambiguus.

3.3.2 Adycap1^{nAmb} and Npy2r^{nAmb} Neurons Selectively Innervate the Heart

Since the Npy2r^{nAmb} and Adcyap1^{nAmb} neurons showed distinct molecular and anatomical profiles from the Crhr2^{nAmb} and Vipr2^{nAmb} neurons, we explored the innervation patterns of these neurons. To map the projections of Npy2r^{nAmb} and Adcyap1^{nAmb} neurons, we injected AAV-DIO-tdTomato into the ventrolateral medulla of Tbx3-CreERT2 mice. We used this mouse line to access Adcyap1^{nAmb} and Npy2r^{nAmb} neurons since *Tbx3* is

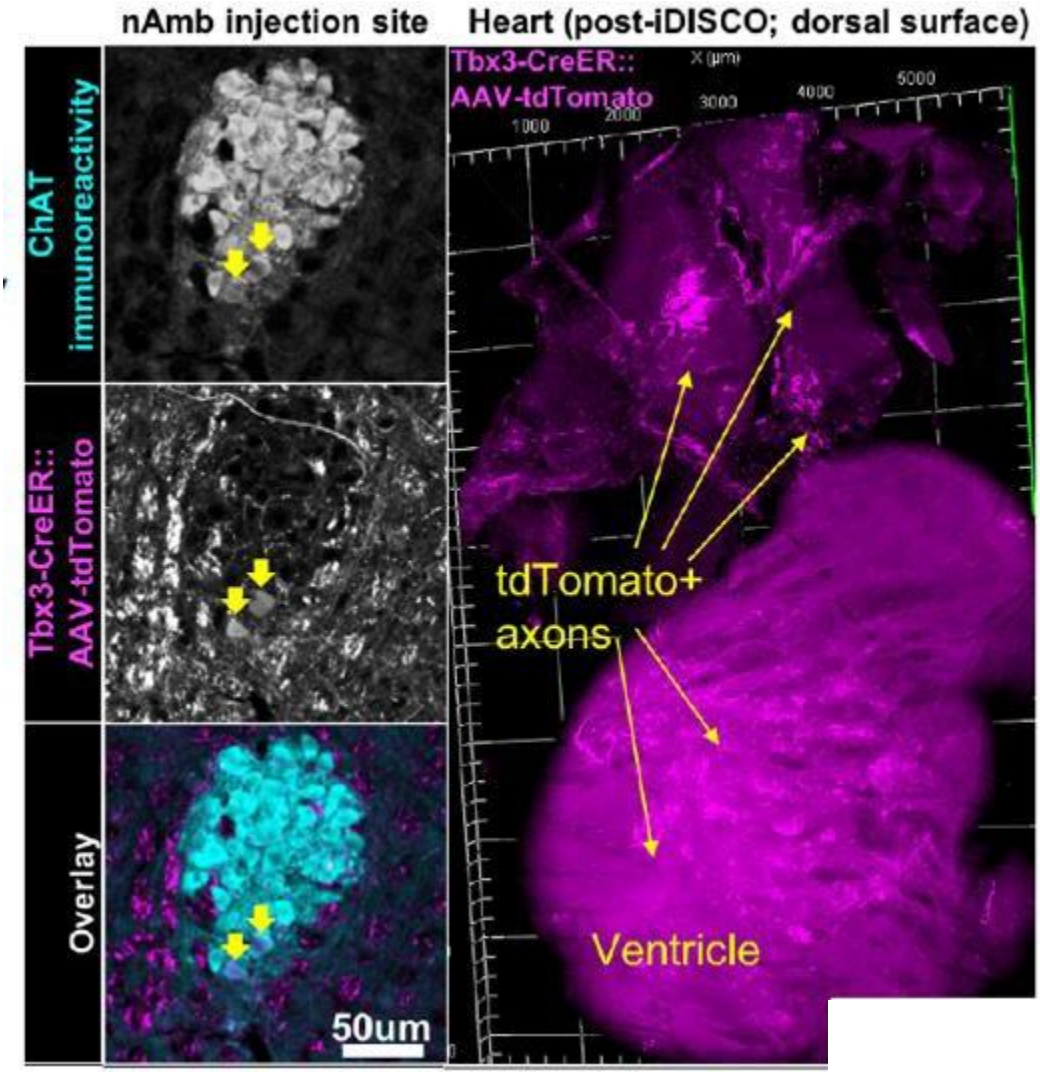

Figure 3-3. Tbx3^{nAmb} Neurons Innervate the Atria and Ventricles of the Heart

Figure 3-3 Legend

Left panels: Chat+ and Tbx3-Cre::AAV-tdTomato cells in the nAmb. Right panel: tdTomato+ axons innervating the dorsal aspect of an optically-cleared heart

marker gene that is highly colocalized with *Adycap1* and *Npy2r* in our single-cell RNA-sequencing data (Figure 3-1). To visualize the axons of tdTomato+ neurons, we optically cleared the heart and imaged whole hearts using confocal imaging. Confocal imaging of the hearts (n=3) showed extensive innervation of the heart by tdTomato+ axons (Figure 3-3). To confirm these tdTomato+ axons came from the nucleus ambiguus, we analyzed tdTomato and ChAT immunofluorescence on hindbrain sections. Our analysis showed AAV-tdTomato labeling of a subset of nucleus ambiguus neurons, typically 2-3 neurons per 30 um-thick nucleus ambiguus section (Figure 3-3). Importantly, no labeling was seen in other heart-projecting regions, e.g., dorsal motor nucleus of the vagus, DMV. These data indicate that Tbx3^{nAmb} neurons innervate heart and so support our hypothesis that they are cardiovagal neurons.

Of note, we originally used the Tbx3-CreERT2 mouse line to access Adcyap1^{nAmb} and Npy2r^{nAmb} neurons; however, this mouse line showed inefficient tamoxifen induction of Cre activity, leading us to search for a more effective mouse line. To map the projections of Npy2r^{nAmb} and Adcyap1^{nAmb} neurons, we obtained Npy2r-Cre and Adcyap1-Cre mice. We confirmed Cre expression in these mouse lines by co-localizing mRNA of the driver gene (i.e. *Npy2r* or *Adcyap1*) and Cre using RNA FISH. In Npy2r-Cre mice, 92% (145 of 157) *Npy2r*+ neurons in the hindbrain were also Cre+ (n=3). In Adcyap1-Cre mice, 89% (41 of 46) of *Adcyap1*+ neurons were also Cre+ (n=2). Furthermore, in the hindbrain of both Cre mouse lines, Cre mRNA was limited to cells in which the driver gene mRNA was also detected, confirming the specificity of these Cre lines. Ongoing studies investigating the innervation of the heart by Adcyap1^{nAmb} and Npy2r^{nAmb} neurons are using these two Cre lines.

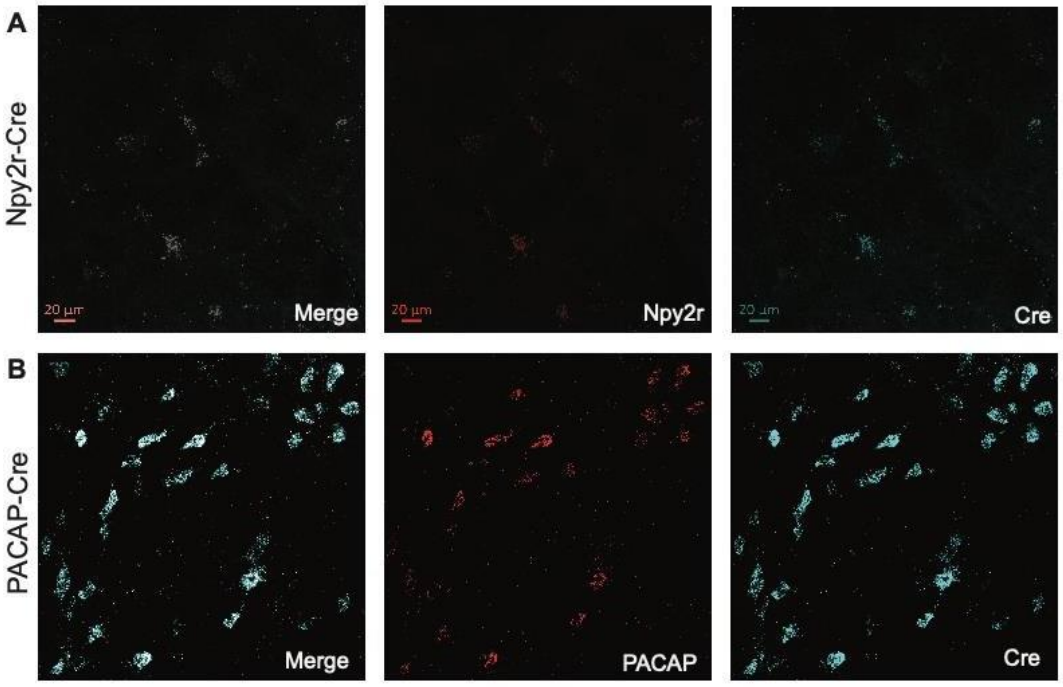

Figure 3-4. Validation of Npy2r-Cre and Adcyap1-Cre Activity

Figure 3-4 Legend

A. Co-localization of Cre mRNA and Npy2r mRNA of Npy2r-Cre mice by RNA fluorescence in situ hybridization (n=3).
B. Co-localization of Cre mRNA and Adcyap1 mRNA of Adcyap1-Cre mice by RNA fluorescence in situ hybridization (n=2).

3.3.3 Activating Npy2r^{nAmb} and Adcyap1^{nAmb} Neurons Reduces Heart Rate

Since the Npy2r^{nAmb} and Adcyap1^{nAmb} neuron subtype innervates the heart, we hypothesized that activation of these neurons would reduce heart rate. To investigate this, we used intersectional optogenetics to activate nucleus ambiguus subtypes, excluding neurons around the nucleus ambiguus that may express *Npy2r* or *Adcyap1*, while recording EKG in anesthetized and awake mice. To do so, we first intersectionally targeted Npy2r^{nAmb} neurons by crossing Npy2r-Cre mice to Chat-Flp mice, which we previously validated by co-localizing ChAT mRNA with Flp mRNA by RNA FISH (Coverdell et al., 2022) . To intersectionally target Adcyap1^{nAmb} neurons, we crossed Adcyap1-Cre mice to Phox2b-Flp mice. Then, we bred the Cre::Flp mice to a transgenic mouse line that intersectionally expresses Cre- and Flp- dependent CaTCh, a calcium-permeable channelrhodopsin2 (Daigle et al., 2018). We used the Cre::Flp::CaTCh offspring to optogenetically activate different nucleus ambiguus neuron populations as follows: all nucleus ambiguus neurons using Chat-Cre::Phox2b-Flp::CaTCh mice (Chat::Phox2b::CaTCh), Npy2r nucleus ambiguus neurons using Npy2r-Cre::Chat-Flp::CaTCh mice (Npy2r::Chat::CaTCh), and Adcyap1 nucleus ambiguus neurons using Adcyap1-Cre::Phox2b-Flp::CaTCh mice (Adcyap1::Phox2b::CaTCh). As a negative control, we also included a group of “CaTCh-only” mice which lacked Cre and Flp activity.

We performed central photostimulation of the nucleus ambiguus in awake and anesthetized mice. This approach allowed us to assess heart rate changes without confounding effects of either anesthesia or movement. Central stimulation of the right nucleus ambiguus of Chat::Phox2b::CaTCh mice targeting all nucleus ambiguus neurons

resulted in an immediate and profound decrease in heart rate, which recovered following cessation of photostimulation (Figure 3-5, Figure 3-6). We observed a very similar effect when targeting the Npy2r^{nAmb} and Adcyap1^{nAmb} neurons. Photostimulation of CaTCh-only mice resulted in no observable change in heart rate.

We observed a reduction in heart rate from a baseline of 500 bpm to 200 bpm when photostimulating all nucleus ambiguus neurons (Figure 3-5). Similarly, when photostimulating Npy2r^{nAmb} neurons, we observed a reduction in heart rate from approximately 600 bpm to 400 bpm (Figure 3-5). Our results when stimulating the Adcyap1^{nAmb} neurons was similar – heart rate reduced from around 500 bpm to 200 bpm (Figure 3-5). Of note, the physiological range of heart rate for mice is ~200 – 800 bpm, indicating that photostimulation of the Npy2r^{nAmb} and Adcyap1^{nAmb} nucleus ambiguus neurons possibly reduced heart rate to this minimum physiological limit. Indeed, closer analysis of the EKGs from the Chat::Phox2b::CaTCh and Npy2r::Chat::CaTCh mice show a cessation of heart beats. Photostimulation of Adcyap1::Phox2b::CaTCh mice showed a similar result; however, heart rate took longer to recover following cessation of photostimulation.

Reduction of heart rate by photostimulation of nucleus ambiguus neurons was frequency-dependent (Figure 3-5). Photostimulating at a frequency of 5 Hz reduced heart rate by approximately 150 bpm; at 10 Hz, by 200 – 300 bpm; and at 20 Hz, by 300 to 400 bpm. Stimulation of the nucleus ambiguus in CaTCh only mice resulted in no detectable change in heart rate.

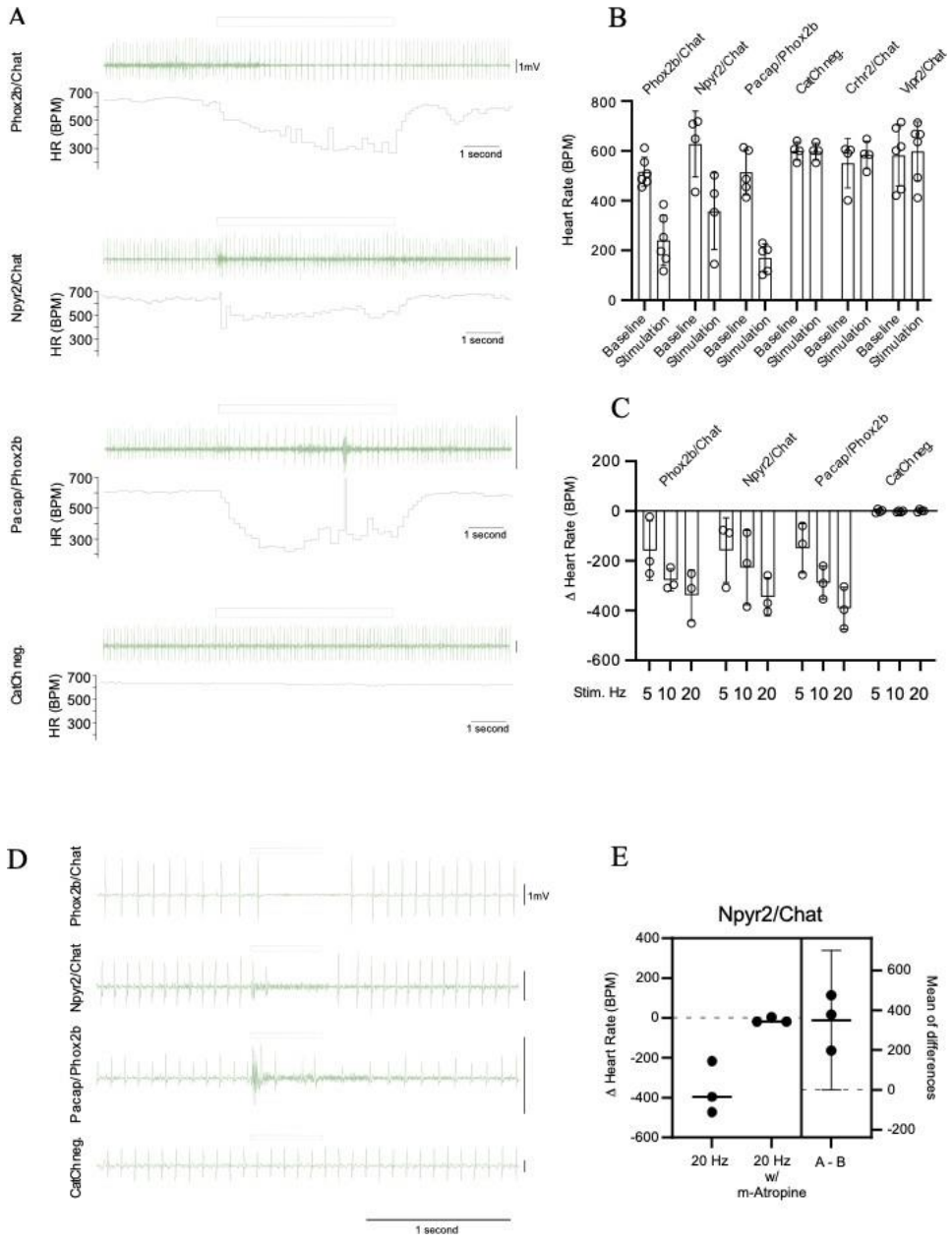

Figure 3-5. Npy2r^{nAmb} and Adcyap1^{nAmb} Neurons Selectively Reduce Heart Rate

Figure 3-5 Legend

A. EKG and heart rate recordings of before, during, and after optogenetic stimulation of the nAmb in Chat-Cre::Phox2b-Flp::CaTCh, Npy2r-Cre::Chat-Flp::CaTCh, PACAP-Cre::Phox2b-Flp::CaTCh, and CaTCh mice.
B. Heart rate at baseline and during nAmb stimulation in Chat-Cre::Phox2b-Flp::CaTCh, Npy2r-Cre::Chat-Flp::CaTCh, PACAP-Cre::Phox2b-Flp::CaTCh, CaTCh, Crhr2-Cre::Chat-Flp::CaTCh, and Vipr2-Cre::Chat-Flp::CaTCh mice.
C. Change in heart rate at different stimulation frequencies (5 Hz, 10 Hz, 20 Hz) in Chat-Cre::Phox2b-Flp::CaTCh, Npy2r-Cre::Chat-Flp::CaTCh, PACAP-Cre::Phox2b-Flp::CaTCh, and CaTCh mice.
D. EKG recordings of before, during, and after ontogenetic stimulation of the nAmb in Chat-Cre::Phox2b-Flp::CaTCh, Npy2r-Cre::Chat-Flp::CaTCh, PACAP-Cre::Phox2b-Flp::CaTCh, and CaTCh mice.
E. Change in heart rate during stimulation of Npy2r-Cre::Chat-Flp::CaTCh mice at 20 Hz frequency and after administration of atropine, a muscarinic receptor antagonist.

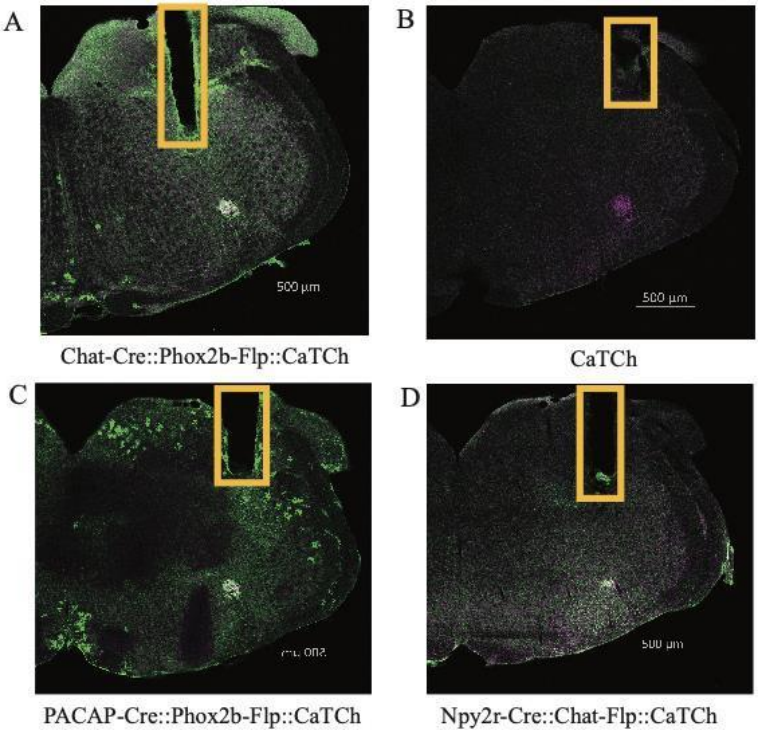

Figure 3-6. Fiber Placements from Optogenetic Experiments

Figure 3-6 Legend

A. Representative image of a fiber placement above the right nAmb in a Chat-Cre::Phox2b-Flp::CaTCh mouse
B. Representative image of a fiber placement above the right nAmb in a CaTCh mouse
C. Representative image of a fiber placement above the right nAmb in a PACAP-Cre::Phox2b-Flp::CaTCh mouse
D. Representative image of a fiber placement above the right nAmb in a Npy2r-Cre::Chat-Flp::CaTCh mouse

We also observed heart rate followed administration of methyl atropine (m-atropine)(Figure 3-5), a competitive antagonist of muscarinic acetylcholine receptors. Administration of m-atropine to mice blocked the effect of photostimulation on heart rate, suggesting that activation of Npy2r^{nAmb} neurons reduces heart rate through muscarinic signaling of the postganglionic neurons in the heart.

Ongoing studies are assessing whether the other nucleus ambiguus neuron subtypes innervate the heart; however, our previous study showed that these subtypes innervate the esophagus, pharynx, and larynx, respectively (Coverdell et al., 2022). We also centrally stimulated the nucleus ambiguus of Crhr2-Cre:Chat-Flp::CaTCh and Vipr2-Cre::Chat-Flp::CaTCh mice while recording EKG. We found no detectable change in heart rate while activating these two nucleus ambiguus subtypes, thus leading us to conclude that these neurons are not involved in heart rate control. Collectively, our data suggests that the nucleus ambiguus is comprised of genetically defined neuron subtypes that play unique physiological roles. Of these neuron subtypes, our results indicate that Npy2r^{nAmb} and Adcyap1^{nAmb} neurons innervate the heart to reduce heart rate.

3.4 DISCUSSION

The nucleus ambiguus is the primary source of parasympathetic input to the heart, lungs, and trachea and motor input to the esophagus, pharynx, and larynx. By using single nuclei RNA sequencing, RNA FISH, anterograde tracing, and intersectional optogenetics, we show one subtype marked by the genes *Npy2r* and *Adcyap1* are cardiovagal preganglionic neurons. This subtype, as studied using the Tbx3-CreERT2 mouse line, innervates both the atria and ventricle of the heart. Furthermore, when Npy2r^{nAmb} and

Adcyap1^{nAmb} neurons are activated, heart rate immediately decreases. Although previous studies have shown that there are some molecular identifiers of cardiovagal preganglionic neurons, this study outlines the molecular organization of these neurons in the nucleus ambiguus and connects it to their anatomy and function.

Our results further solidify the idea of a "labeled line" approach to organizing vagal motor neurons. Two other recent studies exploring the organization of the DMV and nucleus ambiguus showed a similar organization (Coverdell et al., 2022; Tao et al., 2021). Tao et al. showed that the DMV is composed of seven molecular subtypes of vagal motor neurons, two of which selectively innervate the stomach. Our previous study showed that the nucleus ambiguus is organized into three distinct molecularly defined subtypes, two of which innervate the esophagus, pharynx, and larynx. We have shown that one of these subtypes controls striated esophageal muscle contraction. Our current study now further supports this idea of a "labeled line" approach to organizing vagal motor neurons by identifying a third subtype, Npy2r^{nAmb} neurons, which innervate the heart and are capable of suppressing heart rate.

This study raises many questions for future study. For example, is there a division of labor among CVNs? Vagal input controls many aspects of heart function beyond heart rate, for instance – atrioventricular (AV) node conductivity, ventricular contractility, and coronary artery flow (Coote, 2013; Gourine et al., 2016). Several previous studies have shown that CVNs innervate different cardiac ganglia and have distinct functions (Cheng and Powley, 2000; Wake and Brack, 2016). Targeting of specific aspects of cardiovagal function could bring much progress in treating heart disease.

Our sequencing analysis vastly underrepresents the true diversity of nucleus ambiguus neurons. We profiled ~15% of neurons present in just one hemisphere of the nucleus ambiguus. Therefore, it is very likely that additional neuron subtypes exist within the nucleus ambiguus. For example, although we discovered that Npy2r^{nAmb} and Adycap1^{nAmb} neurons innervate the heart to reduce heart rate, it is possible that this subtype consists of multiple subtypes, some of which may influence atrioventricular node conductivity, ventricular contractility, and coronary artery flow.

Another question raised is where do these nucleus ambiguus cardiovagal neurons receive synaptic inputs? Cardiovagal tone is dependent on synaptic input; without it, CVNs are intrinsically silent (Mendelowitz, 1996a). Despite this knowledge, the sources and identities of these afferent neurons is still unknown. Although studies have examined synaptic inputs to the nucleus ambiguus, no studies to our knowledge have specifically traced synaptic inputs to the CVNs.

Lastly, what are the underlying synaptic circuits for key cardiac reflexes such as respiratory sinus arrhythmia and the baroreflex? CVNs are responsible for decreasing heart rate during expiration and in response to baro-/chemoreceptor activation. However, the synaptic circuits relaying reflex signals to the CVNs are unknown.

3.5 METHODS

3.5.1 Experimental Model and Subject Details

All animal care and experimental procedures were approved in advance by the University of Virginia Institutional Animal Care and Use Committee. The fluorescent *in situ* hybridization experiments used C57BL/6J mice from the Jackson Laboratory (JAX,

000664). The following mouse lines were used for optogenetic studies: Chat-IRES-Cre (JAX strain #028861); Phox2b-Flp (JAX strain #22407); CaTCh (JAX strain #025109); Adcyap1-2A-Cre ("PACAP-2A-Cre"; JAX strain #030155), Npy2r-IRES-Cre (Steven Liberles, Harvard Medical School, Howard Hughes Medical Institute; (Chang et al., 2015)) and a novel Chat-p2a-Flp mouse line (Steven Liberles, Harvard Medical School, Howard Hughes Medical Institute; (Coverdell et al., 2022)). The anterograde tracing experiments used Tbx3-CreERT2 mice. Unless otherwise specified, all experiments used adult mice with approximately equal numbers of male and female mice. Mice were housed at 22-24 °C with a 12-hour light:12-hour dark cycle and unlimited access to standard mouse chow and water.

3.5.2 Fluorescence in Situ Hybridization (FISH)

FISH experiments were performed on brain tissue from mice that received one intraperitoneal injection of 2% Fluorogold (Fluorochrome) a minimum of 5 days prior to euthanasia. Mice were terminally anesthetized with ketamine (20 mg/kg) and xylazine (2 mg/kg) diluted in PBS, followed by transcardial perfusion with 0.9% saline plus heparin and 4% paraformaldehyde (Thomas Scientific). Brains were extracted and post-fixed for 24 hours at 4°C. Following fixation, brains were sectioned coronally at 30 - 35 um thickness on a vibratome (Leica). The day before FISH, the sections were rinsed in PBS and then mounted on slides (Fisher) and left to dry overnight. An ImmEdge Hydrophobic Barrier Pen was used to draw a barrier around the sections. The sections were then incubated in Protease IV in a HybEZ II Oven for 30 minutes at 40°C, followed by incubation with target probes (*Chat*, *Phox2b*, *Adcyap1*, *Npy2r*, *Phox2b,* and *Cre*) for 2

hours at 40°C. Slides were then treated with AMP 1-3, HRP-C1, HRP-C2, HRP-C3, and HRP Blocker for 15-30 minutes at 40°C, as previously described (Wang et al., 2012). FITC, Cy3, and Cy5 (Perkin Elmer) were used for probe visualization. Fluorogold was imaged in its native state. Images were taken using a confocal microscope (Zeiss). The three subregions of the nucleus ambiguus correspond to the following bregma levels according to Paxinos and Franklin (2013) (Compact nAmb: -6.47 mm through -6.75 mm from bregma, Intermediate NAmb: -6.83 mm through -7.10mm from bregma, loose nAmb: -7.19 mm through -7.46 mm from bregma).

3.5.3 Anterograde Tracing Viral Injections

Mice were anesthetized with ketamine (20 mg/kg) and xylazine (2 mg/kg) diluted in PBS and positioned in into a stereotaxic apparatus (Kopf). A pulled glass micropipette was used for stereotaxic injections of an adeno-associated virus vector, AAV-DIO-tdTomato using the following stereotaxic coordinates for the nucleus ambiguus: anterior/posterior -2.1, -2.4, -2.7 mm, lateral/medial +/- 1.3 mm, and dorsal/ventral -5.8 mm, from lambda. Following local anesthetization with bupivacaine, virus was injected (200 nl/injection, 2-3 injections/side) using a Nanoject III system. This injection strategy was designed to fully cover the nucleus ambiguus, not to restrict viral infection to only nucleus ambiguus neurons. The pipette was removed 3-5 minutes after injections, followed by wound closure using sutures or surgical wound glue (Vetbond). Meloxicam SR (5 mg/kg; sustained release, SR) was injected subcutaneously for post-operative analgesia.

3.5.4 Tamoxifen Induction

After 3-4 weeks following injection of AAV-tdTomato into the hindbrain of Tbx3-CreERT2 mice, mice were treated with tamoxifen to induce Cre activity. Tamoxifen (100 mg/kg) was injected intraperitoneally for five consecutive days. Following one week after the last tamoxifen injection, mice were perfused with 0.9% saline and 4% paraformaldehyde, followed by harvest of the brain for histology and heart for tissue clearing using iDISCO.

3.5.5 iDISCO Tissue Clearing

iDISCO was perfomed on whole isolated organs according to iDISCO protocol (https://idisco.info/idisco-protocol/). Briefly, hearts were fixed overnight then washed, dehydrated with methanol, and permeabilized with Triton-X. The tissue was then immunolabeled with an iDISCO-compatible anti-tdTomato primary antibody and an Alexa 647-tagged secondary antibody. The immunolabeled tissue was washed, dehydrated with methanol, and optically cleared with dibenzyl ether. Cleared tissue was then imaged for Alexa 647 fluorescence on a LaVision Ultramicroscope II (UNC Chapel Hill, Microscopy Services Laboratory; MSL). Stacked images were used to generate 3D reconstructions with Imaris software (Oxford Instruments; UNC-CH MSL). These reconstructions were analyzed to identify fluorescently labeled axons as evidence of organ innervation.

3.5.6 Optogenetic Physiology

Cre-expressing mouse lines were crossed to Chat-Flp or Phox2b-Flp mouse lines to generate Cre::Flp lines, which were then crossed to transgenic mice that express eYFP tagged calcium-permeable channelrhodopsin 2 (CaTCh) only after recombination by both

Cre and Flp recombinases. Mice from these Cre::Flp::CaTCh lines were implanted with an optical fiber over the right nucleus ambiguus.

Optical fibers for central stimulation and headsets to record electrocardiogram (ECG) were implanted under anesthetized with ketamine (150 mg/kg) and dexmedetomidine (1 mg/kg). Depth of anesthesia was assessed by absence of the corneal and hind-paw withdrawal reflex. Body temperature was maintained at 37.2 ± 0.5 °C with a servo-controlled temperature pad (TC-1000; CWE). Following confirmation of anesthesia, mice were prepped for surgery, positioned in a stereotaxic headframe, and the local anesthetic, Bupivacaine (50 ul of 5 mg/ml), was injected at surgical sites. The tissue overlying the dorsal surface of the skull was retracted and the surface of the skull prepped for headset and optical fiber implants.

EKG headsets were constructed from 4-pin miniature connectors soldered to 2 lengths of Teflon-coated multi-strand stainless steel wire (AM-systems) for positive and negative leads and a stainless steel screw implanted in the skull for the ground. The screw was implanted above the frontal cortex and the leads were tunneled subcutaneously to opposing locations near the base of the ribcage. An optical fiber cannula constructed (200um 0.39NA fiber, Thorlabs) was implanted to stimulated cell bodies in the nucleus ambiguus neurons using the following coordinates from Lambda: Anterior/posterior: -2.1 mm, medial/lateral: +1.3 mm, dorsal/ventral: -5.0 mm for Crhr2-Cre::Chat-Flp::CaTCh mice. Fibers were only implanted on the right side of the brain. The same coordinates were used for Npy2r-Cre::Chat-Flp::CaTCh, Adcyap1-Cre::Phox2b-Flp::CaTCh, Vipr2-Cre::Chat-Flp::CaTCh mice, but at a 10-degree angle to access these neurons, which are found in the semi compact and caudal nucleus ambiguus. The fiber and ECG headset was

secured to the skull with dental cement and wounds were closed with sutures and surgical glue. Mice were given ketoprofen (5 mg/kg) for 3 days after surgery and allowed to recover for a minimum of 5 days before optogenetic physiology experiments.

To assess the cardiac effects of stimulating nucleus ambiguus neurons without anesthesia, mice were scuffed to connect the ECG head set and implanted fiber optic cannula to an amplifier and laser respectively. After a period of habituation to the recording set-up, stimulation was performed with a diode laser (473 nm; LaserGlow) controlled by Spike 2 software (CED). ECG (gain: 2K, band pass filter: 10-1000 Hz) signal was acquired (sampling rate: 1K) and heart rate calculated using Spike 2 software. Stimulation consisted of a 10 s period of stimulation at 10 Hz (5 ms pulse) with a power output at the tip of the connecting fiber of 12 mW.

3.6 ACKNOWLEDGEMENTS

We gratefully acknowledge Patrice G. Guyenet and Ruth Stornetta for thoughtful discussion and feedback on the experimental design and manuscript; Bradford Lowell for the Chat-p2a-Flp mouse; Patrice G. Guyenet and Hui Zong for co-acquisition of pilot funding; Ruth Stornetta for training in microscopy and Neurolucida; Daniel Stornetta for training in the RNAscope method; and Natalie Schiavone, Virginia Owen Trinkle, and Veronica Gutierrez for technical support. We also acknowledge these core facilities: ICCB-Longwood Screening Facility at Harvard Medical School; the Bauer Core Facility at Harvard University; and the Boston Nutrition Obesity Research Center Functional Genomics and Bioinformatics Core and Transgenic Mouse Core. Funding for this study was provided by a University of Virginia 3 Cavaliers award to John Campbell, Patrice G.

Guyenet, and Hui Zong; NIH R01 HL148004to S.B.G.A.; NIH T32 GM007055 and NIH F31 HL158187 to Tatiana Coverdell; and a Pathway to Stop Diabetes Initiator Award 1-18-INI-14, NIH R01 HL153916, pilot grant funding, and transgenic core service from the Boston Nutrition Obesity Research Center (NIH grant no. P30 DK046200) and the Boston Area Diabetes Endocrinology Research Center (BADERC; NIH, grant no. P30 DK057521) to John Campbell.

3.7 AUTHOR CONTRIBUTIONS

Tatiana Coverdell, Stephen Abbott, and John Campbell designed the experiments. John Campbell generated the sNuc-seq data and Tatiana Coverdell analyzed it. Tatiana Coverdell performed the RNA FISH studies. Tatiana Coverdell and Nicholas Conley injected mice for the anterograde tracing studies. Ruei-Jen Abraham-Fan implemented the heart tissue clearing methods and performed the iDISCO clearing and heart immunohistochemistry studies. Tatiana Coverdell and Stephen Abbott performed the optogenetic studies. Tatiana Coverdell and Jiachen Shi completed the mouse line validation experiments. Tatiana Coverdell and Jiachen Shi obtained images for the fiber placements. Tatiana Coverdell, Stephen Abbott, and John Campbell prepared the figures.

CHAPTER 4. CONCLUSIONS AND FUTURE DIRECTIONS

4.1 SUMMARY

The present dissertation outlines an emerging paradigm shift in which vagal motor neurons are organized not only by their anatomy and function, but also at a transcriptomic level. We find that the nucleus ambiguus, a region found within the medullary reticular formation of the brainstem, is composed of multiple genetically defined labeled lines that project to individual organs and control functions related to those organs. The nucleus ambiguus has been previously understood to control aspects of swallowing, vocalization, respiration, and parasympathetic cardiac function through its innervation of the heart, airways, pharynx, larynx, and striated esophageal muscle. However, despite the importance of this region, little was previously known about what neuronal subtypes exist within the nucleus ambiguus, which organ(s) each subtype innervates, and how they control physiological functions.

The above studies outlined in this thesis have identified three molecularly distinct neuronal subtypes localized in the nucleus ambiguus. Our data shows that one of these nucleus ambiguus subtypes innervates the esophagus; another innervates the pharynx and larynx; and a third innervates the heart. Furthermore, when we optogenetically activated the subtype that innervated the esophagus, we saw esophageal muscle contraction, but no change in heart rate. We observed no change in heart rate when activating the subtype innervating the larynx and pharynx. When we optogenetically activated the subtype that innervated the heart, we saw an immediate and drastic decrease in heart rate.

Overall, these studies provide three major advances to understanding the neuronal control of esophageal and cardiorespiratory function: (1) identifies the primary motor and parasympathetic neurons for the esophagus and heart molecularly, anatomically, and functionally, (2) reveals a genetic logic for the functional organization of the nucleus ambiguus; and (3) comprehensively characterizes the gene expression profile of esophageal motor neurons and cardiac vagal preganglionic neurons, which can be mined for potential drug targets to treat swallowing and cardiorespiratory disorders.

4.2 DISCUSSION

Neuronal control over organ function is orchestrated in part by the interplay between the afferent and efferent neurons of the autonomic nervous system. In 1897, the term “autonomic nervous system” was first used to describe nerves that innervate cardiac muscle, smooth muscle, and glandular tissue (Langley, 1897). The vagus nerve, which directly translates from Latin as “the wanderer,” is the longest cranial nerve of the parasympathetic nervous system, the branch of the autonomic nervous system that is responsible for “rest and digest” functions (Neuhuber and Berthoud, 2021). Initial studies of the vagus nerve date as far back as 1855, when a nucleus of the vagus nerve was identified in the hindbrain (Bieger and Hopkins, 1987). As time has progressed from these initial discoveries of the vagus nerve, numerous studies have all pointed to the vast diversity in organ innervation and functional control of this nerve, characterizing its command over organs including the pharynx, larynx, esophagus, heart, airways, pancreas,

stomach, small and large intestines, and the liver (Neuhuber and Berthoud, 2021).

Although around 70% - 80% of the vagus nerve consists of afferent fibers providing sensory information back to the brain (Prescott and Liberles, 2022), efferent fibers of the vagus nerve provide more direct control over organ function and are divided into two primary components: the general visceral efferent component (GVE) and the special visceral efferent component (SVE) (Drake. et al., 2010). GVEs are efferent fibers that innervate smooth muscle, cardiac muscle, and glandular tissue, usually synapsing with postganglionic neurons to produce an outcome. SVEs are efferent fibers that directly innervate striated muscle, such as those found in the pharynx, striated muscle of the esophagus, and larynx.

Studies have identified two major nuclei in the hindbrain that house the cell bodies of the GVEs and SVEs and send efferent axon projections through the vagus nerve: the nucleus ambiguus (nAmb) and the dorsal motor nucleus of the vagus (DMV) (Gibbons, 2019). In 1921, a German physiologist by the name of Otto Loewi identified the first known neurotransmitter, which he named “vagusstoff” (Loewi, 1921). Vagusstoff, translated directly from German as “Vagus Substance,” is now currently identified as acetylcholine, the neurotransmitter that is released at the axon terminals of vagal motor neurons (Loewi, 1921; Zimmer, 2006). Both the nucleus ambiguus and the DMV are now currently identified not only by their anatomical locations in the brainstem, but molecularly by their universal expression of choline acetyltransferase (ChAT), the enzyme that catalyzes the biosynthesis of acetylcholine (Oda, 1999).

The nucleus ambiguus, the smaller of the two vagal nuclei, provides parasympathetic

input to the heart and airways, as well as motor input to the striated esophagus, larynx, and pharyngeal muscles (Bieger and Hopkins, 1987 ; Bieger and Hopkins, 1987; Holstege et al., 1983; Lawn, 1966; Powley et al., 2013; Taylor et al., 1999; Taylor et al., 2014). Thus, vocalization, swallowing, bronchoconstriction, and reduction of heart rate are under the control of this hindbrain nucleus. The DMV contains neurons projecting to the heart, stomach, smooth muscle of the esophagus, liver, pancreas, small intestine, spleen, and colon, thus playing a major role in regulating gastric contraction, gastric relaxation, gastric acid secretion, pancreatic endocrine and exocrine secretions, intestinal mobility, gallbladder contraction, and some ventricular cardiac functions (Liddle, 2018; Mawe et al., 2018; Rogers and Hermann, 2012; Schubert and Peura, 2008).

Given the involvement of the vagus nerve in so many necessary physiological functions, damage or dysfunction of the nucleus ambiguus, DMV, or vagus nerve can have severe clinical implications. Studies have previously characterized some of these clinical complications. Dysphagia (difficulty swallowing), dysphonia and dysarthria (difficulty with speech), and cardiorespiratory complications can all result from issues with the nucleus ambiguus and vagus nerve (Petko and Tadi, 2022). For example, lesioning of the nucleus ambiguus in rats attenuated baroreflex sensitivity by over 80% (Cheng et al., 2004). Furthermore, atonia (loss of muscle tone) of the esophagus and stomach and increased circulating inflammatory cytokines, can also result from dysfunction with the DMV (Zhao et al., 2019). As studies have continued to uncover the significance of the vagal motor neurons, emerging therapies for vagus nerve related disorders have been at the forefront of research. One such therapy has been vagus nerve

stimulation.

Vagus nerve stimulation (VNS) is an approved therapy by the US Food and Drug Administration for treatment in some disorders such as treatment-resistant epilepsy, depression, and stroke (Bonaz et al., 2013; Johnson and Wilson, 2018). This therapy involves implanting a pulse generator under the skin and then wrapping a wire electrode around the left cervical vagus. The pulse generator then delivers electrical pulses to the vagus nerve, thereby repetitively activating it. Given the success of this treatment in epilepsy, depression, and stroke, it has been explored as a potential treatment of obesity, diabetes, cardiovascular disease, and pain management, among other disorders.

Unfortunately, vagus nerve stimulation has been limited in its ability to address many vagus nerve related disorders due to side effects or complications with the implantation surgery (Yap et al., 2020). Although the surgery is minimally invasive, it can still pose significant risks to the patient due to the location of the electrode placement, which is very close to the carotid artery. Side effects or off-target effects are also rampant with VNS since VNS activates all fibers of the vagus nerve, including the afferent fibers. For example, issues with bradyarrhythmia and respiratory complications can develop following treatment with VNS (Fahy, 2010; Marzec et al., 2003; Yap et al., 2020). Thus, further exploration as to whether there are “functional units” of the DMV and nucleus ambiguus that can be uniquely accessed is necessary in order to more comprehensively understand the vagus nerve and provide more targeted treatments for vagus nerve related disorders.

Previous ways to characterize vagal motor neuron diversity

Given that the vagus nerve innervates most visceral organs to control a variety of different functions, it has been hypothesized that vagal motor neurons are organized into "functional units" that project to distinct organs to control unique organ functions. Previous studies have attempted to characterize vagal motor neuron diversity by their molecular, anatomical, morphological, and physiological characteristics (Zeng and Sanes, 2017). Specifically, molecular characterization of vagal neurons has utilized pharmacological studing and retrograde tracing studies with the goal of finding molecular markers unique to subsets of vagal motor neurons. Molecular studies have also attempted to uncover proteins specific to organs as well as proteins involved in functional control of these organs. Studies attempting to organize vagal motor neurons by their anatomical locations have also utilized retrograde and anterograde tracing to determine whether there is a viscerotopic organization of vagal motor neurons in the brainstem. Additionally, morphological characteristics of vagal motor neurons (e.g. dendritic shape, axon shape, branching patterns, soma size, and spine density) have also been utilized to characterize these neurons into cell types (Zeng and Sanes, 2017). Lastly, physiological characteristics of vagal motor neurons (e.g. resting potential, biophysical properties, firing rate) have been utilized to understand differences between vagal motor neurons (Zeng and Sanes, 2017).

Previous studies have been very helpful in characterization of vagal motor neuron diversity and have provided clues as to whether the nucleus ambiguus and DMV are composed of distinct neuronal subtypes that act to control specific organ functions. The initial identification of "Vagusstoff" and ChAT first identified all vagal motor neurons.

Since then, numerous studies have uncovered more information about the identities of vagal motor neurons. Below are some of the highlights of these studies and various methodologies.

Retrograde tracing studies have utilized a variety of different retrograde tracers, which are taken up by axon terminals to travel back to the cell body, to map the connections from vagal motor neuron cell bodies to specific organs. This technique has been useful understanding whether there are molecular markers specific to vagal motor neurons projecting to distinct visceral organs. One such study labeled the thoracic vagus and the superior laryngeal nerve with the retrograde tracer horseradish peroxidase (HRP) and found that nucleus ambiguus neurons labeled with HRP from the thoracic vagus were not immunoreactive for the protein calcitonin gene related peptide (CGRP; gene name: *Calca*)(P.N. McWILLIAM, 1989). However, many of the neurons labeled from the superior laryngeal nerve and the cervical vagus were immunoreactive for CGRP. Another study took this one step further and found through retrograde tracing that over 70% of esophageal projecting nucleus ambiguus neurons expressed CGRP (McGovern and Mazzone, 2010). Thus, it appears CGRP levels may be a way to distinguish between preganglionic parasympathetic nucleus ambiguus neurons and motor neurons of the nucleus ambiguus projecting to the larynx, pharynx, and esophagus. Similarly, retrograde tracing studies in the DMV have provided clues as to whether there are molecular markers of DMV neuronal subtypes. Retrograde tracing studies found that injection of the retrograde tracer, Fluorogold, into the greater curvature of the rat stomach resulted in bilateral labeling of DMV neurons, with some of the Fluorogold labeled DMV neurons

also immunoreacting with the protein neurokinin 1 receptor (NK1R)(Ladic and Buchan, 1996). Interestingly, most of the NK1R labeled DMV neurons were found in the rostral DMV, indicating that a subset of vagal neurons located in the rostral DMV send axonal projections to the greater curvature of the rat stomach.

Additionally, the absence of markers has been useful in uncovering differences between neuron subtypes. For examples, studies have tried to uncover more specific molecular markers of the esophageal nucleus ambiguus motor neurons through retrograde tracing, and in doing so, found that substance P, neuronal nitric oxide synthase (nNOS), vasoactive intestinal peptide (VIP), neurofilament, calretinin, and calbindin are all proteins that are absent from nucleus ambiguus esophageal motor neurons (Mazzone and Canning, 2013; McGovern and Mazzone, 2010).

Another method for uncovering potential molecular differences between vagal neuron subtypes has been through analysis of organ tissue. For example, a study in rats showed through RT-PCR and real-time quantitative PCR that the esophagus mucosa, longitudinal muscle of the esophagus, and lower esophageal sphincter had abundant expression of corticotrophin-releasing factor type 2 (CRF2) –thus uncovering a potential molecular marker of nucleus ambiguus esophageal motor neurons and DMV lower esophageal neurons (Wu et al., 2007). Another study identified a molecular marker of relevance to striated muscle: the inwardly rectifying potassium channel, Kir2.4 (gene name: *Kcjn14*) (Topert et al., 1998). This protein is only found in motor neurons that innervate striated muscle. Lastly, a study in guinea pigs found that the protein pituitary adenylate cyclase-activating polypeptide (PACAP; gene name: *Adcyap1*) was present in

fibers innervating cardiac ganglia, and that these fibers were also ChAT positive (Calupca et al., 2000). Within the DMV, a study looking at gastrin releasing peptide (GRP) immunoreactivity found that GRP was abundant in nerve fibers innervating the exocrine pancreas (Shimosegawa et al., 1993).

Pharmacological studies have also been useful in parsing out vagal motor neuron subtypes by exploring whether certain molecular markers have an impact on organ function. Studies in rats have found that intravenously injecting 5-hydroxtryptamine (5-HT) increased activity of the pharyngeal branch of the vagus nerve, which was abolished with a 5-HT3 receptor (5-HT3R)(gene name: *5Htr3a*) antagonist (Yoshioka et al., 1994). Injection of 5-HT also increased pharyngeal pressure, which was abolished with a 5-HT3R antagonist. Thus, 5-HT3R could serve as a marker for nucleus ambiguus pharyngeal projecting neurons. Additional studies have attempted to uncover molecular identifiers of nucleus ambiguus neurons involved in vocalization. For example, deletion of the gene Teashirt 3 (*Tshz3*) caused significant breathing impairment and death of nucleus ambiguus neurons, including those located in the subregion of the nucleus ambiguus containing laryngeal projecting neurons (Caubit et al., 2010). Deletion of MET receptor tyrosine kinase+ neurons in the hindbrain significantly impaired vocalization and causes a significant reduction of nucleus ambiguus neurons (Kamitakahara et al., 2021). Another study found that CGRP is present in the larynx and is involved in the activity of sensory and motor pathways of the superior laryngeal nerve (Bauman et al., 1999). Thus, it’s possible that some of these genes may be acting in laryngeal motor neurons to control vocalization. Lastly, a study involving the DMV neurons found that activation of NK1R

in DMV vagal motor neurons resulted in inhibition of intragastic pressure and gastric motility (Krowicki 1999).

In addition to finding molecular markers of vagal motor neuron subtypes, studies have also attempted to characterize vagal motor neuron diversity by their anatomical locations within the nucleus ambiguus and the DMV. Both the nucleus ambiguus and the DMV show a viscerotopic organization. Neurons in the nucleus ambiguus are densely packed together in the rostral hindbrain but slowly spread out as the nucleus ambiguus approaches the caudal hindbrain (Bieger and Hopkins, 1987). The rostral nucleus ambiguus is therefore referred to as the compact nucleus ambiguus; the intermediate as the semi-compact nucleus ambiguus; and the caudal as the loose nucleus ambiguus. The DMV is divided into four major columns which each correspond to different organ functions and different branches of the vagus nerve (Berthoud et al., 1991). Furthermore, based on its rostral to caudal and dorsal to ventral organization, there also appears to be multiple subdivisions of the DMV: dorsorostral (DoR), ventrorostral (VeR), rostrointermediate (RoI), dorsointermediate (DoI), centrointermediate (CeI), ventrointermediate (VeI), caudointermediate (CaI), caudal division, and medial fringe subnucleus of the DMV (Huang et al., 1993).

Retrograde tracing studies have attempted to pinpoint whether there is an organization of subtypes within distinct nucleus ambiguus or DMV subregions. For example, retrograde tracing studies labeling the pharynx found that neurons projecting to the pharynx were located in the semi-compact nucleus ambiguus and the rostral extension of the compact nucleus ambiguus (Bieger and Hopkins, 1987). Other retrograde studies

have found that the nucleus ambiguus neurons projecting to the cricothyroid and cricoarytenoid muscles, both groups of laryngeal muscles, are located in the semi-compact and loose nucleus ambiguus, respectively (Hayakawa et al., 1999). The striated muscle of the esophagus is innervated by nucleus ambiguus neurons located in the compact formation (Bieger and Hopkins, 1987).

Similar studies have been performed in an attempt to uncover a viscerotopic organization of organ innervation within the DMV. Many retrograde and anterograde tracing studies have been useful in attempting to distinguish between DMV neuronal subtypes. For example, retrogradely labeling the lower esophageal sphincter showed that DMV neurons projecting to this area were localized to two opposite ends of the DMV – the rostral DMV and the caudal DMV (Rossiter et al., 1990). Other studies have suggested that the rostral division of the DMV contains neurons innervating the abdominal organs and lungs (Huang et al., 1993). The intermediate DMV appears to contain neurons innervating the stomach, ventricles of the heart, and pancreas (Huang et al., 1993). Lastly, the caudal DMV neurons send axonal projections to the smooth muscle of the esophagus (Huang et al., 1993).

Pharmacological studies activating different subregions of the DMV have uncovered some clues as to the functional role of each subregion. In a study in cats, injection of L-glutamic acid into the rostral area of the DMV caused increases in LES pressure (Rossiter et al., 1990). On the other hand, injection of L-glutamic acid into the caudal area of the DMV caused decreases in LES pressure. Thus, it appears that the rostral and caudal end of the DMV, both of which project to the LES, may play distinct functional roles in LES

relaxation and inhibition. Another study found that electrically stimulating the medial caudal DMV elicits the greatest response in gastric acid secretion compared to other areas in the DMV. Stimulation of the lateral caudal DMV elicits the greatest pancreatic response (Laughton and Powley, 1987).

Cell shape has also been a commonly used approach to attempting to characterize neuronal cell types. Both nucleus ambiguus and DMV neurons have been characterized by shape. Motor neurons of the nucleus ambiguus innervating the cricothyroid muscle and the posterior cricoarytenoid muscle are large, oval or polygonal in shape, containing a spherical nucleus and well-developed organelles (Hayakawa et al., 1999). Within the DMV, the ventrorostral and the ventrointermediate DMV neurons are small round or oval shaped (Huang et al., 1993). The dorsorostral, centointermediate, and caudal DMV consist of medium sized oval shaped cells (Huang et al., 1993). The caudointermediate DMV is composed of medium-sized fusiform and multipolar cells (Huang et al., 1993). Lastly, the dorsointermediate DMV neurons are mostly large and triangular in shape.

Taken together, these studies have provided much insight into potential neuronal subtypes of vagal motor neurons. However, although these studies have been useful in attempting to organize neurons into neuronal subtypes, there is a greater need for characterization of vagal motor neurons in an unbiased and comprehensive manner. Previous methods have been limited in doing so because of technical challenges and biases towards specific markers. Additionally, previous methods did not provide scientists with a standard definition of what these cell types are – thus there is a greater need for a commonly understood definition of vagal motor neuron subtypes within the

DMV and nucleus ambiguus in order to effectively study their anatomical and functional roles. Thus, a deeper understanding of the nucleus ambiguus and DMV and further exploration as to whether molecular cell types are the "functional units" of the vagal motor system is of great importance to advancing the field.

Organization of Neuron Subtypes at a Transcriptomic Level

Single cell RNA-sequencing (scRNA-Seq) has become an emerging technique that has the potential to address previous limitations in comprehensively uncovering vagal motor neuron subtypes in an unbiased manner. This technique allows for assessment of genome-wide mRNA expression in individual cells (Haque et al., 2017), thus opening the door for unbiased profiling of thousands of genes per cell, spanning a tremendous scalability as well the ability to profile the transcriptomes of thousands of cells at a time. Furthermore, it provides many benefits to understanding vagal motor neuron subtypes that previous methods were not able to do (Zeng and Sanes, 2017). One such benefit is the genetic access that it provides (Zeng and Sanes, 2017). Because scRNA-seq provides details about the transcriptomes of individual cells, this allows for utilization of marker genes to identify and further study these cell types, thus giving genetic access to neuronal cell types and allowing for identification and manipulation of these cell types in order to more fully understand their anatomical and functional roles. Another benefit of scRNA-seq is its reproducibility (Zeng and Sanes, 2017). scRNA-seq provides scientists with the means to repeatedly study vagal motor neuron cell types through identification of subtype

marker genes. Lastly, scRNA-seq opens the door to further studying diseases and addressing questions such as, is there a specific cell type that is more vulnerable to disease or that plays a greater role in disease phenotypes (Zeng and Sanes, 2017)? Taken together, scRNA-seq has opened the door for a more comprehensive and unbiased profiling of vagal motor neuron cell types.

Since its development in 2009, increasing commercial availability of single cell RNA-sequencing platforms and more developed bioinformatics approaches have allowed this technique to become more readily accessible to scientists (Haque et al., 2017; Tang et al., 2009). RNA-sequencing was first performed on pooled samples that contained millions of cells. Although this gave insight into the transcriptomic profile of these samples, it was not able to give a detailed picture of the transcriptome of individual cells. Since then, the development of single cell RNA-sequencing has allowed for a comparison of transcriptomes between individual cells, which often uncovers a vast degree of heterogeneity.

Many different methodologies have now been developed to study the transcriptomic profile of individual cells in an attempt to uncover different neuronal cell types (Haque et al., 2017). Although each methodology gives insight into the transcriptomic profiles of cell types, they vary in their ability to detect genes (high expression vs low expression) and to determine how many transcripts of each gene exists. Different methods also vary in ability to detect other cellular characteristics such as morphology, spatial distribution, functional, electrophysiological characteristics. This is of great importance because the transcriptomic profile of neurons must be integrated with other cellular properties in

order to fully understand neuronal cell types. Below are some sequencing methods which combine other cellular properties with transcriptomic profiling.

Multiplexed error-robust fluorescence in situ hybridization (MERFISH) is one such method which combines transcriptomic profiling of individual cells with their spatial location within the brain (Chen et al., 2015; Xia et al., 2019). This technique expanded on a previous technique called single-molecule FISH (smFISH), in which fluorescently labeled probes bind to transcript targets, which are then counted using fluorescence microscopy. Due to the limitation of this technique in only being able to measure a few genes at a time, MERFISH emerged to increase the multiplexing capacity of smFISH. MERFISH uses a barcoding approach in which each transcript is assigned a unique barcode, which are then stained with probes, allowing for readout of the barcode, thus providing both transcriptomic and spatial information about a given cell. MERFISH offers high multiplexing power (thousands of genes per sample), high cell throughput (sequencing of thousands of cells per sample), high sensitivity (accurate identification of RNA), and high resolution (ability to detect single cell to sub-cellular localization). Many studies using this approach have uncovered a strong correlation between anatomical location within the brain and transcriptomic profiles of neurons (Chen 2021; Zhang 2021). The ability to combine transcriptomics with spatial information of a cell have provided many advancements in the field of neuroscience and medicine (Crosetto et al., 2015). One such advancement is in understanding development by measuring chromatic abundance, gene expression, and protein levels in developing embryos at different developmental stages. Another advancement is in measuring how gene expression

profiles change during different physiological conditions. Lastly, these approaches can allow for advancement in understanding the heterogeneity of tumors in an attempt to provide more individually targeted treatments for cancers.

Patch-sequencing (Patch-seq) is another RNA-sequencing method that allows for identification of cell types based on transcriptomic, electrophysiological, and morphological characteristics. By combining patch clamping electrophysiological recordings, morphological analysis, and transcriptomic profiling, patch-seq links functional properties, cellular morphology, and gene expression profiles (van den Hurk et al., 2018). Electrophysiological recordings are first performed on neurons in acute brain slices, neuronal cultures, or in vivo (Lipovsek et al., 2021). In some cases, the neurons are labeled fluorescently, which allows for morphological reconstruction and study. Following recording and in some cases, imaging, the neurons are collected and processed for scRNA-seq. Although this method allows for combination of multiple data modalities, it is not high throughput compared to other sequencing approaches. However, it poses many benefits in understanding vagal motor neuron cell types. These include a study of neuron cell types based on multiple modalities, including anatomical location within the brain, functional properties of each neuron, morphological assessment, and transcriptomic profiling of individual neurons (Lipovsek et al., 2021).

Genetic targeting and technology – a new approach to understanding the vagal motor system

Cell types as defined by transcriptomics data must be combined with anatomical

and functional studies in order to validate their transcriptomics and further understand their true nature. Combining single cell transcriptomics with other techniques allows for a fully comprehensive understanding of vagal motor neuron cell types. Given the discovery of transcriptomic profiling and the emergence of genetic targeting and technology, genetic markers can be assessed to further study the anatomy and function of vagal motor neuron subtypes. For example, recombinase-expressing mouse lines, which insert a DNA recombinase (i.e. Cre) into a targeted gene locus, can be used to genetically access vagal motor neuron subtypes to study their axonal projections, physiological functions, and synaptic inputs (Luo et al., 2018). Researchers could also use viruses which express genetic tools driven by cell type-specific genetic elements, also allowing for genetic targeting of vagal motor neuron subtypes.

One crucial piece of information to understanding vagal motor neurons cell types is mapping the connections between the neurons and organs. Combining retrograde mapping with fluorescence in situ hybridization (FISH) studies can give some clues as to where vagal motor neurons are projecting to. For example, injection of a retrograde tracer into specific organs of interest allows for labeling of vagal motor neuron cell bodies, which can then be assessed with FISH for specific markers of vagal motor neuron cell types as revealed through their transcriptomic profiles.

Access to the transcriptional profile of vagal motor neuron cell types also allows for studying this question through anterograde tracing studies. Injection of Cre-dependent viruses encoding for fluorescent or chromogenic reporters into the hindbrain of mice with Cre inserted into a marker gene of interest allows for analysis of vagal motor neuron

innervation of specific organs. Fluorescent reporter labeling approaches can be combined with tissue clearing methods such as immunolabeling-enabled three-Dimensional Imaging of Solvent-Cleared Organs (iDISCO), in which organs are made optically transparent after fluorescent labeling axons, and then imaged using light sheet microscopy (Rajendran et al., 2019; Renier et al., 2014). This approach has been successfully applied to studies looking at global parasympathetic and sympathetic innervation of the whole mouse heart (Rajendran et al., 2019).

Chromogenic reporter systems, such as alkaline phosphatase, are another useful method to study vagal motor neuron subtype innervation patterns (Coverdell et al., 2022; Prescott et al., 2020; Tao et al., 2021). This method utilizes Cre recombinase mouse lines and Cre-dependent reporter viruses carrying placental alkaline phosphatase (PLAP), which fills the cell bodies and axons of neurons expressing Cre with PLAP. From here, organs can be collected and immersed in a solution in which the substrate reacts with PLAP to form a dark blue to purple precipitate. Organs can then be optically cleared and imaged. This approach has been successfully applied to studies looking at vagal sensory innervation of the airways (Prescott et al., 2020). Thus, tissue clearing combined with a chromogenic reaction allows for identification of vagal motor neuron organ innervation.

Beyond anatomical mapping, the functional roles of each vagal motor neuron cell type can also be studied by utilizing the transcriptomic profiles of vagal motor neuron subtypes and genetic technologies. Intersectional optogenetics is one such approach that allows for this. Cre recombinase expressing mouse lines bred with mouse lines expressing Cre dependent opsins dallows for opsin expression localized to specific cell

types, which then allows for those cell types to be individually activated or inhibited with light while assessing for functional changes. Similarly, Cre recombinase expressing mouse lines can also be injected with viruses containing Cre-dependent opsins, allowing for targeted functional assessment of vagal motor neuron cell types. Furthermore, combining Cre recombinase expressing mouse lines with Flp recombinase expressing mouse lines and a Cre-dependent and Flp-dependent channelrhodopsin mouse line allows for more targeted analysis of vagal motor neuron cell types. One such example is the CaTCh mouse line, which Cre and Flp dependently expresses channelrhodopsin (Daigle et al., 2018). Similarly, Cre and Flp mouse lines can be injected with Cre and Flp dependent viruses encoding for activating or inhibiting opsins, allowing for even greater specificity.

Intersectional chemogenetics is another approach that can be used to assess more long-term functions of vagal motor neuron cell types, especially in the context of disease and other physiological reflex functions (Dyavanapalli, 2020). The Cre-Lox recombination system can also be utilized to achieve highly selective expression of designer receptors exclusively activated by designer drugs (DREADDS) in vagal motor neurons. These are G-protein coupled human muscarinic receptors that can be selectively activated by injection of clozapine N-oxide (CNO). Two different DREADDS of interest to studying the functional role of vagal motor neuron cell types exist: hM4Di, which inhibits neuronal activity when activated, and hM3Dq, which activates neuronal activity when activated. Furthermore, activation of inhibition of neurons using DREADDS lasts for approximately 8 hours. Cre recombinase expression can be driven by a marker gene

promotor and co-injected with flexed excitatory or inhibitory DREADDS to induce expression of DREADDS within vagal motor neuron cell types.

Despite the emergence of these technologies, some concern has been raised as to how reliably and reproducibly single cell transcriptomics can define vagal motor neuron cell types. Below, we identify a few studies that have successfully applied single cell transcriptomics with other existing methodologies to identifying vagal motor neuron subtypes within the nucleus ambiguus and the DMV.

Two recent studies identified nucleus ambiguus neuron subtypes based in part by their transcriptomic profiles (Coverdell et al., 2022; Veerakumar et al., 2022). One study combined single nuclei RNA-sequencing with anterograde mapping and intersectional optogenetics to reveal a genetically defined circuit for vagal motor control of the esophagus (Coverdell et al., 2022). Using single nuclei RNA-sequencing, this study found that the nucleus ambiguus is composed of three molecularly distinct subtypes, which were annotated using the subtype-specific genes: *Crhr2*, *Vipr2*, and *Adcyap1*. Mapping the axon projections of the $Crhr2^{nAmb}$ and $Vipr2^{nAmb}$ neurons using Cre recombinase mouse lines and a Cre dependent chromogenic reporter virus showed that the $Crhr2^{nAmb}$ neurons selectively innervated the esophagus, whereas the $Vipr2^{nAmb}$ neurons did not innervate the esophagus but instead innervated the pharyngeal and laryngeal muscles. Furthermore, optogenetically activating cholinergic Crhr2+ fibers in the esophagus caused esophageal muscle contraction. No effect on heart rate was detected when activating $Crhr2^{nAmb}$ neurons. Additionally, activation of cholinergic Vipr2+ neurons did not cause any esophageal contractions. Taken together, this study

successfully combined single cell transcriptomics with anatomical tracing and functional studies to reveal a genetic logic for the functional organization of the nucleus ambiguus.

Another study used retrograde neuronal tracing, single cell RNA sequencing, and optogenetics to uncover a cardiac parasympathetic control circuit in mice (Veerakumar et al., 2022). Heart projecting nucleus ambiguus neurons were labeled with a retrograde tracer injected into the pericardial space, followed by collection and transcriptional profiling of labeled nucleus ambiguus neurons. The same approach was applied to labeling the cricothyroid laryngeal muscle. These results yielded three nucleus ambiguus neuronal cell types: one laryngeal nucleus ambiguus cell type and two cardiovagal nucleus ambiguus cell types. Furthermore, this study found that nucleus ambiguus cardiovagal neurons molecularly, anatomically, and functionally distinct subtypes: ambiguus cardiovascular (ACV) neurons and ambiguus cardiopulmonary (ACP) neurons. Anterograde tracing using a Cre dependent fluorescent protein GFP and Cre recombinase expressing mouse lines showed that the ACV neurons innervate cardiac parasympathetic ganglion, whereas the ACP neurons innervate cardiac ganglion and lung parasympathetic ganglion. Furthermore, optogenetic activation of either the ACP neurons or ACV neurons showed very similar effects on heart rate: activation of these vagal neuron subtypes results in an immediate and drastic decrease in heart rate. Furthermore, studies looking at the role of ACV or ACP neurons in baroreflex or diving reflex control found that the ACP neurons mediate the diving reflex, whereas the ACV neurons mediate the baroreflex. Taken together, these two studies support the idea that the nucleus ambiguus communicates with visceral organs through genetically-defined labeled lines to control

unique physiological functions specific to each organ, and that nucleus ambiguus neurons are organized at a transcriptomic level.

Another study focused on characterizing the DMV neurons found that there is a labeled line organization of DMV neurons and that two DMV neuronal subtypes project to the stomach (Tao et al., 2021). Using single nuclei RNA-sequencing of DMV neurons, this study uncovered seven molecularly distinct DMV motor neurons. Furthermore, anterograde tracing studies utilizing subtype specific Cre driver mice found that two of these subtypes, Cck^{DMV} and $Pdyn^{DMV}$, innervated the glandular stomach in mice. Interestingly, the Cck^{DMV} neurons make contact with enteric neurons releasing acetylcholine, characteristic of neurons acting to control gastric contraction and acid secretion. On the other hand, the $Pdyn^{DMV}$ contact with enteric neurons releasing nitric oxide, characteristic of neurons acting to control gastric relaxation. Taken together, this study also supports the idea that vagal motor neurons are organized functionally at a transcriptomic level.

4.3 FUTURE DIRECTIONS

Our studies show that the nucleus ambiguus is comprised of three molecularly, anatomically, and functionally defined neuronal subtypes. The $Crhr^{nAmb}$ subtype innervates the esophagus to control striated esophageal muscle contraction. The $Npy2r^{nAmb}$ subtype innervates the heart to reduce heart rate. The $Vipr2^{nAmb}$ subtype innervates the pharynx and larynx. These findings have raised many additional questions, which are described below.

4.3.1 Role of Vipr2^{nAmb} neurons in vocalization

Our previous studies have pointed to a role of the Vipr2^{nAmb} neurons in swallowing and vocalization. These neurons are located in the pharyngeal and laryngeal subregions of the nucleus ambiguus; indeed, we found that this subtype innervates the pharynx and larynx (Coverdell et al., 2022). We are further interested in elucidating the functional role of the Vipr2^{nAmb} subtype; thus, studies are currently underway to determine how this subtype controls different aspects of pharyngeal and laryngeal function.

Specifically, we are further interested in this subtype's role in vocalization. To explore this, we plan to perform a more detailed anatomical analysis of the larynx following injection of a viral tracer into the nucleus ambiguus of Vipr2-Cre mice. Following ample time for virus infection and expression of the reporter, larynxes will be harvested and sectioned for histological analysis using DAB immunohistochemistry for the virus reporter and H&E staining to visualize muscle and connective tissue. A more detailed exploration of laryngeal muscle innervation by the Vipr2^{nAmb} neurons will give further clues about their functional roles.

We also plan to use intersectional optogenetics to assess what happens in the larynx when the Vipr2^{nAmb} neurons are activated. To do so, we will harvest the larynxes from Vipr2-Cre::Chat-Flp::CaTCh mice and perform ex vivo optogenetic stimulation of the larynxes while recording changes in glottal opening. This data will provide information on whether activation of the Vipr2^{nAmb} neurons causes changes in the larynx that are associated with vocalization.

To assess the impact of Vipr2^{nAmb} neurons on vocalization in a mouse model, we will cross Vipr2-cre::Chat-Flp mice to a dsDTR mouse line, which Cre and Flp

dependently expressed diphtheria toxin receptor. We will then take adult male Vipr2-Cre::Chat-Flp::dsDTR mice and record their vocalizations when placed in a chamber with a female mouse in estrus to obtain a baseline vocalization recording for each mouse. After this, we will inject diphtheria toxin into the hindbrain of these mice to ablate Vipr2+Chat+ nucleus ambiguus neurons. We will then repeat the experiment and record vocalization when these neurons are ablated. Mice will be perfused and brains harvested following these experiments to histologically confirm that Vipr2+Chat+ nucleus ambiguous neurons were ablated. We expect that ablation of Vipr2 nAmb neurons will cause a reduction in vocalization.

4.3.2. Functional role of the Crhr2^{nAmb} neurons in swallowing

Although our studies addressed a functional role of the Crhr2^{nAmb} neurons in contracting esophageal striated muscle, our studies could be extended into assessing how this impacts the process of swallowing. To explore this, we plan to ablate Crhr2^{nAmb} neurons using diphtheria toxin. Briefly, we will cross Crhr2-Cre::Chat-Flp mice to a dsDTR mouse line, which Cre and Flp dependently expresses diphtheria toxin receptor. We will then use fluoroscopy to record the process of swallowing in these mice prior to diphtheria toxin injection. After obtaining these videos, we will inject diphtheria toxin into the hindbrain of Crhr2-Cre::Chat-Flp::dsDTR mice. Following time for recovery, we will then repeat the experiment and record swallowing when the Crhr2+/Chat+ neurons are ablated. Mice will be perfused and brains harvested following these experiments to histologically confirm that Crhr2r+/Chat+ nucleus ambiguus neurons were ablated. Given that activation of these neurons results in contractions of the striated muscle of the esophagus, we expect that ablation of these neurons will impede this process and therefore create significant issues in swallowing.

4.3.3 Necessity of Npy2r^{nAmb} and Adcyap1^{nAmb} subtypes in heart rate reduction

Our studies have shown that Npy2r^{nAmb} and Adcyap1^{nAmb} neurons are sufficient in reducing heart rate. We are now interested in whether these neurons are necessary in reducing heart rate. To address this, we will utilize the dsDTR (diphtheria toxin receptor)

mouse line. Briefly, we will cross Npy2r-Cre::Chat-Flp mice and PACAP-Cre::Phox2b-Flp mice to a dsDTR mouse line, which Cre and Flp dependently expresses diphtheria toxin receptor. We will then record a baseline heart rate. After obtaining this, we will inject diphtheria toxin into the hindbrain of Npy2r-Cre::Chat-Flp::dsDTR and PACAP-Cre::Phox2b-Flp::dsDTR mice. Following time for recovery, we will then record heart rate. Mice will be perfused and brains harvested following these experiments to histologically confirm that nucleus ambiguus neurons were ablated. Given that activation of these neurons resulted in a decrease in heart rate, we expect that ablation of them will increase heart rate.

To further assess the necessity of Npy2r^{nAmb} and Adcyap1^{nAmb} neurons in reducing heart rate, we will use a lentivirus (LV) inhibitory stGtACR2-mCherry to optogenetically inhibit these neurons while recording heart rate. This virus will be injected into the nucleus ambiguus of Chat-Cre::Phox2b-Flp::dsHTB (positive control to target all nAmb neurons), Chat-Cre::dsHTB (no Flp, negative control), Npy2r-Cre::Chat-Flp::dsHTB (Npy2r^{nAmb} subtype), and PACAP-Cre::Phox2b-Flp::dsHTB (Adcyap1^{nAmb}) mice, followed by 6 weeks of recovery to allow time for virus infection and expression (Figure 4-1). Since the dsHTB transgene is necessary for lentivirus infection and requires the presence of both Cre and Flp to be expressed, this will allow for selective infection of the lentivirus in these neurons and therefore, specific targeting of the Npy2r^{nAmb} and Adcyap1^{nAmb} subtypes. Following this, EKG recordings will be obtained before, during, and after optogenetic inhibition. We expect that optogenetic inhibition of these neurons will increase heart rate. Our preliminary studies show successful infection of all nucleus ambiguus neurons (Figure 4-1). Furthermore, our studies show that optogenetic inhibition of Adcyap1+Phox2b+

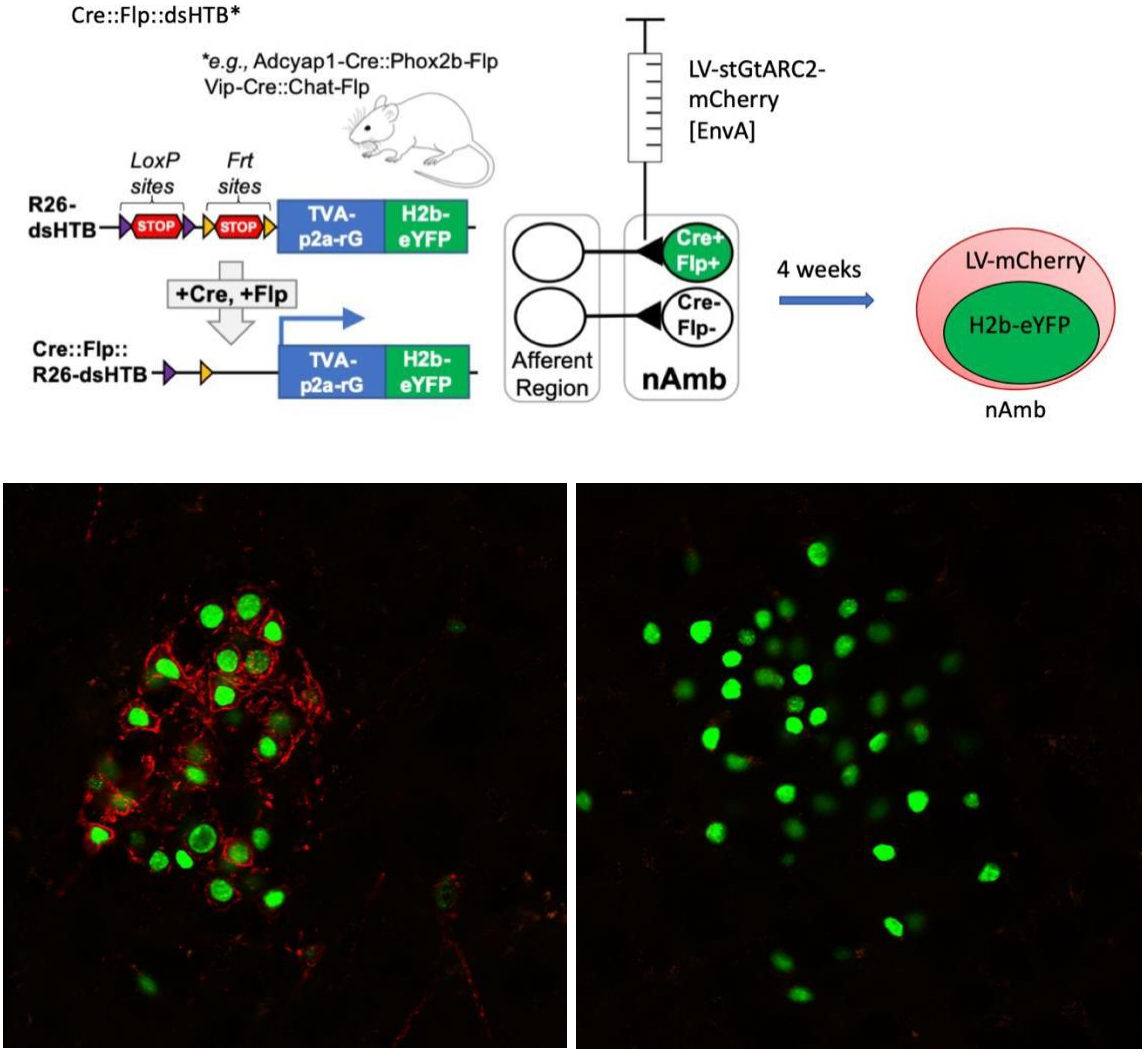

Figure 4-1. Use of LV-stGtARC2-mCherry to target nucleus ambiguus neurons for loss of function studies.

Figure 4-1 Legend

Schematic showing injection strategy for LV-stGtARC2-mCherry [EnvA] targeting of nucleus ambiguus neurons (top panel). Successful infection of nucleus ambiguus neurons (bottom left panel) compared to control side in the same mouse with no injection (bottom right panel)

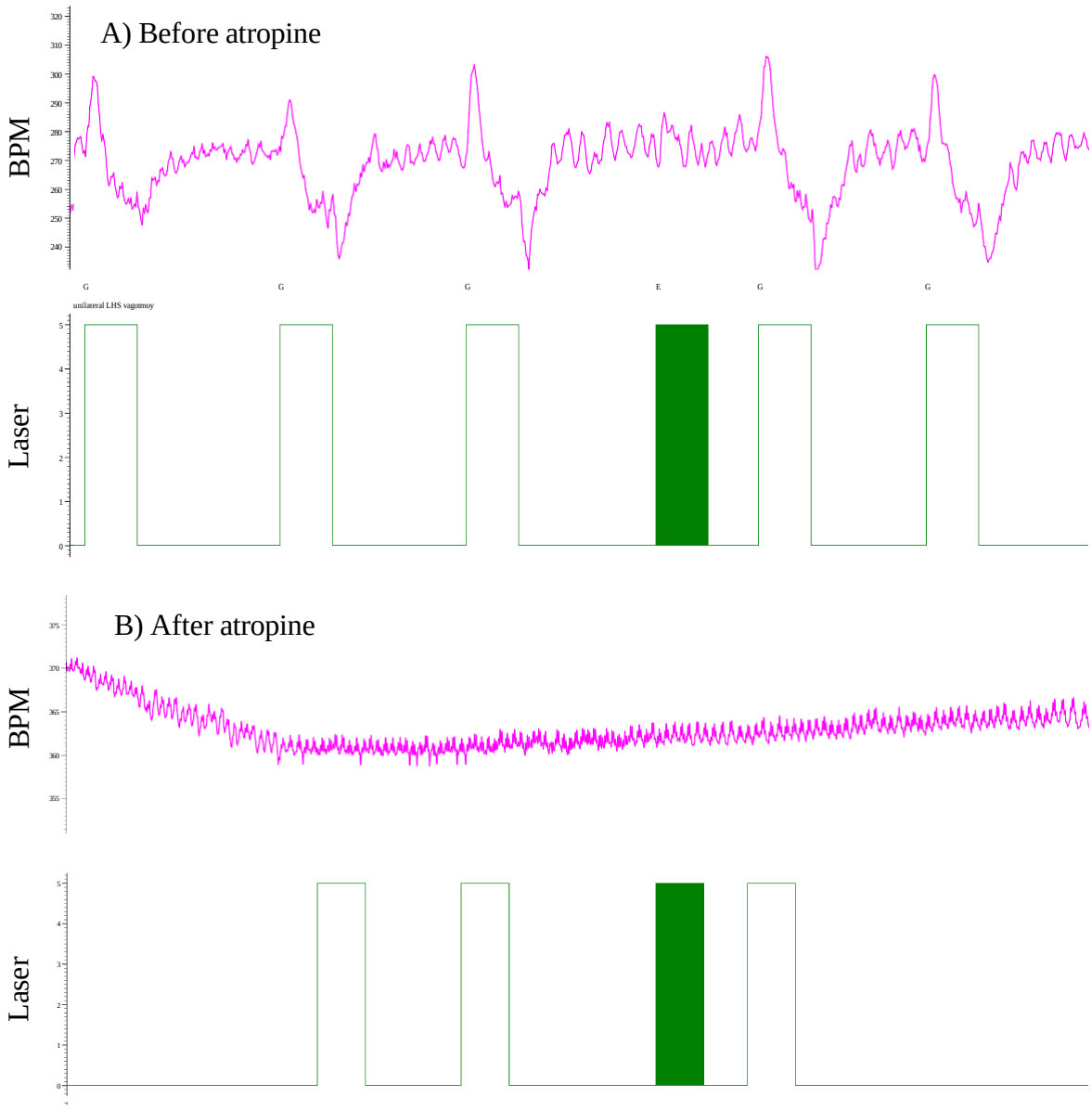

Figure 4-2. Heart rate response to optogenetic inhibition of Adcyap1+Phox2b+ nucleus ambiguus neurons before and after atropine administration.

Figure 4-2 Legend

A) Optogenetic inhibition of Adcyap1+Phox2b+ neurons in the nucleus ambiguus produces a biphasic response after left vagus nerve vagotomy in which heart rate initially increases but decreases shortly after this increase
B) Atropine abolished effect of optogenetic inhibition of Adcyap1+Phox2b+ nucleus ambiguus neurons

neurons in the nucleus ambiguus produces a biphasic response in which heart rate initially increases but decreases shortly after this increase (Figure 4-2).

4.3.4 Npy2r^{nAmb} and Adcyap1^{nAmb} neurons involvement in cardiac reflexes

Previous studies have shown that CVNs in the nucleus ambiguus mediate key cardiovascular reflexes in response to internal and external stimuli (Silvani et al., 2016). For example, the diving reflex, the most powerful autonomic reflex known, occurs when the apex of the nose contacts water during breath-holding (Godek and Freeman, 2021). This causes profound decreases in heart rate, blood pressure, and breathing, which are each generated through distinct circuits and neurons (Foster and Sheel, 2005; Hult et al., 2019). Though previous research has identified certain brain regions that are activated during the diving reflex, specific neuron types and neural circuits remain unknown (Kapa et al., 2016; Panneton et al., 2014). Therefore, there is a clear need for a deeper understanding of cardiovagal circuits that mediate this and other cardiorespiratory reflexes.

To address this question, we plan to again utilize the dsDTR (diphtheria toxin receptor) mouse line. Briefly, we will cross Npy2r-Cre::Chat-Flp mice and PACAP-Cre::Phox2b-Flp mice to a dsDTR mouse line. We will then implant telemetry probes which will record heart rate. Following recovery from the probe implant surgery, the mice will be trained to dive underwater and a baseline heart rate will be recorded during this dive. We expect to see a decrease in heart rate during the dive. After this training, we will inject diphtheria toxin into the hindbrain of Npy2r-Cre::Chat-Flp::dsDTR and PACAP-Cre::Phox2b-Flp::dsDTR mice. Following time for recovery, we will then record heart rate again while the mice are diving. Mice will be perfused and brains harvested following these

experiments to histologically confirm that nucleus ambiguus neurons were ablated. We expect that heart rate will no longer drop during the dive in mice with ablated Npy2r^{nAmb} and PACAP^{nAmb} neurons.

4.3.5 Synaptic inputs to Npy2r^{nAmb} and Adcyap1^{nAmb} neurons

CVNs are intrinsically silent and thus rely constantly on synaptic inputs (Mendelowitz, 1996a). One major source of synaptic input to nucleus ambiguus neurons is the nucleus tractus solitarius (NTS). The NTS provides both excitatory and inhibitory input to the nucleus ambiguus and is likely involved in cardiac reflex activities to the CVNs and other nucleus ambiguus neurons. Furthermore, underwater submersion activates numerous neurons in the medullary dorsal horn (MDH). Previous studies have separately shown that (1) diving activates MDH and NTS neurons (Panneton, 2013; Panneton and Gan, 2020) and (2) that MDH and NTS neurons innervate the nucleus ambiguus. However, it remains unknown whether these diving reflex-activated neurons are connected to the cardiovagal nucleus ambiguus neurons. Discovering the circuits which mediate this powerful, highly conserved reflex will shed light on the underlying mechanisms of cardiovagal function, which can further allow for targeted research of cardiac illness diagnosis and treatment.

Another major source of synaptic input to the nucleus ambiguus originates from a region called the “post-inspiratory complex” (PiCo). These neurons are responsible for driving the post-inspiratory phase of respiration (Anderson et al., 2016a). Previous studies have shown that during post-inspiration, glutamatergic synaptic input to cardiovagal nucleus ambiguus neurons increases (Dergacheva et al., 2010). However, the source of this synaptic input remains unknown. Therefore, we hypothesize that glutamatergic PiCo

neurons synapse directly on Npy2r^{nAmb} and PACAP^{nAmb} neurons. Consistent with this hypothesis, PiCo neurons are cholinergic, and cholinergic respiratory neurons in particular are thought to activate nucleus ambiguus neurons during respiratory sinus arrhythmia (Anderson et al., 2016a). Importantly, a circuit which connects excitatory PiCo neurons to cardioinhibitory nucleus ambiguus neurons could explain the coupling of post-inspiration with bradycardia that defines respiratory sinus arrhythmia.

Although previous studies have identified afferent neurons around the nucleus ambiguus and in the MDH and NTS, it is not known what the identities of these neurons are and whether they synapse onto cardiovagal nucleus ambiguus neurons. To explore these questions, we will map the monosynaptic inputs to each nucleus ambiguus neuron subtype using a modified rabies virus, [EnvA]SADΔG-H2B-mCherry ("rabies-H2b-mCherry"). This modified rabies virus expresses a nuclear localized fluorescent protein, H2b-mCherry, which robustly labels infected cells. It is also pseudotyped with EnvA glycoprotein and so it can only infect cells that express the avian viral receptor, TVA 88. Lastly, rabies-H2b-mCherry lacks the gene encoding rabies G protein (rG) and so cannot spread trans-synaptically from a neuron unless rG is also expressed by that neuron. Thus, by targeting TVA and rG expression to a specific neuronal population via "helper" viruses or a transgenic reporter mouse, rabies infection can be restricted to the TVA+/rG+ neuronal population ("starter neurons") and their primary synaptic afferents ("input neurons"). This approach labels neurons across the nervous system that directly connect to the starter neurons.

To explore the synaptic inputs to the Npy2r^{nAmb} and PACAP^{nAmb} neurons, we will cross Npy2r-Cre::Chat-Flp mice and PACAP-Cre::Phox2b-Flp mice to dsHTB mice (a

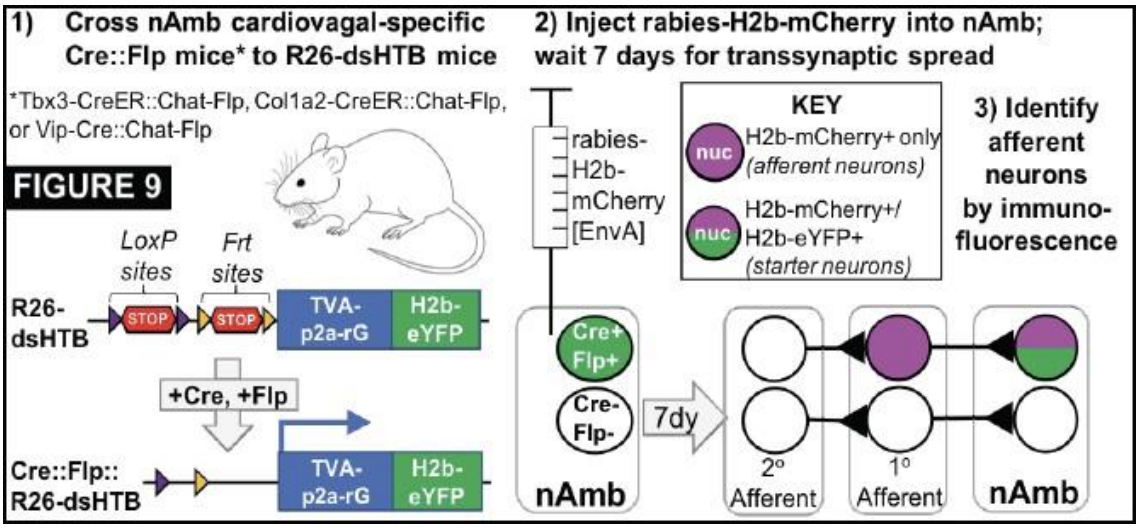

Figure 4-3. Schematic of rabies input mapping.

Figure 4-3 Legend

Cre::Flp mice are crossed to dsHTB mice. Cre::Flp::dsHTB offspring are then injected with rabies-h2b-mCherry, followed by 7 days of waiting for infection and transsynaptic spread. Afferent neurons are then identified by expression of mCherry only. Starter neurons are identified by expression of mCherry and GFP.

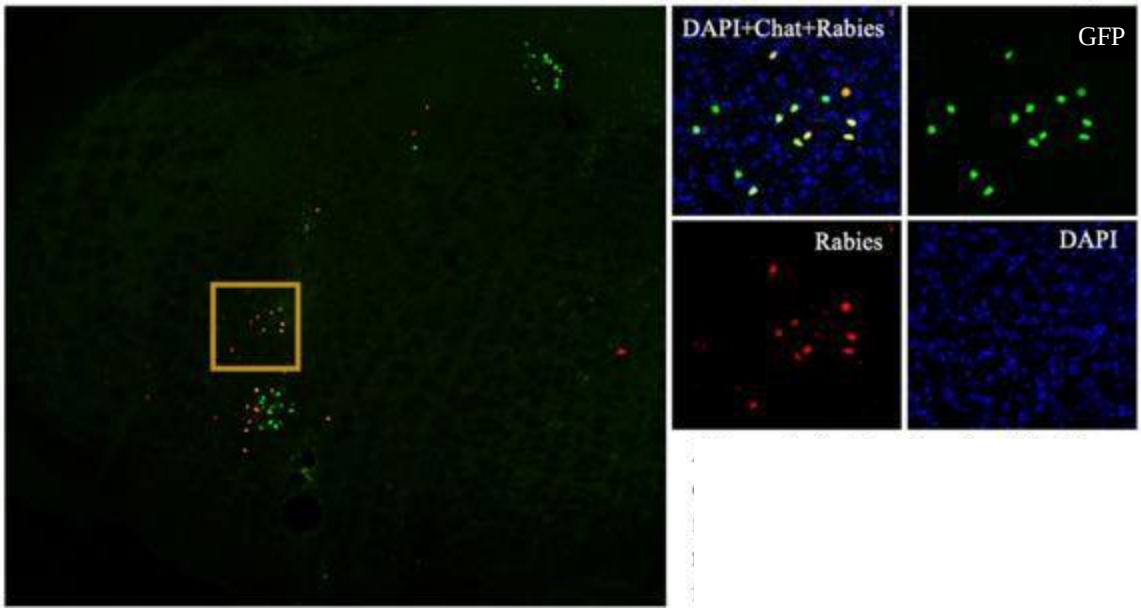

Figure 4-4. Rabies mapping in Chat-Cre::Phox2b-Flp::dsHTB mice.

Figure 4-4 Legend

Positive control results show successful infection of nucleus ambiguus neurons (green and red) and neurons projecting onto those (red) from various regions of the hindbrain.

reporter line that Cre- and Flp-dependently expresses TVA, rG, and a nuclear-localized GFP). The nuclear-localized GFP marks the Cre+/Flp+ starter neurons so that they can be distinguished from their input neurons, which are labeled by H2b-mCherry+ only (Figure 4-3). Following 10 days after injection of the virus, brains will be harvested and assessed for mCherry and GFP. Our preliminary studies show robust infection of the starter neuron population (Figure 4-4); however, further optimization is needed to identify input neurons.

4.3.6. GRP DMV neurons may be inhibitory LES neurons

Gastroesophageal reflux disease (GERD) is a medical condition that occurs when the contents of the stomach flow back into the esophagus, causing heartburn and in more severe cases, chest pain, dental erosions, and asthma (Antunes et al., 2021). This reflux of stomach contents back into the esophagus is caused by relaxation or incomplete closure of the lower esophageal sphincter – a ring of muscle that connects the esophagus to the stomach (Antunes et al., 2021; Mittal et al., 2006). Approximately 20% of adults in the US are diagnosed with GERD, making it one of the most common digestive disorders in the US (Antunes et al., 2021). Currently, therapies are focused on drug treatment or surgical therapies. However, these therapies can often have adverse effects or be invasive. Therefore, a more targeted therapy for GERD is needed.

Opening and closing of the lower esophageal sphincter (LES) is controlled by a region in the hindbrain called the dorsal motor nucleus of the vagus (DMV), which sends neuron axon projections to the LES to control sphincter tone and opening (Mittal et al., 2006). Inhibitory neurons located in the more caudal region of the DMV are involved in relaxing the sphincter, which may have some association with GERD

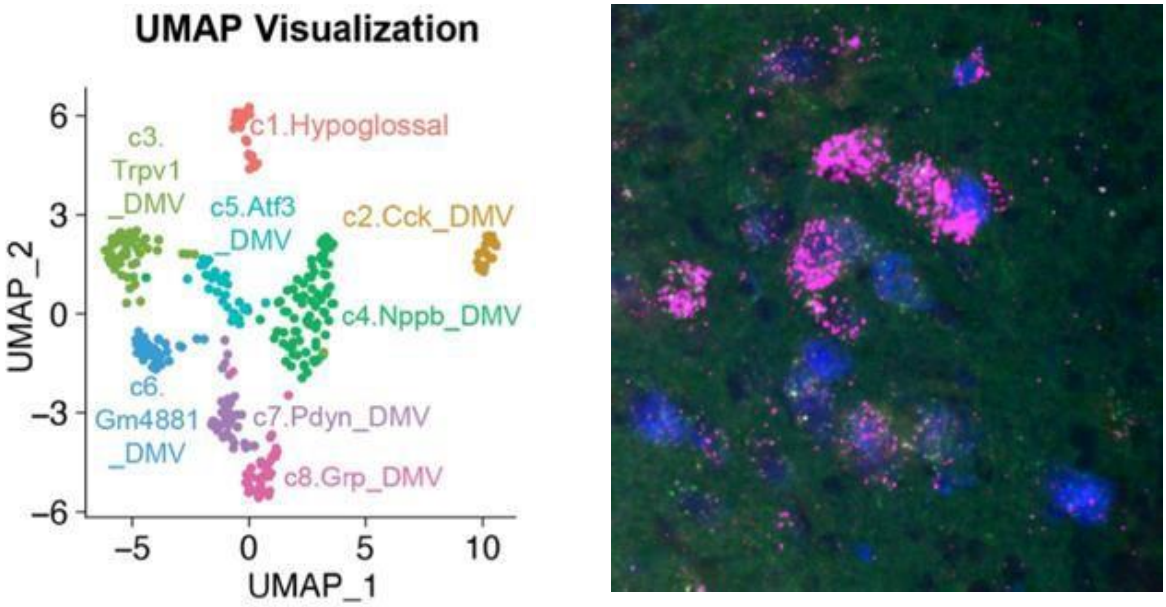

Figure 4-5. Identification of GRP DMV neurons in the caudal DMV

Left panel taken from Tao., J., Campbell, J.N., Tsai, L.T., Wu, C., Liberles, S.D., and Lowell, B.B. (2021). Highly selective brain-to-gut communication via genetically defined vagus neurons. Neuron *109*, 2106-2115.

Figure 4-5 Legend

UMAP visualization plot from single nuclei RNA-sequencing of all DMV neurons (left) (Tao. et al., 2021). Different DMV subtypes are grouped by color and determined by differential gene expression. Fluorescence in situ hybridization studies found GRP neurons exclusively in the caudal DMV (right, GRP in magenta, fluorogold neurons in blue)

(Antunes et al., 2021; Ogilvie et al., 1985). Thus, there is a need for a greater understanding of these neurons in the context of GERD.

Our preliminary single nuclei RNA-sequencing of the DMV uncovered seven different neuronal cell types in this region (Figure 4-5, left)(Tao. et al., 2021). In preliminary studies, we found that one of these subtypes identified by the gene marker GRP (gastrin releasing peptide), is found exclusively in the caudal DMV (Figure 4-5, right), leading us to hypothesize that this might be the DMV subtype involved in LES control. However, anatomical and functional studies are needed to further determine whether this subtype projects to the LES to control LES relaxation.

Further studies will be twofold – "mapping" of the GRP DMV neurons to determine if they send axons to the LES, and chronically activating these neurons to determine if this causes GERD in mice. To determine if the GRP DMV neurons project to the LES, the DMV of GRP-Cre (in which Cre recombinase is only expressed in GRP neurons) mice will be injected with a Cre recombinase dependent reporter virus. This will label all DMV GRP neurons and their axons. Following injection of this virus, the esophagus and stomach of these mice will be taken out and made optically transparent to allow for visualization of any axonal projections to the LES. This method has already been established in a positive control model in which all DMV neurons were labeled and the stomach and esophagus were harvested to visualize axonal innervations (Figure 4-6).

To determine if the GRP DMV neurons are responsible for inhibiting the LES, we will use intersectional genetics and chemogenetics to allow for targeted chronic activation of GRP DMV neurons. Using a mouse model in which GRP DMV neurons are activated

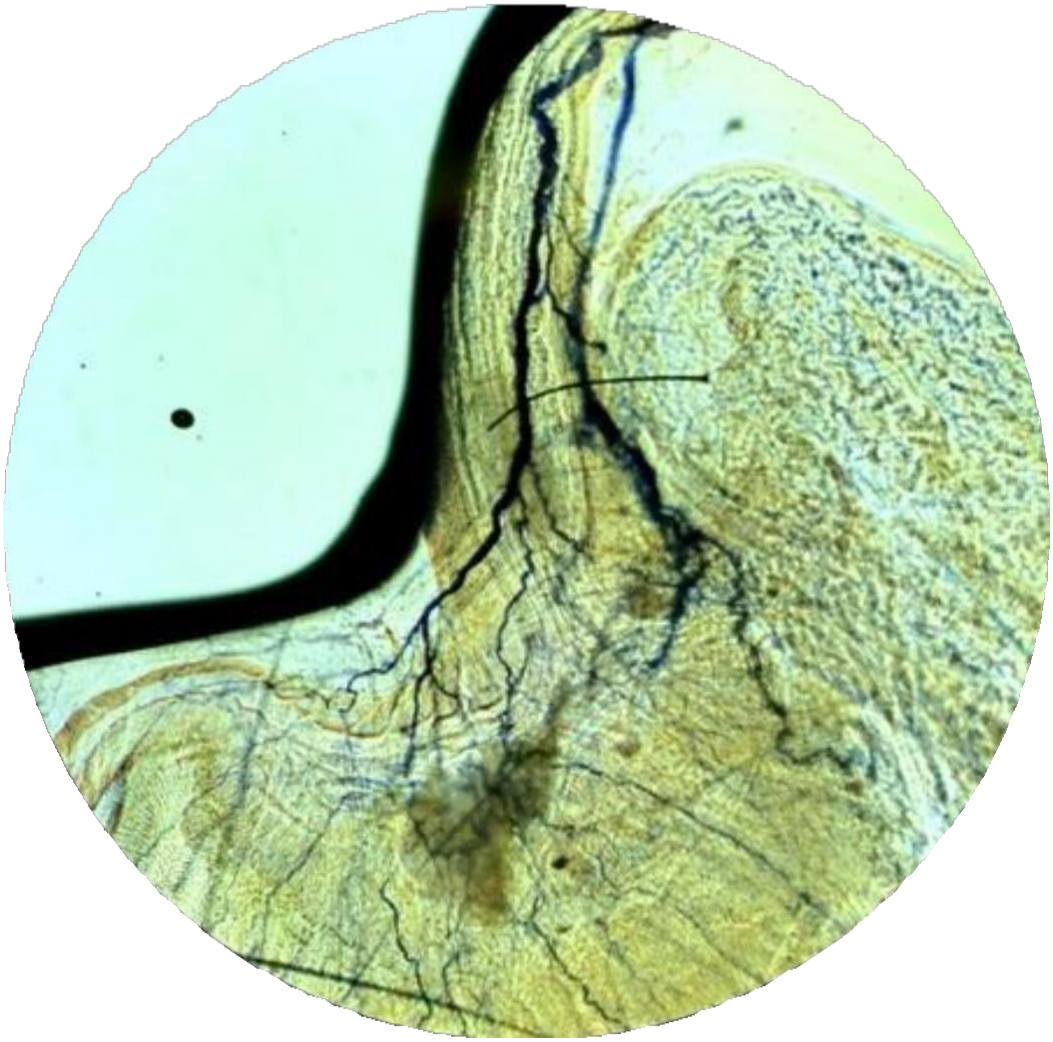

Figure 4-6. Axon projections to the LES and stomach from DMV neurons.

Figure 4-6 Legend

Labeling of all DMV neurons allowed for visualization of projections to the LES and stomach. Axons are shown in dark blue.

following intraperitoneal injection of CNO, we will chronically activate the GRP DMV neurons for 4 weeks in order to allow for possible GERD manifestations to be visible. Previous mouse models of GERD in which GERD was surgically induced saw drastic changes in the esophageal lining of mice following 4 weeks of induced GERD. Therefore, we will look at the esophagus of mice in which GRP DMV neurons are chronically activated and compare this to wildtype mice to see if there are any visible changes in the esophagus that are characteristic of GERD. Following completion of these studies, we expect to have projection profiling images of GRP DMV neurons projecting to the LES similar to what is seen in the positive control model. We also expect that chronic activation of GRP DMV neurons will also keep the LES chronically relaxed, which will cause GERD symptoms in mice. Therefore, given these results, we can make the conclusion that the GRP DMV neurons are responsible for projecting to the LES to control relaxation of this sphincter.

This study will reveal specific neural circuits that cause relaxation of the LES and thus allow for more targeted treatments of GERD. Furthermore, since we have the complete gene expression profile of GRP DMV neurons, we will also have a list of receptors, neuropeptides, and other signaling molecules that these neurons express, which are potential druggable targets for treating GERD. Together, these studies will reveal the cellular and molecular basis for neural control of LES relaxation and shed light on the underlying neurocircuitry of one of the most common digestive disorders: GERD.

CHAPTER 5. REFERENCES

Anderson, T.M., Garcia, A.J., 3rd, Baertsch, N.A., Pollak, J., Bloom, J.C., Wei, A.D., Rai, K.G., and Ramirez, J.M. (2016). A novel excitatory network for the control of breathing. Nature *536*, 76-80.

Bieger, D., and Hopkins, D.A. (1987). Viscerotopic representation of the upper alimentary tract in the medulla oblongata in the rat: the nucleus ambiguus. J Comp Neurol *262*, 546-562.

Cheng, Z., and Powley, T.L. (2000). Nucleus ambiguus projections to cardiac ganglia of rat atria: an anterograde tracing study. J Comp Neurol *424*, 588-606.

Daigle, T.L., Madisen, L., Hage, T.A., Valley, M.T., Knoblich, U., Larsen, R.S., Takeno, M.M., Huang, L., Gu, H., Larsen, R., *et al.* (2018). A Suite of Transgenic Driver and Reporter Mouse Lines with Enhanced Brain-Cell-Type Targeting and Functionality. Cell *174*, 465-480 e422.

Habib, N., Li, Y., Heidenreich, M., Swiech, L., Avraham-Davidi, I., Trombetta, J.J., Hession, C., Zhang, F., and Regev, A. (2016). Div-Seq: Single-nucleus RNA-Seq reveals dynamics of rare adult newborn neurons. Science *353*, 925-928.

Holstege, G., Graveland, G., Bijker-Biemond, C., and Schuddeboom, I. (1983). Location of motoneurons innervating soft palate, pharynx and upper esophagus. Anatomical evidence for a possible swallowing center in the pontine reticular formation. An HRP and autoradiographical tracing study. Brain Behav Evol *23*, 47-62.

Kobler, J.B., Datta, S., Goyal, R.K., and Benecchi, E.J. (1994). Innervation of the larynx, pharynx, and upper esophageal sphincter of the rat. J Comp Neurol *349*, 129-147.

Lee, B.H., Lynn, R.B., Lee, H.S., Miselis, R.R., and Altschuler, S.M. (1992). Calcitonin gene-related peptide in nucleus ambiguus motoneurons in rat: viscerotopic organization. J Comp Neurol *320*, 531-543.

Leong, S.K., and Ling, E.A. (1990). Labelling neurons with fluorescent dyes administered via intravenous, subcutaneous or intraperitoneal route. J Neurosci Methods *32*, 15-23.

McGovern, A.E., and Mazzone, S.B. (2010). Characterization of the vagal motor neurons projecting to the Guinea pig airways and esophagus. Front Neurol *1*, 153.

McWilliam, P.N., Maqbool, A., and Batten, T.F. (1989). Distribution of calcitonin gene-related peptide-like immunoreactivity in the nucleus ambiguus of the cat. J Comp Neurol *282*, 206-214.

Penagini, R., Picone, A., and Bianchi, P.A. (1996). Effect of morphine and naloxone on motor response of the human esophagus to swallowing and distension. Am J Physiol *271*, G675-680.

Picelli, S., Faridani, O.R., Bjorklund, A.K., Winberg, G., Sagasser, S., and Sandberg, R. (2014). Full-length RNA-seq from single cells using Smart-seq2. Nat Protoc *9*, 171-181.

Powley, T.L., Mittal, R.K., Baronowsky, E.A., Hudson, C.N., Martin, F.N., McAdams, J.L., Mason, J.K., and Phillips, R.J. (2013). Architecture of vagal motor units controlling striated muscle of esophagus: peripheral elements patterning peristalsis? Auton Neurosci *179*, 90-98.

Prescott, S.L., Umans, B.D., Williams, E.K., Brust, R.D., and Liberles, S.D. (2020). An Airway Protection Program Revealed by Sweeping Genetic Control of Vagal Afferents. Cell *181*, 574-589 e514.

Roh, H.C., Tsai, L.T., Lyubetskaya, A., Tenen, D., Kumari, M., and Rosen, E.D. (2017). Simultaneous Transcriptional and Epigenomic Profiling from Specific Cell Types within Heterogeneous Tissues In Vivo. Cell Rep *18*, 1048-1061.

Rossi, J., Balthasar, N., Olson, D., Scott, M., Berglund, E., Lee, C.E., Choi, M.J., Lauzon, D., Lowell, B.B., and Elmquist, J.K. (2011). Melanocortin-4 receptors expressed by cholinergic neurons regulate energy balance and glucose homeostasis. Cell Metab *13*, 195-204.

Sang, Q., and Young, H.M. (1998). The origin and development of the vagal and spinal innervation of the external muscle of the mouse esophagus. Brain Res *809*, 253-268.

Sherman, D., Worrell, J.W., Cui, Y., and Feldman, J.L. (2015). Optogenetic perturbation of preBotzinger complex inhibitory neurons modulates respiratory pattern. Nat Neurosci *18*, 408-414.

Stanek, E.t., Cheng, S., Takatoh, J., Han, B.X., and Wang, F. (2014). Monosynaptic premotor circuit tracing reveals neural substrates for oro-motor coordination. Elife *3*, e02511.

Tanaka, I., Ezure, K., and Kondo, M. (2003). Distribution of glycine transporter 2 mRNA-containing neurons in relation to glutamic acid decarboxylase mRNA-containing neurons in rat medulla. Neurosci Res *47*, 139-151.

Tao, J., Campbell, J.N., Tsai, L.T., Wu, C., Liberles, S.D., and Lowell, B.B. (2021). Highly selective brain-to-gut communication via genetically defined vagus neurons. Neuron *109*, 2106-2115 e2104.

Todd, W.D., Venner, A., Anaclet, C., Broadhurst, R.Y., De Luca, R., Bandaru, S.S., Issokson, L., Hablitz, L.M., Cravetchi, O., Arrigoni, E., *et al.* (2020). Suprachiasmatic

VIP neurons are required for normal circadian rhythmicity and comprised of molecularly distinct subpopulations. Nat Commun *11*, 4410.

Abrahams, T.P., Partosoedarso, E.R., and Hornby, P.J. (2002). Lower oesophageal sphincter relaxation evoked by stimulation of the dorsal motor nucleus of the vagus in ferrets. Neurogastroenterol Motil *14*, 295-304.

Altschuler, S.M. (2001). Laryngeal and respiratory protective reflexes. Am J Med *111 Suppl 8A*, 90S-94S.

Anderson, T.M., Garcia, A.J., 3rd, Baertsch, N.A., Pollak, J., Bloom, J.C., Wei, A.D., Rai, K.G., and Ramirez, J.M. (2016b). A novel excitatory network for the control of breathing. Nature *536*, 76-80.

Antunes, C., Aleem, A., and Curtis, S. (2021). Gastroesophageal Reflux Disease. (StatPearls Publishing).

Bai, L., Mesgarzadeh, S., Ramesh, K.S., Huey, E.L., Liu, Y., Gray, L.A., Aitken, T.J., Chen, Y., Beutler, L.R., Ahn, J.S., *et al.* (2019). Genetic Identification of Vagal Sensory Neurons That Control Feeding. Cell *179*, 1129-1143 e1123.

Bartlett, D., Jr. (1989). Respiratory functions of the larynx. Physiol Rev *69*, 33-57.

Bauman, N.M., Wang, D., Jaffe, D.A., Sandler, A.D., and Luschei, E.S. (1999). Effect of intravenous calcitonin gene-related peptide antagonist on the laryngeal chemoreflex in piglets. Otolaryngol Head Neck Surg *121*, 1-6.

Bell, Z.W., Lovell, P., Mello, C.V., Yip, P.K., George, J.M., and Clayton, D.F. (2019). Urotensin-related gene transcripts mark developmental emergence of the male forebrain vocal control system in songbirds. Sci Rep *9*, 816.

Bieger, D., and Hopkins, D. (1987). Viscerotopic representation of the upper alimentary tract in the medulla oblongata in the rat: the nucleus ambiguus. The Journal of comparative neurology *262* 546-562.

Blum, J.A., Klemm, S., Shadrach, J.L., Guttenplan, K.A., Nakayama, L., Kathiria, A., Hoang, P.T., Gautier, O., Kaltschmidt, J.A., Greenleaf, W.J., *et al.* (2021). Single-cell transcriptomic analysis of the adult mouse spinal cord reveals molecular diversity of autonomic and skeletal motor neurons. Nat Neurosci *24*, 572-583.

Bonaz, B., Picq, C., Sinniger, V., Mayol, J.F., and Clarencon, D. (2013). Vagus nerve stimulation: from epilepsy to the cholinergic anti-inflammatory pathway. Neurogastroenterol Motil *25*, 208-221.

Borgmann, D., Ciglieri, E., Biglari, N., Brandt, C., Cremer, A.L., Backes, H., Tittgemeyer, M., Wunderlich, F.T., Bruning, J.C., and Fenselau, H. (2021). Gut-brain

communication by distinct sensory neurons differently controls feeding and glucose metabolism. Cell Metab *33*, 1466-1482 e1467.

Calupca, M.A., Vizzard, M.A., and Parsons, R.L. (2000). Origin of pituitary adenylate cyclase-activating polypeptide (PACAP)-immunoreactive fibers innervating guinea pig parasympathetic cardiac ganglia. J Comp Neurol *423*, 26-39.

Carpenter, D. (1989). Central nervous system mechanisms in deglutition and emesis. In Handbook of Physiology The Gastrointestinal System Motility and Circulation
(Bethesda, MD), pp. 685–714.

Caubit, X., Thoby-Brisson, M., Voituron, N., Filippi, P., Bevengut, M., Faralli, H., Zanella, S., Fortin, G., Hilaire, G., and Fasano, L. (2010). Teashirt 3 regulates development of neurons involved in both respiratory rhythm and airflow control. The Journal of neuroscience : the official journal of the Society for Neuroscience *30*, 9465-9476.

Chang, H.Y., Mashimo, H., and Goyal, R.K. (2003). Musings on the wanderer: what's new in our understanding of vago-vagal reflex? IV. Current concepts of vagal efferent projections to the gut. Am J Physiol Gastrointest Liver Physiol *284*, G357-366.

Chang, R.B., Strochlic, D.E., Williams, E.K., Umans, B.D., and Liberles, S.D. (2015). Vagal Sensory Neuron Subtypes that Differentially Control Breathing. Cell *161*, 622-633.

Cheng, Z., and Powley, T.L. (2000). Nucleus ambiguus projections to cardiac ganglia of rat atria: an anterograde tracing study. J Comp Neurol *424*, 588-606.

Compton, D., Hill, P.M., and Sinclair, J.D. (1973). Weight-lifters' blackout. Lancet *2*, 1234-1237.

Coote, J.H. (2013). Myths and realities of the cardiac vagus. J Physiol *591*, 4073-4085.

Costantini, M., Salvador, R., and Costantini, A. (2022). Esophageal Achalasia: Pros and Cons of the Treatment Options. World J Surg *46*, 1554-1560.

Coverdell, T.C., Abraham-Fan, R.J., Wu, C., Abbott, S.B.G., and Campbell, J.N. (2022). Genetic encoding of an esophageal motor circuit. Cell Rep *39*, 110962.

Daigle, T.L., Madisen, L., Hage, T.A., Valley, M.T., Knoblich, U., Larsen, R.S., Takeno, M.M., Huang, L., Gu, H., Larsen, R., *et al.* (2018). A Suite of Transgenic Driver and Reporter Mouse Lines with Enhanced Brain-Cell-Type Targeting and Functionality. Cell *174*, 465-480 e422.

Dergacheva, O., Griffioen, K.J., Neff, R.A., and Mendelowitz, D. (2010). Respiratory modulation of premotor cardiac vagal neurons in the brainstem. Respir Physiol Neurobiol *174*, 102-110.

Desmedt, J. (1981). Motor unit types, recruitment and plasticity in health and disease. Progress in Clinical Neurophysiology *9*, 418.

Diamant, N. (1989). Gastroenterology Clinics of North America. Motility Disorders, Vol 18 (Philadelphia, PA: Saunders).

Dobin, A., Davis, C.A., Schlesinger, F., Drenkow, J., Zaleski, C., Jha, S., Batut, P., Chaisson, M., and Gingeras, T.R. (2013). STAR: ultrafast universal RNA-seq aligner. Bioinformatics *29*, 15-21.

Doty, R. (1968). Neural organization of deglutition, Vol IV (Washington, DC: Am Physiol Soc).

Doty, R., and Bosma, J. (1956). An electromyographic analysis of reflex deglutition. . J Neurophysiol *19*, 44-60.

Drake., R.L., Vogl., W., Mitchell., A.W., and Gray., H. (2010). Gray's Anatomy for Students (Churchill Livingstone/Elsevier).

Duchateau, J., and Enoka, R. (2011). Human motor unit recordings: origins and insight into the integrated motor system. Brain Res *1409*, 42-61.

Edmundowicz, S., and Clouse, R. (1991). Shortening of the esophagus in response to swallowing. . The American journal of physiology *260*, G512-516.

Fahy, B.G. (2010). Intraoperative and perioperative complications with a vagus nerve stimulation device. J Clin Anesth *22*, 213-222.

Fisher, J.T., Vincent, S.G., Gomeza, J., Yamada, M., and Wess, J. (2004). Loss of vagally mediated bradycardia and bronchoconstriction in mice lacking M2 or M3 muscarinic acetylcholine receptors. FASEB J *18*, 711-713.

Foster, G.E., and Sheel, A.W. (2005). The human diving response, its function, and its control. Scand J Med Sci Sports *15*, 3-12.

Franciosi, S., Perry, F.K.G., Roston, T.M., Armstrong, K.R., Claydon, V.E., and Sanatani, S. (2017). The role of the autonomic nervous system in arrhythmias and sudden cardiac death. Auton Neurosci *205*, 1-11.

French, C.A., Groszer, M., Preece, C., Coupe, A.M., Rajewsky, K., and Fisher, S.E. (2007). Generation of mice with a conditional Foxp2 null allele. Genesis *45*, 440-446.

Fujita, E., Tanabe, Y., Shiota, A., Ueda, M., Suwa, K., Momoi, M.Y., and Momoi, T. (2008). Ultrasonic vocalization impairment of Foxp2 (R552H) knockin mice related to speech-language disorder and abnormality of Purkinje cells. Proceedings of the National Academy of Sciences of the United States of America *105*, 3117-3122.

Garamendi-Ruiz, I., and Gomez-Esteban, J.C. (2019). Cardiovascular autonomic effects of vagus nerve stimulation. Clin Auton Res *29*, 183-194.

Gibbons, C.H. (2019). Chapter 27 - Basics of autonomic nervous system function, Vol 160 (Elsevier).

Gidda, J., and Goyal, R. (1984). Swallow-evoked action potentials in vagal preganglionic efferents. . J Neurophysiol *52*, 1169-1180.

Godek, D., and Freeman, A. (2021). Physiology, Diving Reflex (Florida: StatPearls Publishing).

Gourine, A.V., Machhada, A., Trapp, S., and Spyer, K.M. (2016). Cardiac vagal preganglionic neurones: An update. Auton Neurosci *199*, 24-28.

Goyal, R., and Chaudhury, A. (2008a). Physiology of normal esophageal motility. J Clin Gastroenterol *42*, 610-619.

Goyal, R., and Cobb, B. (1981). Motility of the pharynx, esophagus and esophageal sphincters (New York: Raven).

Habib, N., Li, Y., Heidenreich, M., Swiech, L., Avraham-Davidi, I., Trombetta, J.J., Hession, C., Zhang, F., and Regev, A. (2016). Div-Seq: Single-nucleus RNA-Seq reveals dynamics of rare adult newborn neurons. Science *353*, 925-928.

Hao, Y., Hao, S., Andersen-Nissen, E., Mauck, W.M., 3rd, Zheng, S., Butler, A., Lee, M.J., Wilk, A.J., Darby, C., Zager, M., *et al.* (2021). Integrated analysis of multimodal single-cell data. Cell *184*, 3573-3587 e3529.

Haque, A., Engel, J., Teichmann, S.A., and Lonnberg, T. (2017). A practical guide to single-cell RNA-sequencing for biomedical research and clinical applications. Genome Med *9*, 75.

Haselton, J.R., Solomon, I.C., Motekaitis, A.M., and Kaufman, M.P. (1992). Bronchomotor vagal preganglionic cell bodies in the dog: an anatomic and functional study. J Appl Physiol (1985) *73*, 1122-1129.

Haxhiu, M.A., Chavez, J.C., Pichiule, P., Erokwu, B., and Dreshaj, I.A. (2000). The excitatory amino acid glutamate mediates reflexly increased tracheal blood flow and airway submucosal gland secretion. Brain Res *883*, 77-86.

Hayakawa, T., Zheng, J.Q., Maeda, S., Ito, H., Seki, M., and Yajima, Y. (1999). Synaptology and ultrastructural characteristics of laryngeal cricothyroid and posterior cricoarytenoid motoneurons in the nucleus ambiguus of the rat. Anat Embryol (Berl) *200*, 301-311.

Hayano, J., Yasuma, F., Okada, A., Mukai, S., and Fujinami, T. (1996). Respiratory sinus arrhythmia. A phenomenon improving pulmonary gas exchange and circulatory efficiency. Circulation *94*, 842-847.

Hernandez-Miranda, L.R., Ruffault, P.L., Bouvier, J.C., Murray, A.J., Morin-Surun, M.P., Zampieri, N., Cholewa-Waclaw, J.B., Ey, E., Brunet, J.F., Champagnat, J., *et al.* (2017). Genetic identification of a hindbrain nucleus essential for innate vocalization. Proceedings of the National Academy of Sciences of the United States of America *114*, 8095-8100.

Holstege, G., G., G., C., B.-B., and I., S. (1983a). Location of motoneurons innervating soft palate, pharynx and upper esophagus. Anatomical evidence for a possible swallowing center in the pontine reticular formation. An HRP and autoradiographical tracing study. Brain Behav Evol *23*, 47-62.

Holstege, G., Graveland, G., Bijker-Biemond, C., and Schuddeboom, I. (1983b). Location of motoneurons innervating soft palate, pharynx and upper esophagus. Anatomical evidence for a possible swallowing center in the pontine reticular formation. An HRP and autoradiographical tracing study. Brain Behav Evol *23*, 47-62.

Holstege, G., and Subramanian, H.H. (2016). Two different motor systems are needed to generate human speech. J Comp Neurol *524*, 1558-1577.

Huang, X.F., Tork, I., and Paxinos, G. (1993). Dorsal motor nucleus of the vagus nerve: a cyto- and chemoarchitectonic study in the human. J Comp Neurol *330*, 158-182.

Hult, E.M., Bingaman, M.J., and Swoap, S.J. (2019). A robust diving response in the laboratory mouse. J Comp Physiol B *189*, 685-692.

Ingelfinger, F. (1958). Esophageal Motility. Physiol Rev *38*, 533-534.

Jean, A. (1990). Brainstem control of swallowing: localization and organization of the central pattern generator for swallowing (London: MacMillan).

Jean, A. (2001a). Brain Stem Control of Swallowing: Neuronal Network and Cellular Mechanisms. Physiological Reviews *81*, 929-969.

Johnson, R.L., and Wilson, C.G. (2018). A review of vagus nerve stimulation as a therapeutic intervention. J Inflamm Res *11*, 203-213.

Kahrilas, P. (1992). Functional anatomy and physiology of the esophagus (Boston: Little, Brown).

Kamitakahara, A., Wu, H.H., and Levitt, P. (2017). Distinct projection targets define subpopulations of mouse brainstem vagal neurons that express the autism-associated MET receptor tyrosine kinase. J Comp Neurol *525*, 3787-3808.

Kamitakahara, A.K., Ali Marandi Ghoddousi, R., Lanjewar, A.L., Magalong, V.M., Wu, H.H., and Levitt, P. (2021). MET Receptor Tyrosine Kinase Regulates Lifespan Ultrasonic Vocalization and Vagal Motor Neuron Development. Front Neurosci *15*, 768577.

Kapa, S., DeSimone, C.V., and Asirvatham, S.J. (2016). Innervation of the heart: An invisible grid within a black box. Trends Cardiovasc Med *26*, 245-257.

Kc, P., Mayer, C.A., and Haxhiu, M.A. (2004). Chemical profile of vagal preganglionic motor cells innervating the airways in ferrets: the absence of noncholinergic neurons. J Appl Physiol (1985) *97*, 1508-1517.

Kobler, J., Datta, S., Goyal, R., and Benecchi, E. (1994a). Innervation of the Larynx, Pharynx, and Upper Espohageal Sphincter of the Rat. THE JOURNAL OF COMPARATIVE NEUROLOGY *349*, 129-147.

Kobler, J.B., Datta, S., Goyal, R.K., and Benecchi, E.J. (1994b). Innervation of the larynx, pharynx, and upper esophageal sphincter of the rat. J Comp Neurol *349*, 129-147.

Kupari, J., Haring, M., Agirre, E., Castelo-Branco, G., and Ernfors, P. (2019). An Atlas of Vagal Sensory Neurons and Their Molecular Specialization. Cell Rep *27*, 2508-2523 e2504.

Lang, I.M. (2009). Brain stem control of the phases of swallowing. Dysphagia *24*, 333-348.

Langley, J.N. (1897). On the Regeneration of Pre-Ganglionic and of Post-Ganglionic Visceral Nerve Fibres. J Physiol *22*, 215-230.

Lawn, A.M. (1964). The localization, by means of electrical stimulation of the origin and path in the medulla oblongata of the motor nerve fibres of the rabbit oesophagus. J Physiol (Lond) *174*, 232-244.

Lawn, A.M. (1966a). The localization, in the nucleus ambiguus of the rabbit, of the cells of origin of motor nerve fibers in the glossopharyngeal nerve and various branches of the vagus nerve by means of retrograde degeneration. The Journal of comparative neurology *127*, 293-306.

Lawn, A.M. (1966b). The nucleus ambiguus of the rabbit. J Comp Neurol *127*, 307-320.

Lee, B.H., Lynn, R.B., Lee, H.S., Miselis, R.R., and Altschuler, S.M. (1992). Calcitonin gene-related peptide in nucleus ambiguus motoneurons in rat: viscerotopic organization. J Comp Neurol *320*, 531-543.

Lein, E.S., Hawrylycz, M.J., Ao, N., Ayres, M., Bensinger, A., Bernard, A., Boe, A.F., Boguski, M.S., Brockway, K.S., Byrnes, E.J., *et al.* (2007). Genome-wide atlas of gene expression in the adult mouse brain. Nature *445*, 168-176.

Leiter, J.C., and Bohm, I. (2007). Mechanisms of pathogenesis in the Sudden Infant Death Syndrome. Respir Physiol Neurobiol *159*, 127-138.

Leong, S.K., and Ling, E.A. (1990). Labelling neurons with fluorescent dyes administered via intravenous, subcutaneous or intraperitoneal route. J Neurosci Methods *32*, 15-23.

Liddle, R.A. (2018). Physiology of the Gastrointestinal Tract, Vol 6th Edition (Academic Press).

Liu, L., Zhao, M., Yu, X., and Zang, W. (2019). Pharmacological Modulation of Vagal Nerve Activity in Cardiovascular Diseases. Neurosci Bull *35*, 156-166.

Loewi, O. (1921). Über humorale übertragbarkeit der Herznervenwirkung. Pflügers Arch Ges Physiol *189*, 239-242.

Luo, L., Callaway, E.M., and Svoboda, K. (2018). Genetic Dissection of Neural Circuits: A Decade of Progress. Neuron *98*, 256-281.

Marzec, M., Edwards, J., Sagher, O., Fromes, G., and Malow, B.A. (2003). Effects of vagus nerve stimulation on sleep-related breathing in epilepsy patients. Epilepsia *44*, 930-935.

Matsuo, K., and Palmer, J. (2008). Anatomy and Physiology of Feeding and Swallowing - Normal and Abnormal. Phys Med Rehabil Clin N Am *19*, 691-707.

Mawe, G.M., Lavoie, B., Nelson, M.T., and Pozo, M.J. (2018). Physiology of the Gastrointestinal Tract, Vol 6th Edition.

Mazzone, S.B., and Canning, B.J. (2013). Autonomic neural control of the airways. Handb Clin Neurol *117*, 215-228.

McAllen, R.M., and Spyer, K.M. (1978). Two types of vagal preganglionic motoneurones projecting to the heart and lungs. J Physiol *282*, 353-364.

McGovern, A.E., and Mazzone, S.B. (2010). Characterization of the vagal motor neurons projecting to the Guinea pig airways and esophagus. Front Neurol *1*, 153.

McWilliam, P.N., Maqbool, A., and Batten, T.F. (1989). Distribution of calcitonin gene-related peptide-like immunoreactivity in the nucleus ambiguus of the cat. J Comp Neurol *282*, 206-214.

Mendelowitz (1996a). Firing properties of identified parasympathetic cardiac neurons in nucleus ambiguus. Am J Physi *271*, 5.

Mendelowitz, D. (1996b). Firing properties of identified parasympathetic cardiac neurons in nucleus ambiguus. Am J Physiol *271*, H2609-2614.

Mi, H., Ebert, D., Muruganujan, A., Mills, C., Albou, L.P., Mushayamaha, T., and Thomas, P.D. (2021). PANTHER version 16: a revised family classification, tree-based classification tool, enhancer regions and extensive API. Nucleic Acids Res *49*, D394-D403.

Miller, A. (1982). Deglutition. . Physiol Rev *62*, 129–184.

Miller, A.J. (2002). Oral and pharyngeal reflexes in the mammalian nervous system: their diverse range in complexity and the pivotal role of the tongue. Crit Rev Oral Biol Med *13*, 409-425.

Mittal, R., Padda, B., Bhalla, V., Bhargava, V., and Liu, J. (2006). Synchrony between circular and longitudinal muscle contractions during peristalsis in normal subjects. . Am J Physiol Gastrointest Liver Physiol *290*, G431-438.

Miura, H., Quadros, R.M., Gurumurthy, C.B., and Ohtsuka, M. (2018). Easi-CRISPR for creating knock-in and conditional knockout mouse models using long ssDNA donors. Nat Protoc *13*, 195-215.

Molfino, N.A., Slutsky, A.S., Julia-Serda, G., Hoffstein, V., Szalai, J.P., Chapman, K.R., Rebuck, A.S., and Zamel, N. (1993). Assessment of airway tone in asthma. Comparison between double lung transplant patients and healthy subjects. Am Rev Respir Dis *148*, 1238-1243.

Mu, L., and Sanders, I. (2007). Neuromuscular Specializations Within Human Pharyngeal
Constrictor Muscles. Annals of Otology, Rhinology & Laryngology *116*, 604-617.

Neuhuber, W.L., and Berthoud, H.R. (2021). Functional anatomy of the vagus system - Emphasis on the somato-visceral interface. Auton Neurosci *236*, 102887.

Nosaka, S., Yamamoto, T., and Yasunaga, K. (1979). Localization of vagal cardioinhibitory preganglionic neurons with rat brain stem. J Comp Neurol *186*, 79-92.

Nunez-Abades, P.A., Pasaro, R., and Bianchi, A.L. (1992). Study of the topographical distribution of different populations of motoneurons within rat's nucleus ambiguus, by means of four different fluorochromes. Neurosci Lett *135*, 103-107.

Oda, Y. (1999). Choline acetyltransferase: the structure, distribution and pathologic changes in the central nervous system. Pathol Int *49*, 921-937.

Ogilvie, A.L., James, P.D., and Atkinson, M. (1985). Impairment of vagal function in reflux oesophagitis. Q J Med *54*, 61-74.

Olshansky, B., Sabbah, H.N., Hauptman, P.J., and Colucci, W.S. (2008). Parasympathetic nervous system and heart failure: pathophysiology and potential implications for therapy. Circulation *118*, 863-871.

P.N. McWILLIAM, A.M., T.F.C. BATTEN (1989). Distribution of Calcitonin Gene-Related Peptide-Like Immunoreactivity in the Nucleus Ambiguus of the Cat. THE JOURNAL OF COMPARATIVE NEUROLOGY, 9.

Panebianco, M., Marchese-Ragona, R., Masiero, S., and Restivo, D. (2020). Dysphagia in neurological diseases: a literature review. . Neurol Sci *41*, 3067-3073.

Panneton, W.M. (2013). The mammalian diving response: an enigmatic reflex to preserve life? Physiology (Bethesda) *28*, 284-297.

Panneton, W.M., Anch, A.M., Panneton, W.M., and Gan, Q. (2014). Parasympathetic preganglionic cardiac motoneurons labeled after voluntary diving. Front Physiol *5*, 8.

Panneton, W.M., and Gan, Q. (2020). The Mammalian Diving Response: Inroads to Its Neural Control. Front Neurosci *14*, 524.

Penagini, R., Picone, A., and Bianchi, P.A. (1996). Effect of morphine and naloxone on motor response of the human esophagus to swallowing and distension. Am J Physiol *271*, G675-680.

Petko, B., and Tadi, P. (2022). Neuroanatomy, Nucleus Ambiguus. In StatPearls (Treasure Island (FL)).

Picelli, S., Faridani, O.R., Bjorklund, A.K., Winberg, G., Sagasser, S., and Sandberg, R. (2014). Full-length RNA-seq from single cells using Smart-seq2. Nat Protoc *9*, 171-181.

Powley, T.L., Mittal, R.K., Baronowsky, E.A., Hudson, C.N., Martin, F.N., McAdams, J.L., Mason, J.K., and Phillips, R.J. (2013a). Architecture of vagal motor units controlling striated muscle of esophagus: peripheral elements patterning peristalsis? Auton Neurosci *179*, 90-98.

Powley, T.L., Mittal, R.K., Baronowsky, E.A., Hudson, C.N., Martin, F.N., McAdams, J.L., Mason, J.K., and Phillips, R.J. (2013b). Architecture of vagal motor units controlling striated muscle of esophagus: peripheral elements patterning peristalsis? Auton Neurosci *179*, 90-98.

Prescott, S.L., Umans, B.D., Williams, E.K., Brust, R.D., and Liberles, S.D. (2020). An Airway Protection Program Revealed by Sweeping Genetic Control of Vagal Afferents. Cell *181*, 574-589 e514.

Rajendran, P.S., Challis, R.C., Fowlkes, C.C., Hanna, P., Tompkins, J.D., Jordan, M.C., Hiyari, S., Gabris-Weber, B.A., Greenbaum, A., Chan, K.Y., *et al.* (2018). Identification of peripheral neural circuits that regulate heart rate using optogenetic and viral vector strategies. bioRxiv, 456483.

Restivo, D.A., Marchese-Ragona, R., Lauria, G., Squatrito, S., Gullo, D., and Vigneri, R. (2006). Botulinum toxin treatment for oropharyngeal dysphagia associated with diabetic neuropathy. Diabetes Care *29*, 2650-2653.

Robbins, J. (1999). The evolution of swallowing neuroanatomy and physiology in humans: a practical perspective. . Ann Neurol *46*, 279–280.

Rogers, R., Hermann, G., and Travagli, R. (1999). Brainstem pathways responsible for oesophageal control of gastric motility and tone in the rat. J Physiol *514*, 369-383.

Rogers, R.C., and Hermann, G.E. (2012). Physiology of the Gastrointestinal Tract, Vol 5th Edition (Academic Press).

Roh, H.C., Tsai, L.T., Lyubetskaya, A., Tenen, D., Kumari, M., and Rosen, E.D. (2017). Simultaneous Transcriptional and Epigenomic Profiling from Specific Cell Types within Heterogeneous Tissues In Vivo. Cell Rep *18*, 1048-1061.

Roman, C., and Gonella, J. (1987). Extrinsic control of digestive tract motility, Vol 2nd Edition (New York: Raven).

Rossi, J., Balthasar, N., Olson, D., Scott, M., Berglund, E., Lee, C.E., Choi, M.J., Lauzon, D., Lowell, B.B., and Elmquist, J.K. (2011). Melanocortin-4 receptors expressed by cholinergic neurons regulate energy balance and glucose homeostasis. Cell Metab *13*, 195-204.

Rossiter, C.D., Norman, W.P., Jain, M., Hornby, P.J., Benjamin, S., and Gillis, R.A. (1990). Control of lower esophageal sphincter pressure by two sites in dorsal motor nucleus of the vagus. Am J Physiol *259*, G899-906.

Sang, Q., and Young, H.M. (1998). The origin and development of the vagal and spinal innervation of the external muscle of the mouse esophagus. Brain Res *809*, 253-268.

Sataloff, R.T., Chowdhury, F., Portnoy, J., Hawkshaw, M.J., and S., J. (2013). Surgical Techniques in Otolaryngology – Head and Neck Surgery: Laryngeal Surgery (New Delhi, India: Jaypee Brothers Medical Publishers).

Schubert, M.L., and Peura, D.A. (2008). Control of Gastric Acid Secretion in Health and Disease. Gastroenterology *134*, 1842-1860.

Seebeck, J., Schmidt, W.E., Kilbinger, H., Neumann, J., Zimmermann, N., and Herzig, S. (1996). PACAP induces bradycardia in guinea-pig heart by stimulation of atrial cholinergic neurones. Naunyn Schmiedebergs Arch Pharmacol *354*, 424-430.

Sharpey-Schafer, E.P. (1953). The mechanism of syncope after coughing. Br Med J *2*, 860-863.

Sherman, D., Worrell, J.W., Cui, Y., and Feldman, J.L. (2015). Optogenetic perturbation of preBotzinger complex inhibitory neurons modulates respiratory pattern. Nat Neurosci *18*, 408-414.

Shiba, K., Satoh, I., Kobayashi, N., and Hayashi, F. (1999). Multifunctional Laryngeal Motoneurons: an Intracellular Study in the Cat. J Neurosci *19*, 2717-2727.

Shiina, T., Shimizu, Y., Izumi, N., Suzuki, Y., Asano, M., Atoji, Y., Nikami, H., and Takewaki, T. (2005). A comparative histological study on the distribution of striated and smooth muscles and glands in the esophagus of wild birds and mammals. J Vet Med Sci *67*, 115-117.

Shu, W., Cho, J.Y., Jiang, Y., Zhang, M., Weisz, D., Elder, G.A., Schmeidler, J., De Gasperi, R., Sosa, M.A., Rabidou, D., *et al.* (2005). Altered ultrasonic vocalization in mice with a disruption in the Foxp2 gene. Proceedings of the National Academy of Sciences of the United States of America *102*, 9643-9648.

Silvani, A., Calandra-Buonaura, G., Dampney, R.A., and Cortelli, P. (2016). Brain-heart interactions: physiology and clinical implications. Philos Trans A Math Phys Eng Sci *374*.

Smith-White, M.A., Herzog, H., and Potter, E.K. (2002). Role of neuropeptide Y Y(2) receptors in modulation of cardiac parasympathetic neurotransmission. Regul Pept *103*, 105-111.

Stanek, E.t., Cheng, S., Takatoh, J., Han, B.X., and Wang, F. (2014). Monosynaptic premotor circuit tracing reveals neural substrates for oro-motor coordination. Elife *3*, e02511.

Sturrock, R.R. (1990). A comparison of age-related changes in neuron number in the dorsal motor nucleus of the vagus and the nucleus ambiguus of the mouse. J Anat *173*, 169-176.

Suh, M.K., Kim, H., and Na, D.L. (2009). Dysphagia in patients with dementia: Alzheimer versus vascular. Alzheimer Dis Assoc Disord *23*, 178-184.

Tack, J., and Pandolfino, J.E. (2018). Pathophysiology of Gastroesophageal Reflux Disease. Gastroenterology *154*, 277-288.

Takanaga, A., Hayakawa, T., Tanaka, K., Kawabata, K., Maeda, S., and Seki, M. (2003). Immunohistochemical characterization of cardiac vagal preganglionic neurons in the rat. Autonomic Neuroscience *106*, 132-137.

Tanaka, I., Ezure, K., and Kondo, M. (2003). Distribution of glycine transporter 2 mRNA-containing neurons in relation to glutamic acid decarboxylase mRNA-containing neurons in rat medulla. Neurosci Res *47*, 139-151.

Tang, F., Barbacioru, C., Wang, Y., Nordman, E., Lee, C., Xu, N., Wang, X., Bodeau, J., Tuch, B.B., Siddiqui, A., *et al.* (2009). mRNA-Seq whole-transcriptome analysis of a single cell. Nature methods *6*, 377-382.

Tao, J., Campbell, J.N., Tsai, L.T., Wu, C., Liberles, S.D., and Lowell, B.B. (2021). Highly selective brain-to-gut communication via genetically defined vagus neurons. Neuron *109*, 2106-2115 e2104.

Tao., J., Campbell, J.N., Tsai, L.T., Wu, C., Liberles, S.D., and Lowell, B.B. (2021). Highly selective brain-to-gut communication via genetically defined vagus neurons. Neuron *109*, 2106-2115.

Taylor, E.W., Jordan, D., and Coote, J.H. (1999). Central control of the cardiovascular and respiratory systems and their interactions in vertebrates. Physiol Rev *79*, 855-916.

Taylor, E.W., Leite, C.A., Sartori, M.R., Wang, T., Abe, A.S., and Crossley, D.A., 2nd (2014). The phylogeny and ontogeny of autonomic control of the heart and cardiorespiratory interactions in vertebrates. J Exp Biol *217*, 690-703.

Thach, B.T. (2008). Some aspects of clinical relevance in the maturation of respiratory control in infants. J Appl Physiol (1985) *104*, 1828-1834.

Todd, W.D., Venner, A., Anaclet, C., Broadhurst, R.Y., De Luca, R., Bandaru, S.S., Issokson, L., Hablitz, L.M., Cravetchi, O., Arrigoni, E., *et al.* (2020). Suprachiasmatic VIP neurons are required for normal circadian rhythmicity and comprised of molecularly distinct subpopulations. Nat Commun *11*, 4410.

Topert, C., Doring, F., Wischmeyer, E., Karschin, C., Brockhaus, J., Ballanyi, K., Derst, C., and Karschin, A. (1998). Kir2.4: a novel K+ inward rectifier channel associated with motoneurons of cranial nerve nuclei. J Neurosci *18*, 4096-4105.

Urbanus, B.H.A., Peter, S., Fisher, S.E., and De Zeeuw, C.I. (2020). Region-specific Foxp2 deletions in cortex, striatum or cerebellum cannot explain vocalization deficits observed in spontaneous global knockouts. Sci Rep *10*, 21631.

Veerakumar, A., Yung, A.R., Liu, Y., and Krasnow, M.A. (2022). Molecularly defined circuits for cardiovascular and cardiopulmonary control. Nature *606*, 739-746.

Wake, E., and Brack, K. (2016). Characterization of the intrinsic cardiac nervous system. Auton Neurosci *199*, 3-16.

Wang, F., Flanagan, J., Su, N., Wang, L.C., Bui, S., Nielson, A., Wu, X., Vo, H.T., Ma, X.J., and Luo, Y. (2012). RNAscope: a novel in situ RNA analysis platform for formalin-fixed, paraffin-embedded tissues. J Mol Diagn *14*, 22-29.

Wang, X., Guo, R., Zhao, W., and Pilowsky, P.M. (2016). Medullary mediation of the laryngeal adductor reflex: A possible role in sudden infant death syndrome. Respir Physiol Neurobiol *226*, 121-127.

Wehrwein, E.A., and Joyner, M.J. (2013). Regulation of blood pressure by the arterial baroreflex and autonomic nervous system. Handb Clin Neurol *117*, 89-102.

Williams, E.K., Chang, R.B., Strochlic, D.E., Umans, B.D., Lowell, B.B., and Liberles, S.D. (2016). Sensory Neurons that Detect Stretch and Nutrients in the Digestive System. Cell *166*, 209-221.

Wolf, D.C. (1990). Dysphagia. In Clinical Methods: The History, Physical, and Laboratory Examinations, rd, H.K. Walker, W.D. Hall, and J.W. Hurst, eds. (Boston).

Wu, R., Dong, W., Cui, X., Zhou, M., Simms, H.H., Ravikumar, T.S., and Wang, P. (2007a). Ghrelin down-regulates proinflammatory cytokines in sepsis through activation of the vagus nerve. Ann Surg *245*, 480-486.

Wu, S.V., Yuan, P.Q., Wang, L., Peng, Y.L., Chen, C.Y., and Tache, Y. (2007b). Identification and characterization of multiple corticotropin-releasing factor type 2 receptor isoforms in the rat esophagus. Endocrinology *148*, 1675-1687.

Yap, J.Y.Y., Keatch, C., Lambert, E., Woods, W., Stoddart, P.R., and Kameneva, T. (2020). Critical Review of Transcutaneous Vagus Nerve Stimulation: Challenges for Translation to Clinical Practice. Front Neurosci *14*, 284.

Yasuma, F., and Hayano, J. (2004). Respiratory sinus arrhythmia: why does the heartbeat synchronize with respiratory rhythm? Chest *125*, 683-690.

Yoshioka, M., Goda, Y., Ikeda, T., Togashi, H., Ushiki, T., and Saito, H. (1994). Involvement of 5-HT3 receptors in the initiation of pharyngeal reflex. Am J Physiol *266*, R1652-1658.

Zhang, Z. (2016). Mechanics of human voice production and control. J Acoust Soc Am *140*, 2614.

Zimmer, H.G. (2006). Otto Loewi and the chemical transmission of vagus stimulation in the heart. Clin Cardiol *29*, 135-136.